Sgr A*- the galactic center black hole – part 1 A

The COST action "Black Holes in a Violent Universe" (MP-0905) organizes a Summer School on "Black Holes at all scales Ioannina, Greece, September 16 and 18

Andreas Eckart

I.Physikalisches Institut der Universität zu Köln

Max-Planck-Institut für Radioastronomie, Bonn

14:30-16:00 Part I: Observational methods to study the Galactic Center – SgrA and its environment CND/mini-spiral/central stellar cluster - dust sources in the central few arcseconds*

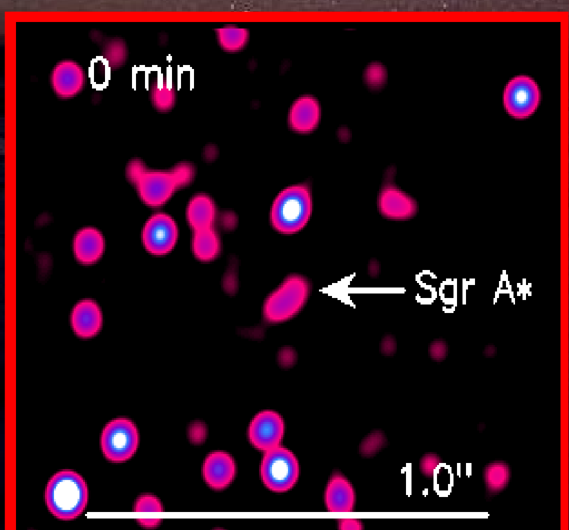

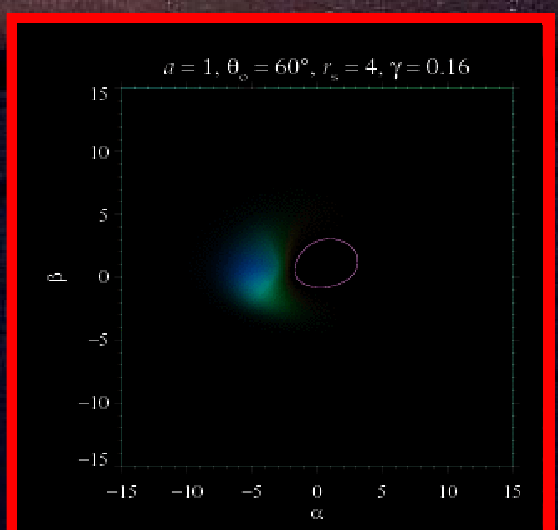

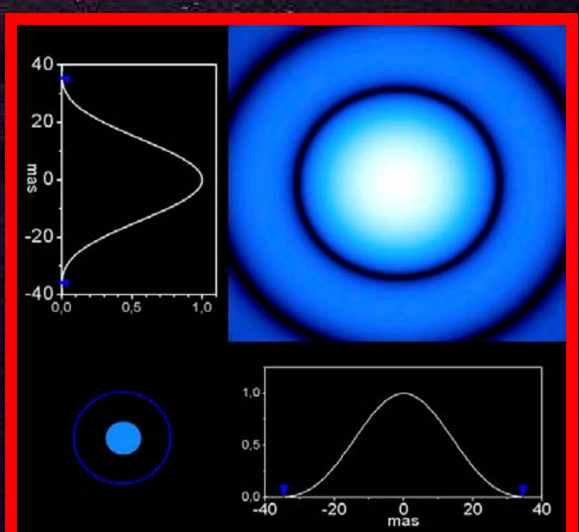

The Galactic Center

I Observational methods to study galaxy nuclei

II Structure of the Galactic Center

*III Variable emission from Sagittarius A**

incomplete and biased

The Center of the Milky Way

Closest galactic center at 8 kpc
High extinction of Av=30 Ak=3
Stars can only be seen in the NIR

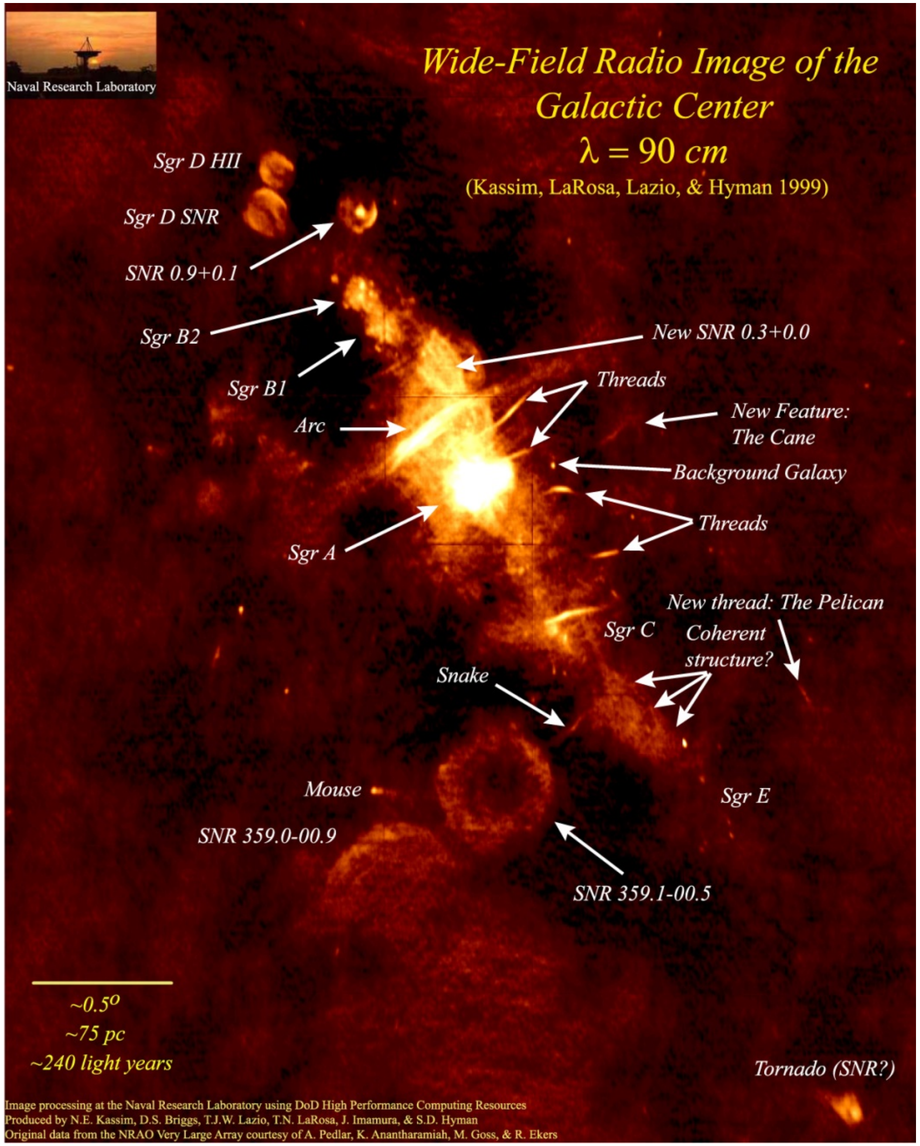

VLA 90cm

Kassim, Briggs, Lasio, LaRosa, Imamura, Hyman

Observational methods to the Galactic Center

- imaging/daptive optics
- Interferometry in the radio
- Interferometry in the mm-domain
- Interferometry in the NIR
- imaging spectroscopy

Direct Imaging

Speckle Interferometry

Via short exposures (typically 100 ms) the influence of the atmosphere on the image can be recorded and corrected for.

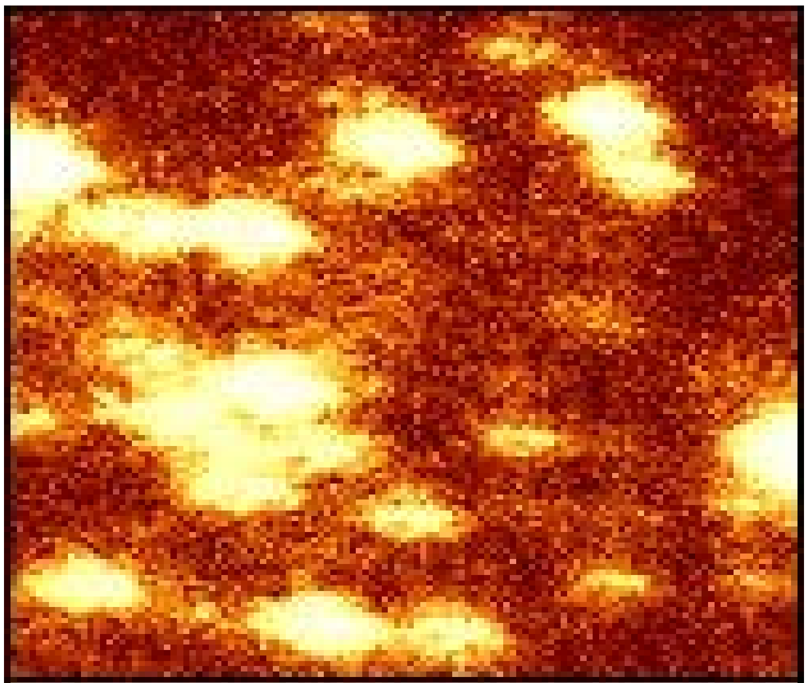

SHARP NTT short exposures

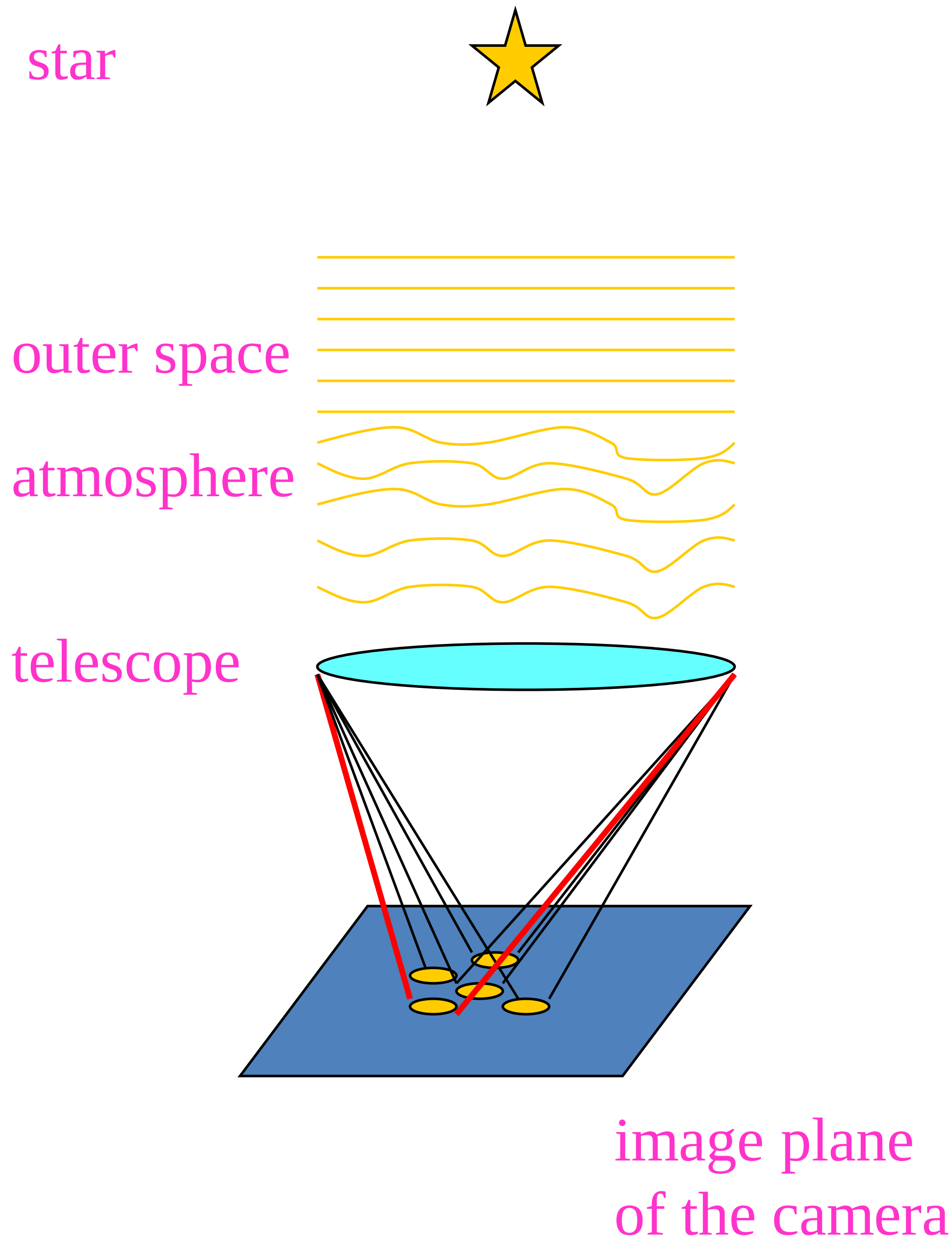

Image Formation

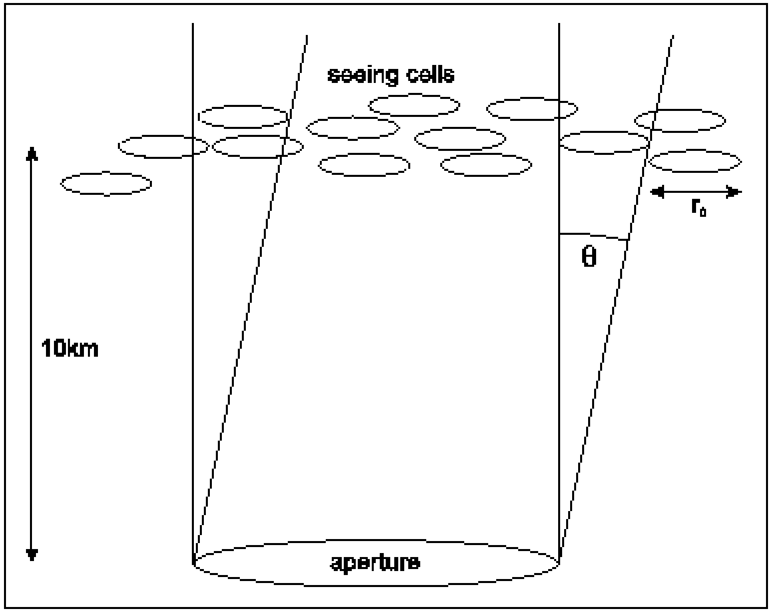

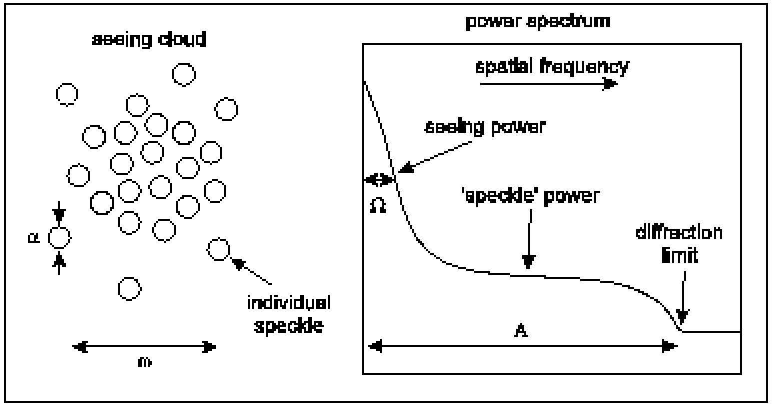

Image Formation

image plane

$$\boxed{I(x,y) = O(x,y) * P(x,y)}$$

image is object convolved with PSF

Fourier plane

$$\boxed{i(u,v) = o(u,v)\, p(u,v)}$$

$$\boxed{|\langle i(u,v)\rangle|^2 = o^2(u,v)\,|\langle T(u,v)\rangle|^2}$$

long exposure power spectrum

$$\boxed{|\langle i\rangle|^2 = |\langle a e^{i\phi}\rangle|^2}$$

$$\boxed{\langle |i(u,v)|^2\rangle = o^2(u,v)\langle |T(u,v)|^2\rangle}$$

short exposure power spectrum

$$\boxed{\langle |i|^2\rangle = \langle i^* \times i\rangle = \langle a^2\rangle\langle e^{-i\phi} e^{i\phi}\rangle = \langle a^2\rangle}$$

information at high spatial frequencies is preserved!

Seeing

$$\langle T(u,v)\rangle = T_S(u,v)T^*(u,v)$$

Telescope tranfer function:T* (autocorrelation of aperture)

Seeing transfer function: Ts

$$w^2 = u^2 + v^2$$

$$T_S(\omega) \approx \exp(-3.44\frac{\lambda|w|^{5/3}}{r_0})$$

assuming a Kolmogorov power law for the atmospheric turbulence

$$r_0 \propto \lambda^{6/5} \times \left(\cos(\gamma)\right)^{3/5}$$

r_0 Fried size of turbulent cells

γ zenith angle

$$\omega \approx \lambda / r_0$$

angular diameter of a (Fried) seeing cell

$$\boxed{\omega \propto \lambda^{-1/5}}$$

The seeing is better in the Infrared wavelength domain!!

Also: γ should be small!
Go to Chile!!

Adaptive Optics

Adaptive Optics

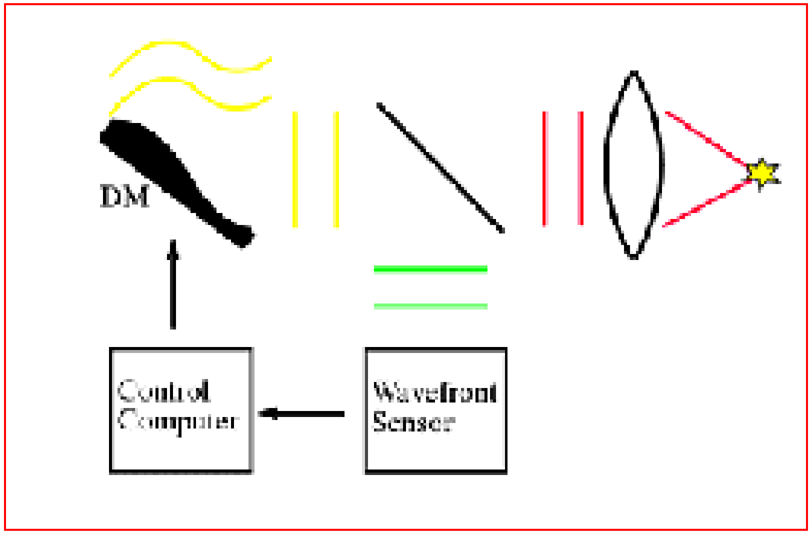

distorted wavefront is measured online and straightened via a deformable mirror

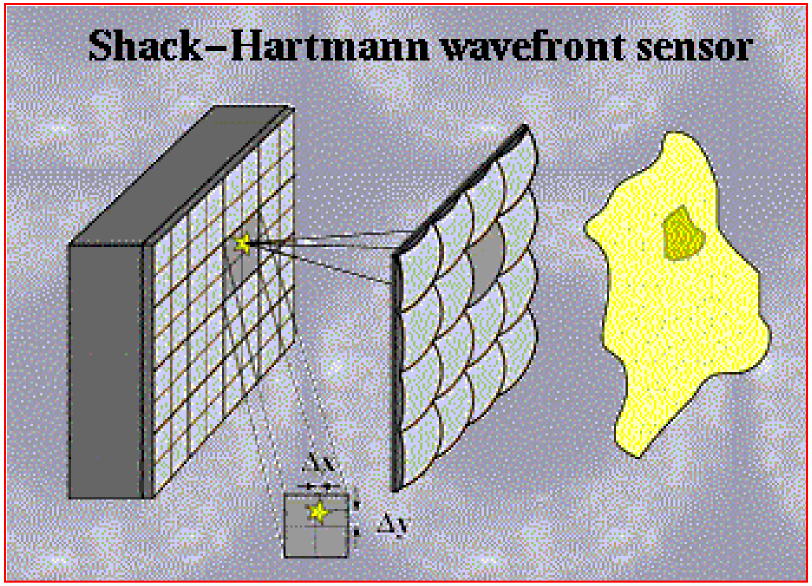

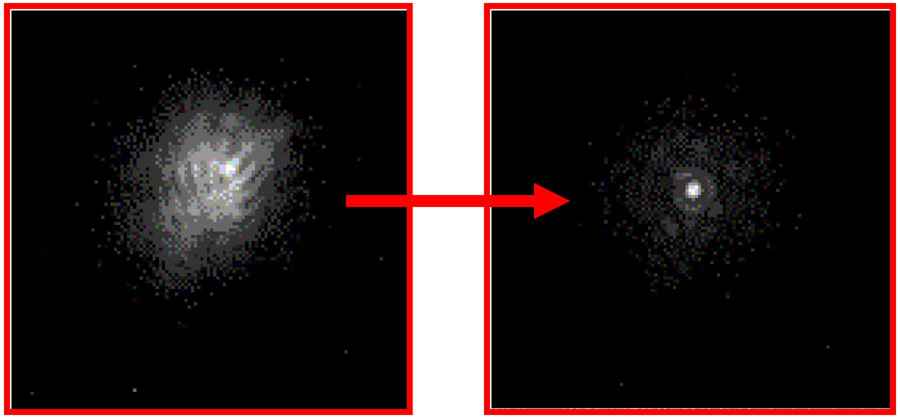

Image Formation

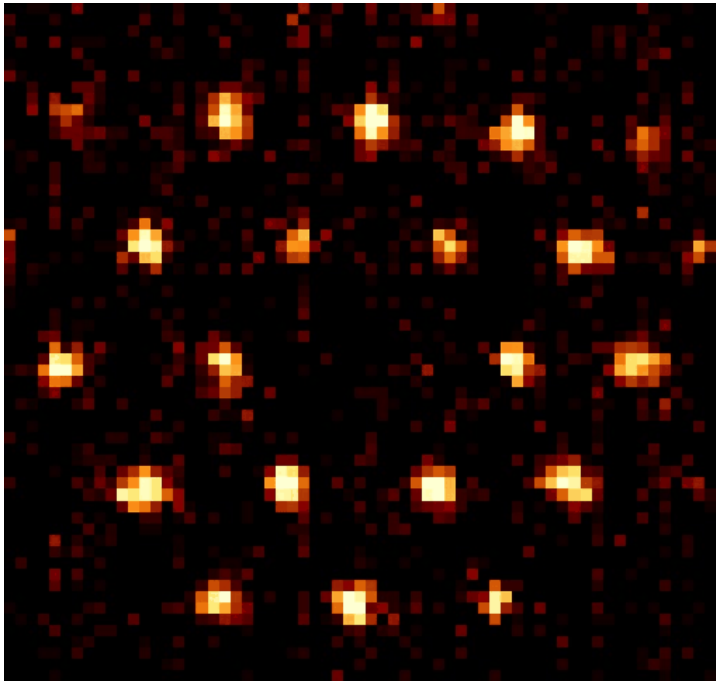

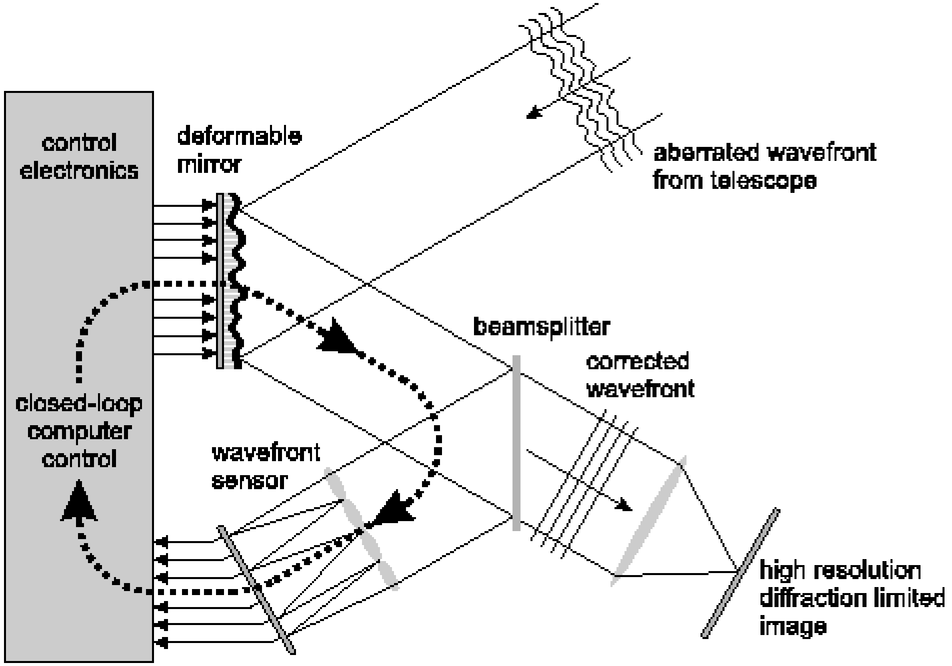

Keck II
AO image
of the GC

Adaptive Optics

Galactic Center
Keck Adaptive Optics

Mosaic of 24 images (total integration time: 120 seconds), this image shows the very central area of our own galaxy, the Milky Way. It was obtained on May 26th, 1999. The central arcsecond (inset) will help to determine the mass of the central back hole Sgr A*.

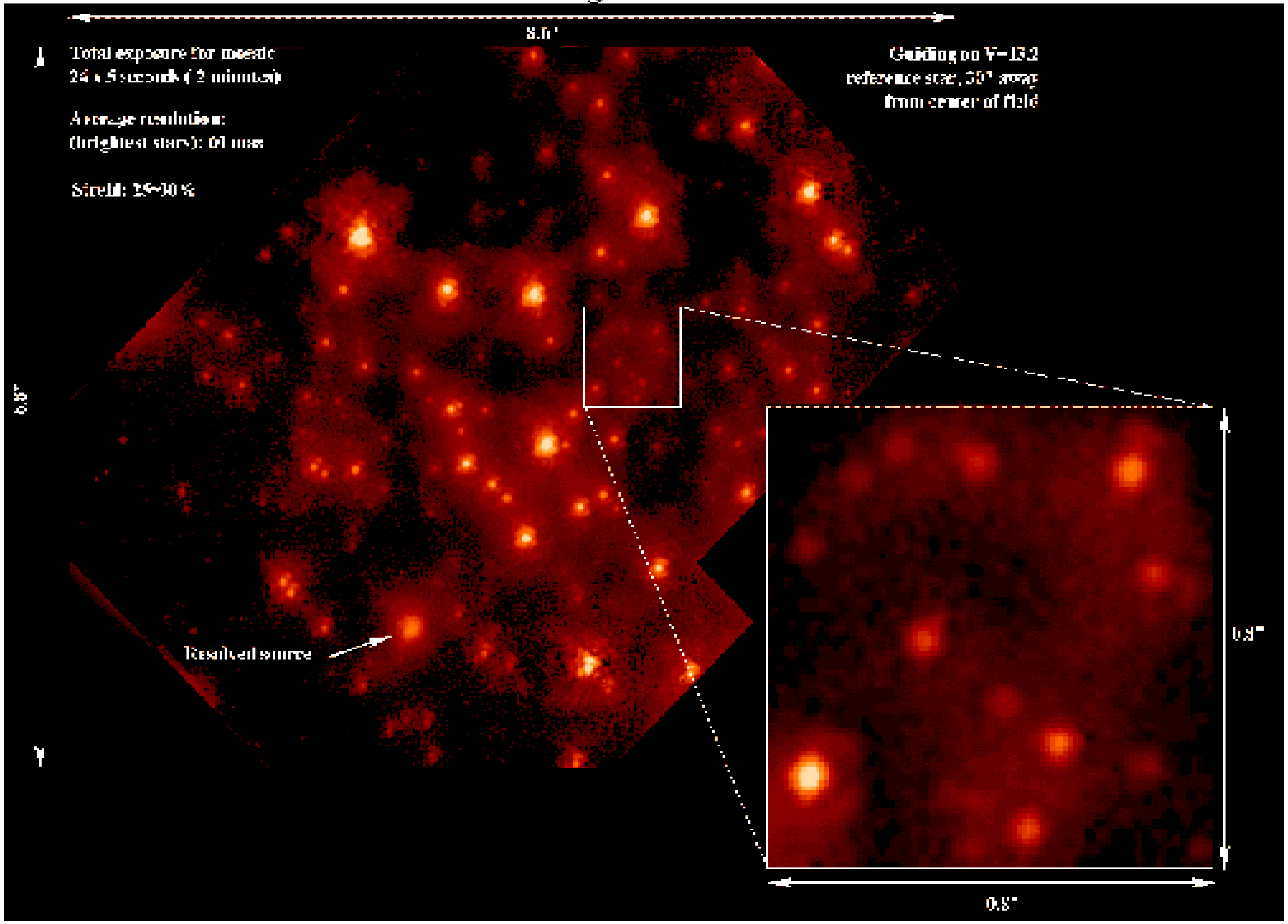

Adaptive Optics at ESO Paranal

CONICA at VLT UT4

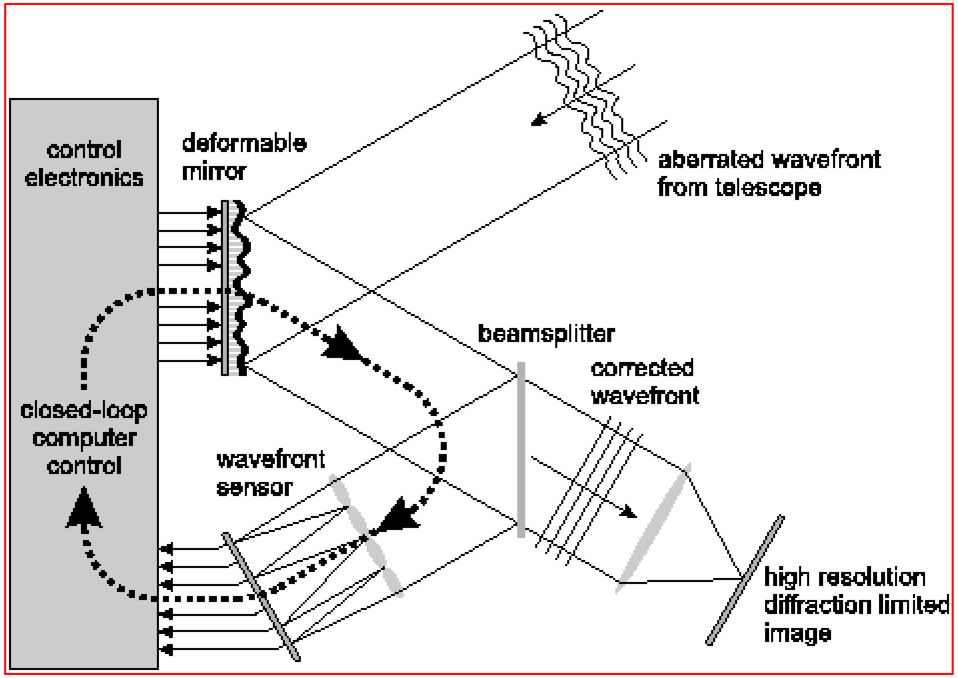

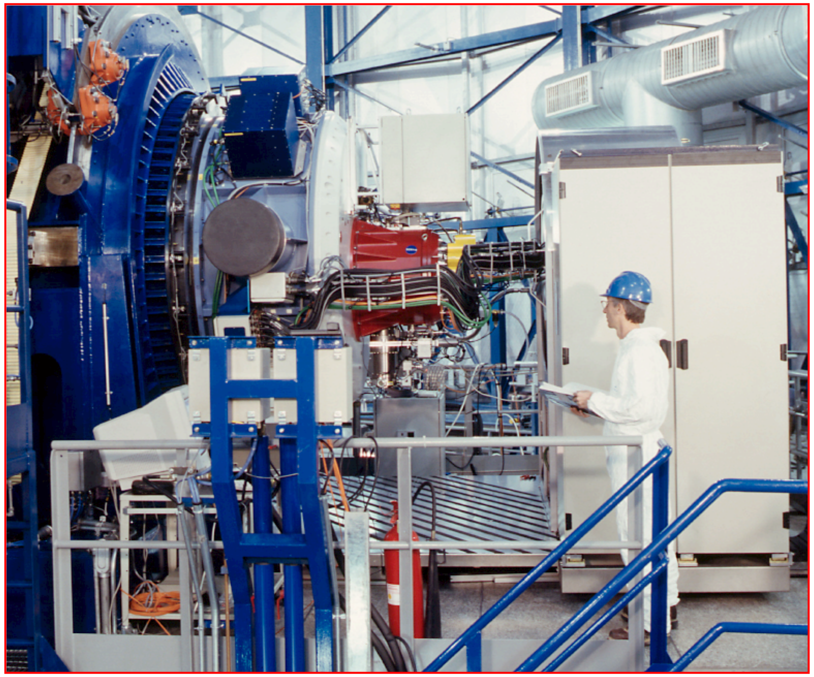

Adaptive Optics

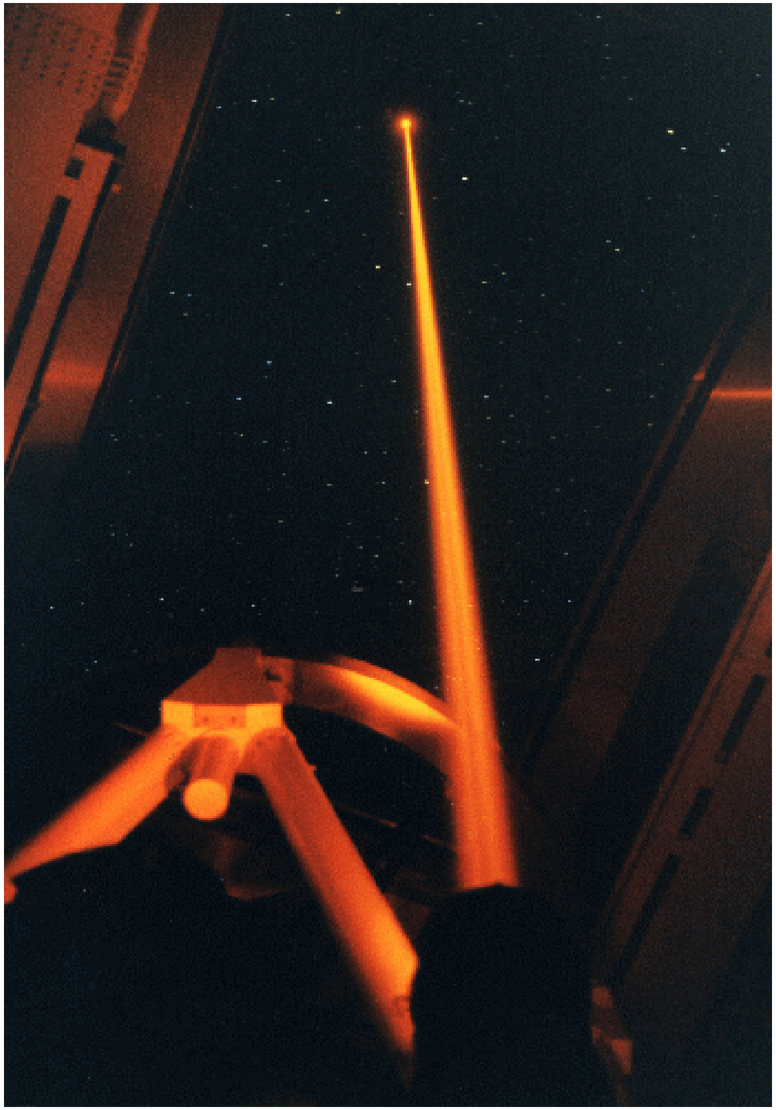

MPE laser guide star at the ALFA Calar Alto AO-System

Adaptive Optics at ESO Paranal

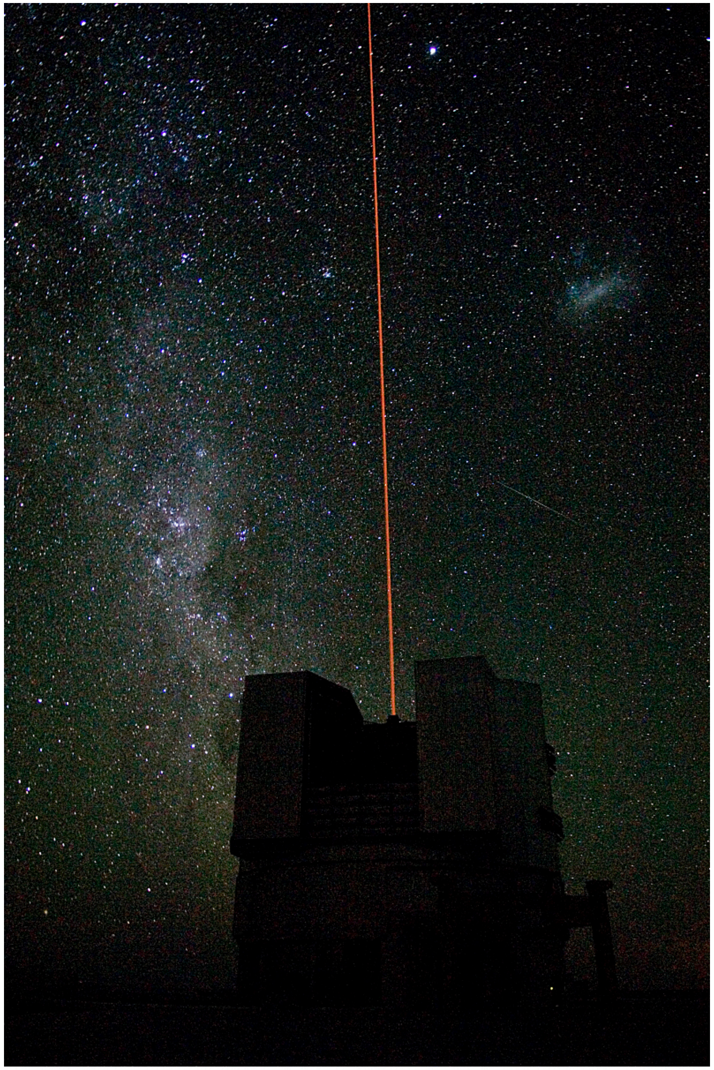

First Light of the VLT Laser Guide Star

ESO PR Photo 07a/06 (23 February 2006)

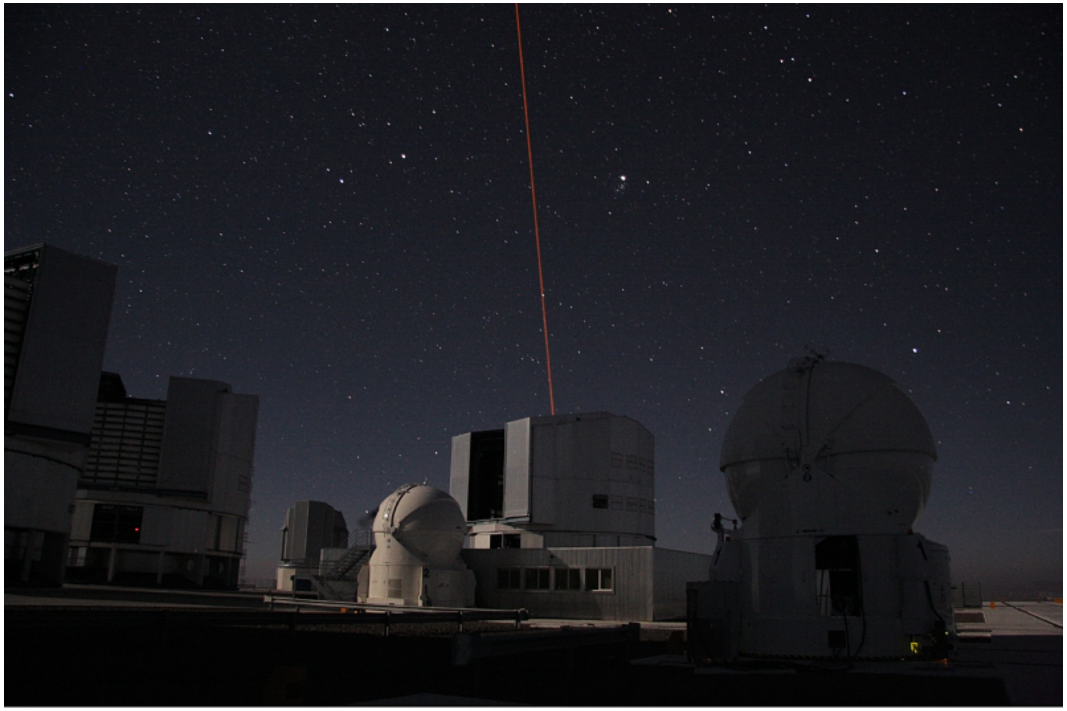

An Artificial Star Above Paranal

ESO PR Photo 07b/06 (23 February 2006)

28 Jan. 2006; 8 W into a fiber

Interferometry in the radio

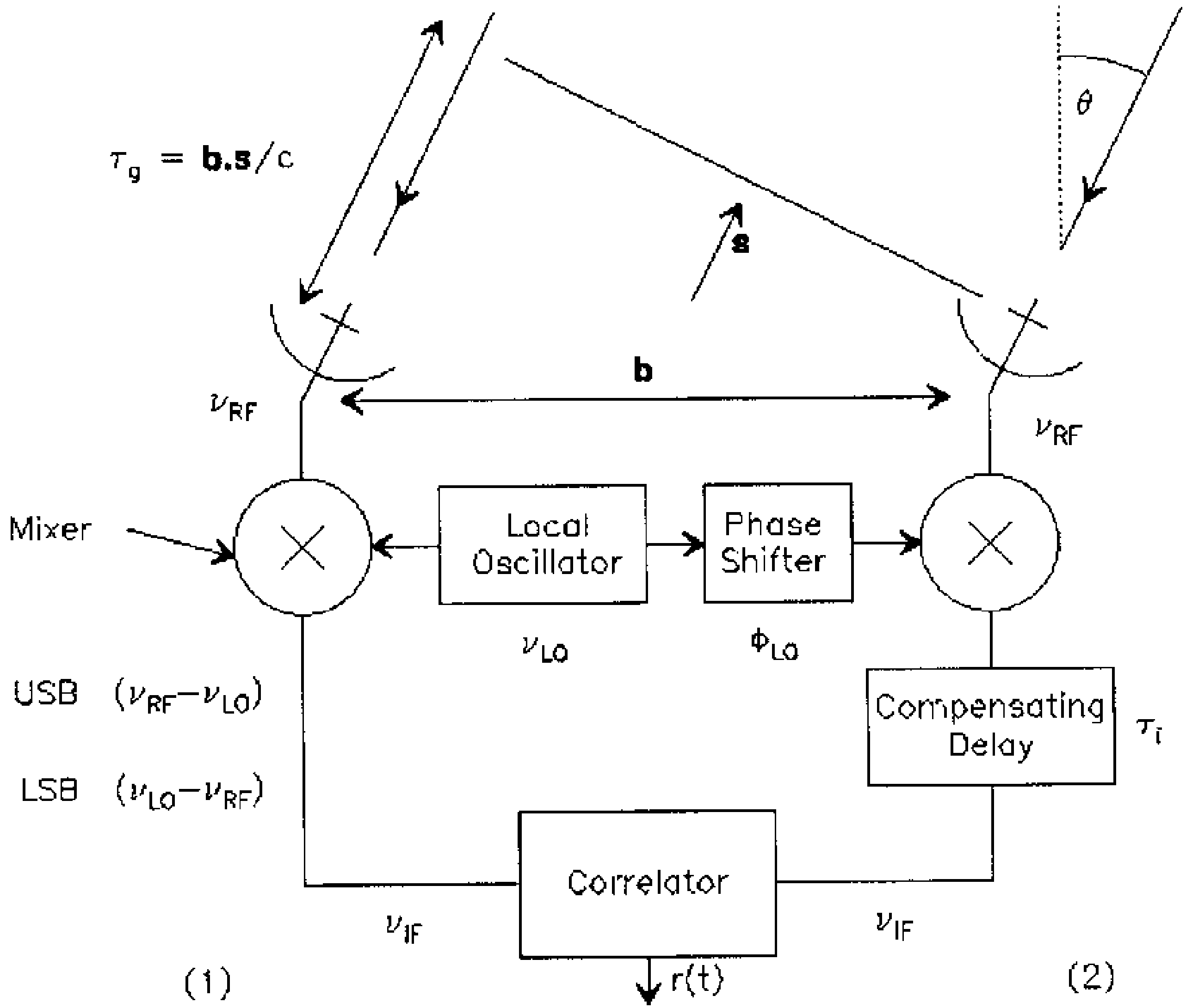

$\tau_g = \mathbf{b.s}/c$
θ
$\mathbf{s}$
$\mathbf{b}$
ν_{RF}
ν_{RF}
Mixer
Local Oscillator
Phase Shifter
ν_{LO}
ϕ_{LO}
USB $(\nu_{RF}-\nu_{LO})$
LSB $(\nu_{LO}-\nu_{RF})$
Compensating Delay
τ_i
Correlator
ν_{IF}
ν_{IF}
r(t)
(1)
(2)

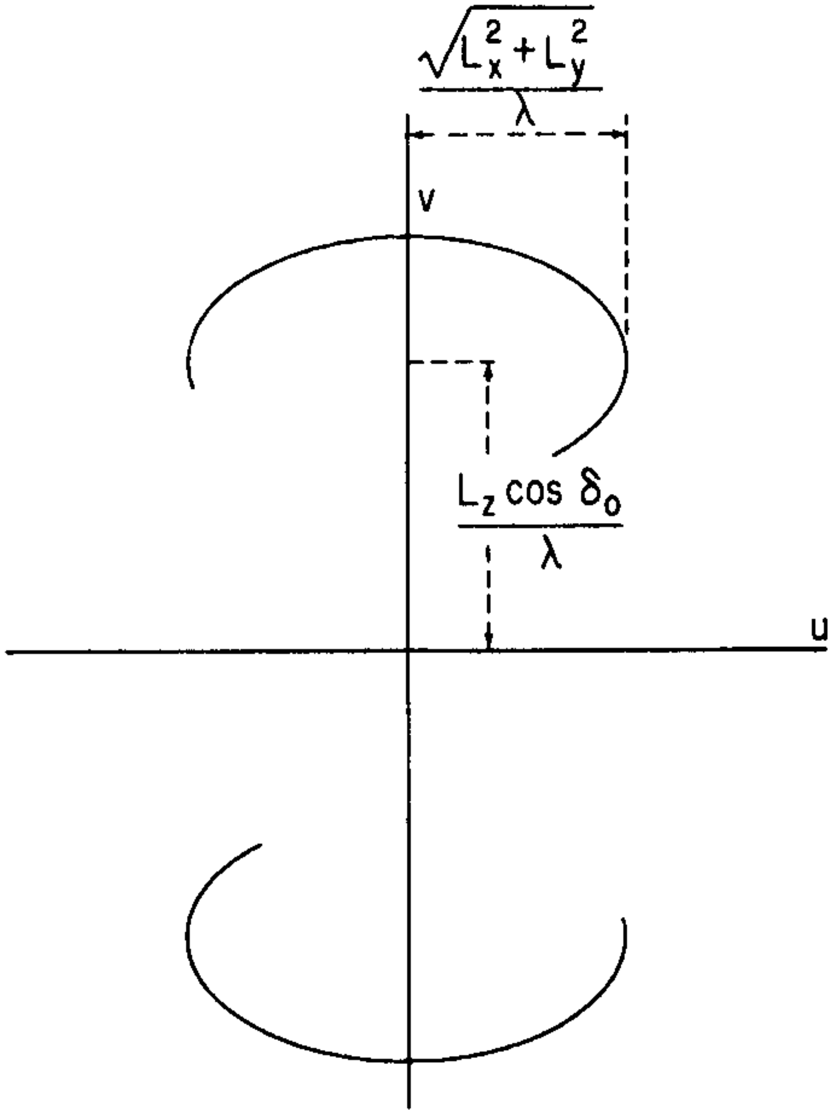
$\frac{\sqrt{L_x^2+L_y^2}}{\lambda}$
v
$\frac{L_z \cos \delta_o}{\lambda}$
u

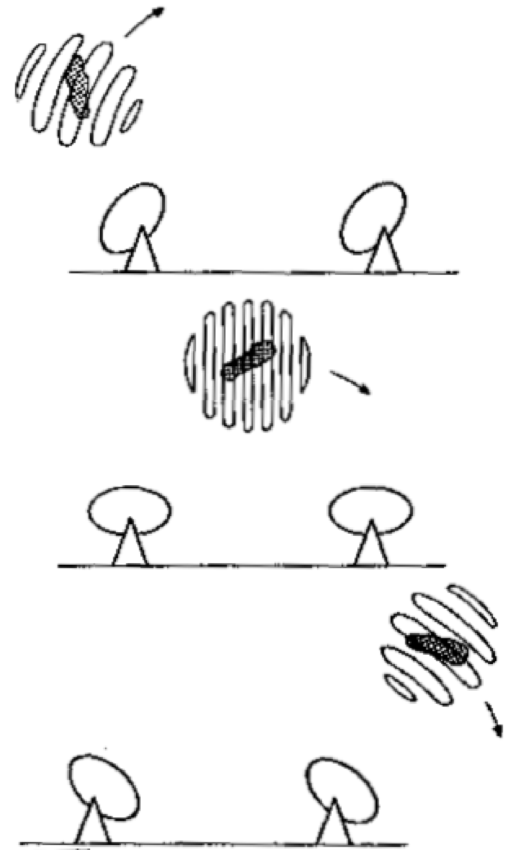

Interferometry in the mm-domain

CARMA mm-interferometer

The Combined Array for Research in Millimeter-wave Astronomy (CARMA) is a university-based interferometer consisting of six 10.4-meter, nine 6.1-meter, and eight 3.5-meter antennas that are used in combination to image the astronomical universe at millimeter wavelengths. Located at a high-altitude site in eastern California,

Atacama Large Millimeter Array

5000m altitude; 50 12m antennas; 70-900 GHz

Linear resolutions of a few parsecs can be reached for nearby active nuclei.

Interferometry in the NIR

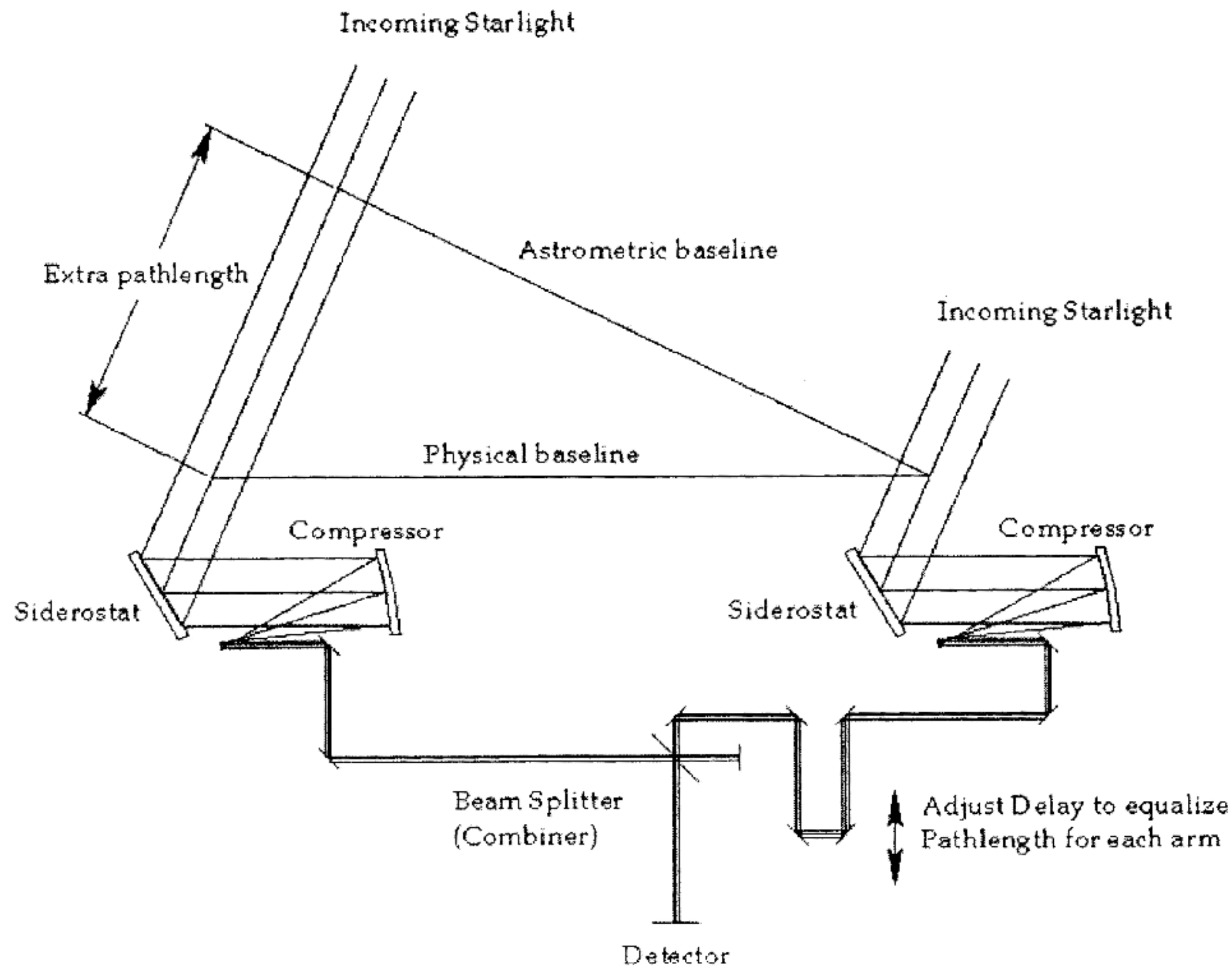
Incoming Starlight
Extra pathlength
Astrometric baseline
Incoming Starlight
Physical baseline
Compressor
Compressor
Siderostat
Siderostat
Beam Splitter
(Combiner)
Adjust Delay to equalize
Pathlength for each arm
Detector

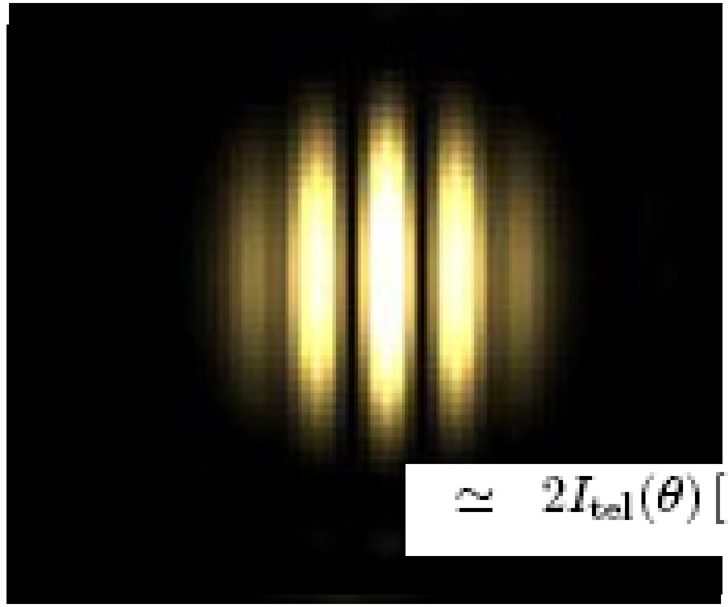

$$\simeq \quad 2I_{\mathrm{tel}}(\theta)\left[1 + V_{\mathrm{UD1}}\cos(2\pi\theta B/\lambda)\right]$$

$$V_{\mathrm{UD}} = \frac{2J_1(\pi B\theta_{\mathrm{UD}}/\lambda)}{\pi B\theta_{\mathrm{UD}}/\lambda}.$$

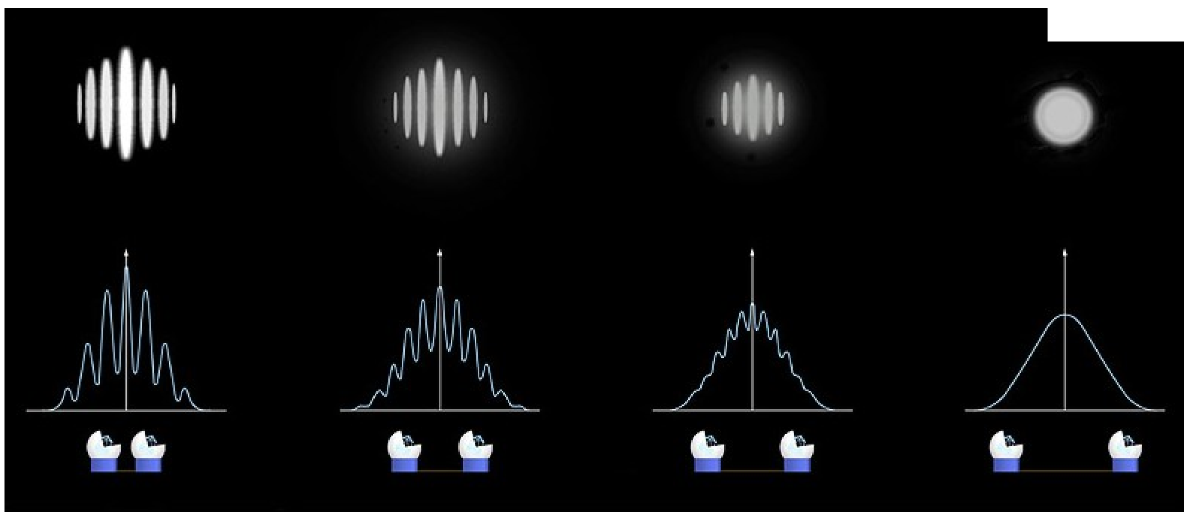

IF simulates a large aperture telescope in terms of resolution

The 8m diameter VLT mirrors combined with high throughput instrumentation and adaptive optics will allow sensitive subarcsecond NIR spectroscopy of active nuclei.

Sgr A*- the galactic center black hole - part 1 B

The COST action "Black Holes in a Violent Universe" (MP-0905) organizes a Summer School on "Black Holes at all scales Ioannina, Greece, September 16 and 18

STRONGGRAVITY EU FP7-SPACE research project 312789 2013 - 2017

SEVENTH FRAMEWORK PROGRAMME

Andreas Eckart

I.Physikalisches Institut der Universität zu Köln

Max-Planck-Institut für Radioastronomie, Bonn

Max-Planck-Institut für Radioastronomie

I. Physikalisches Institut Universität zu Köln

14:30-16:00 Part I: Observational methods to study the Galactic Center – SgrA and its environment CND/mini-spiral/central stellar cluster - dust sources in the central few arcseconds*

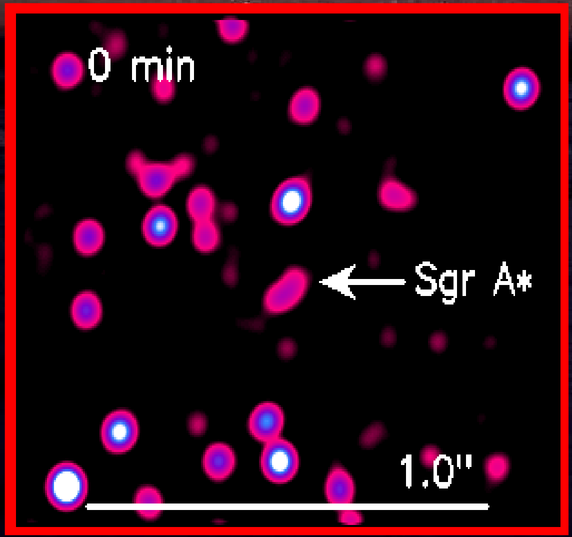

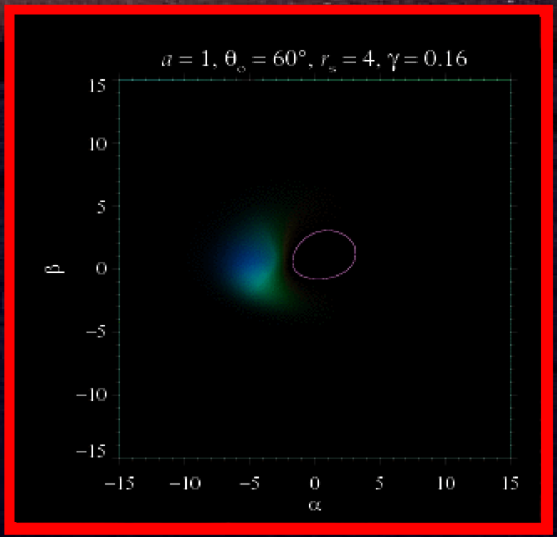

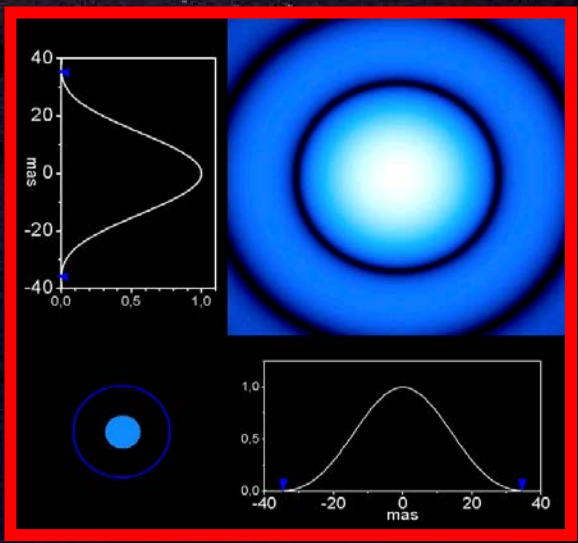

The Evironment of SgrA*

Orbital motion of high-velocity S-stars

On the possibility to detect relativistic and Newtonian peri-center shifts

- Granularity of scatterers
- Search for stellar probes

The Center of the Milky Way

Closest galactic genter at 8 kpc
High extinktion of Av=30 Ak=3
Stars can only be seen in the NIR

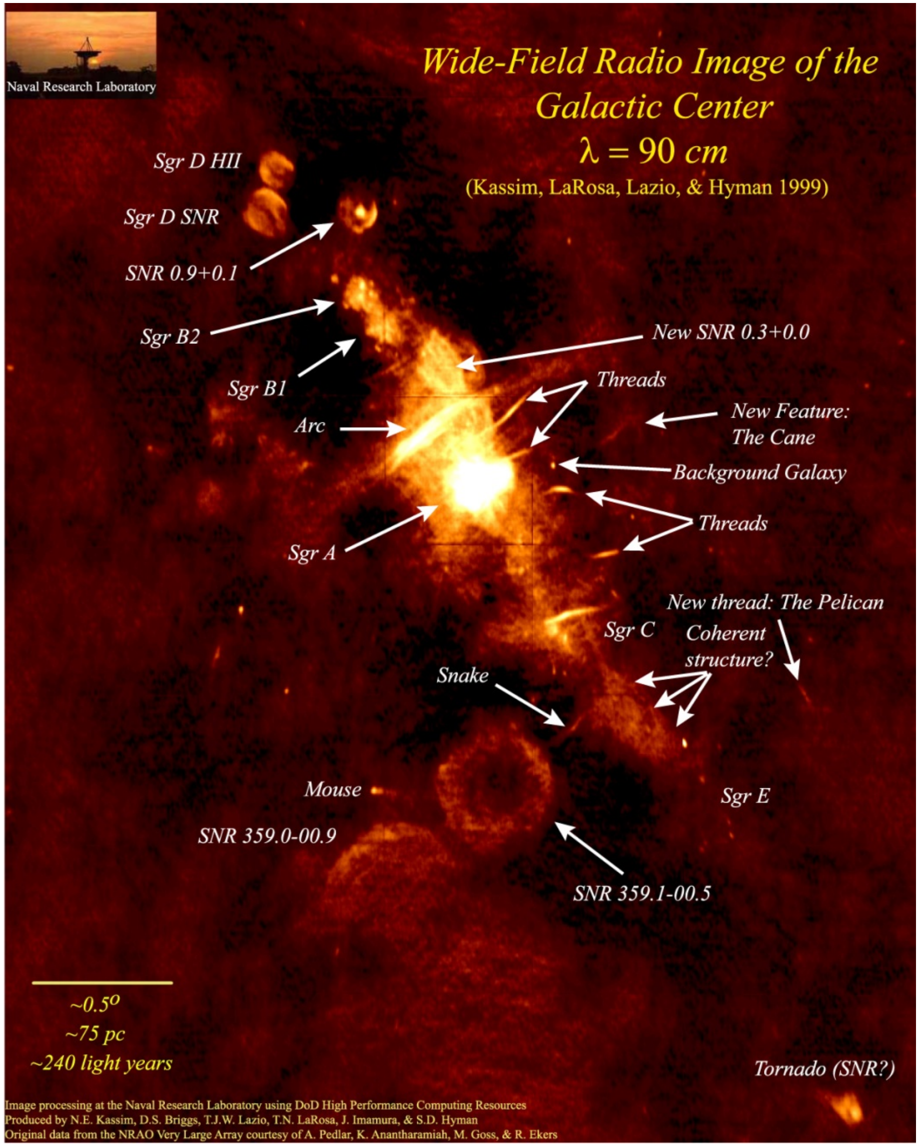

VLA 90cm

Kassim, Briggs, Lasio, LaRosa, Imamura, Hyman

SgrA* and its Environment

Orbits of High Velocity Stars
in the Central Arcsecond

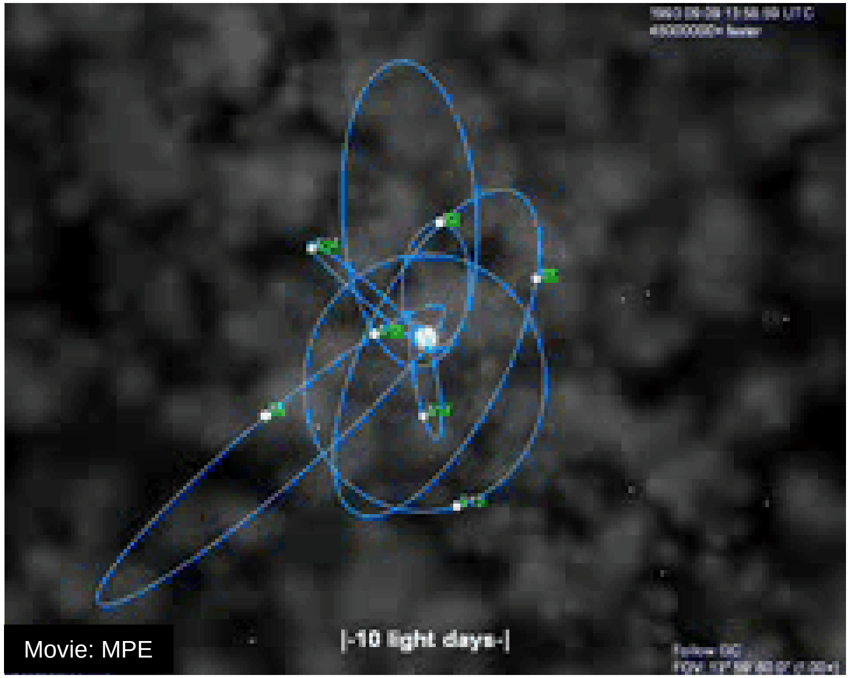

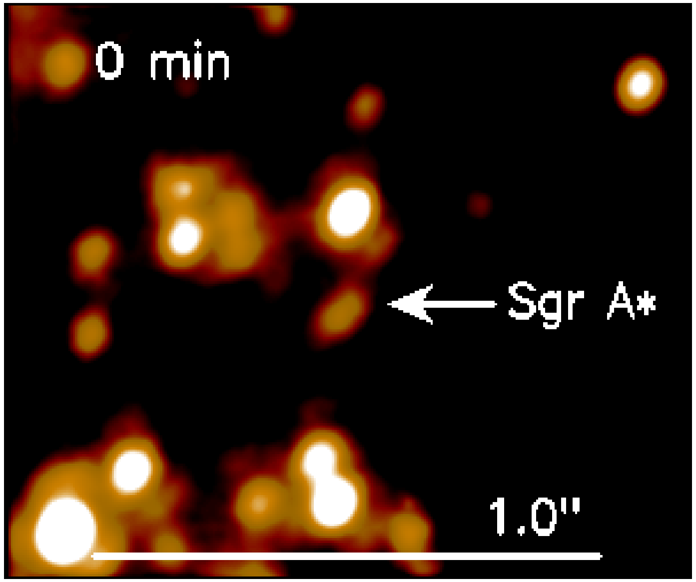

Eckart & Genzel 1996/1997 (first proper motions)
Eckart et al. 2002 (S2 is bound; first elements)
Schödel et al. 2002, 2003 (first detailed elements)
Ghez et al 2003 (detailed elements)
Eisenhauer 2005, Gillessen et al. 2009
(improved elements on more stars and distance)

~4 million solar masses
at a distance of
~8.3+-0.3 kpc

Progress in measuring the orbits

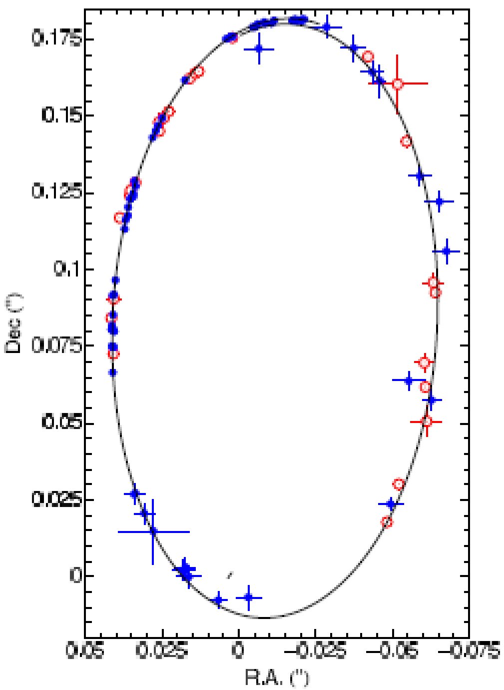

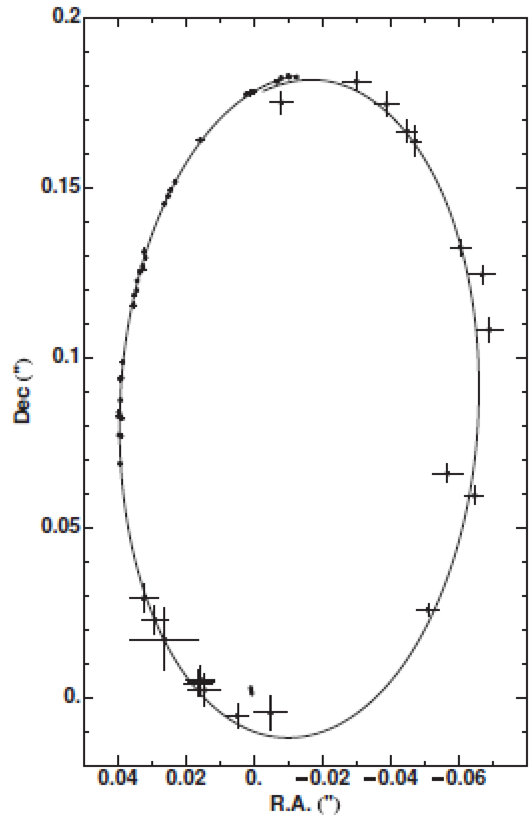

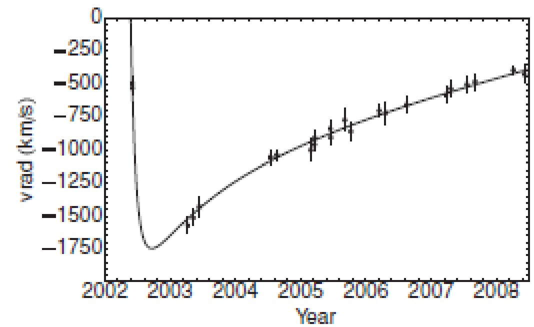

$$T_{orbit} = 15.6 \pm 0.4 yrs$$

$$e = 0.883 \pm 0.003$$

$$a = 0.125 \pm 0.002$$

$$R_0 = 8.28 \pm 0.15|_{\mathrm{stat}} \pm 0.29|_{\mathrm{sys}}\ \mathrm{kpc}$$

$$M_{\mathrm{MBH}} = 4.30 \pm 0.20|_{\mathrm{stat}} \pm 0.30|_{\mathrm{sys}} \times 10^6\ M_{\odot}$$

Gillessen+ 2009

Shortest known period star

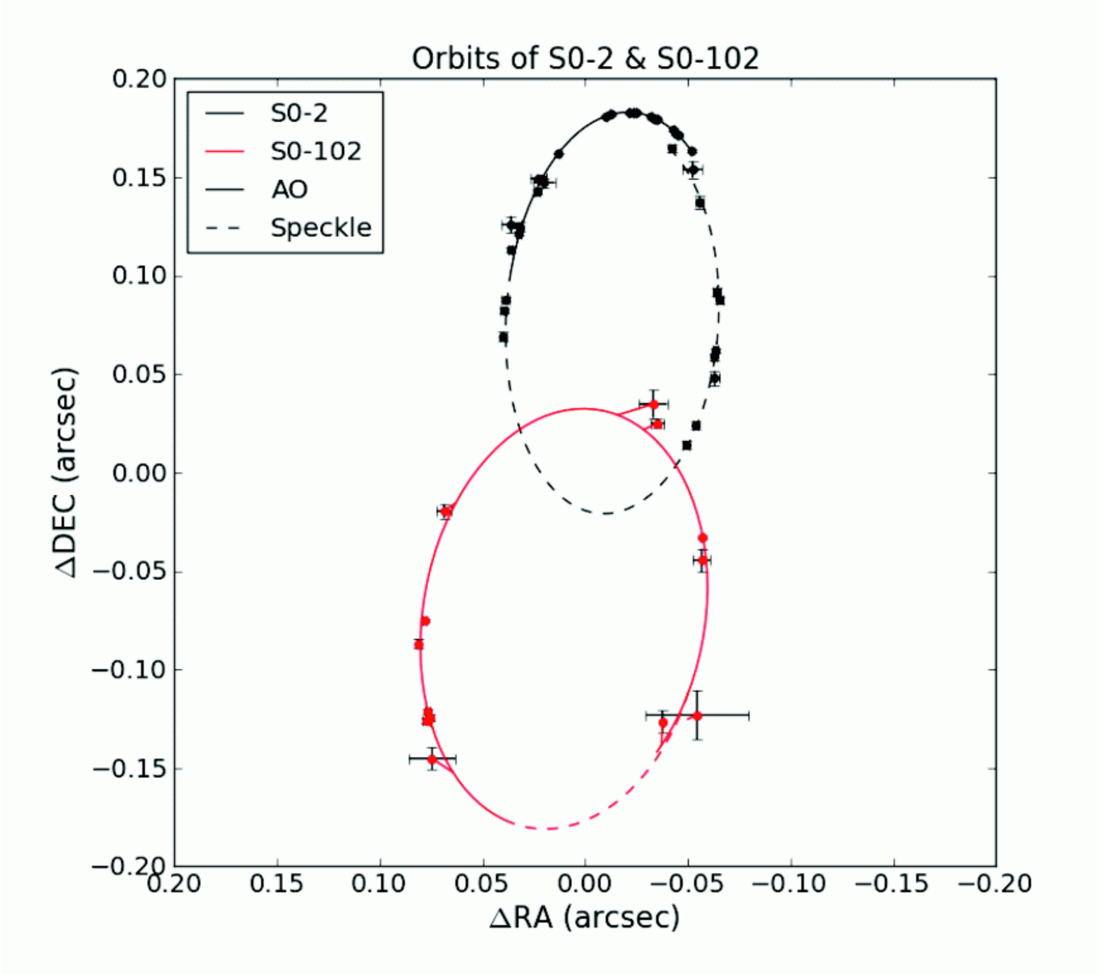

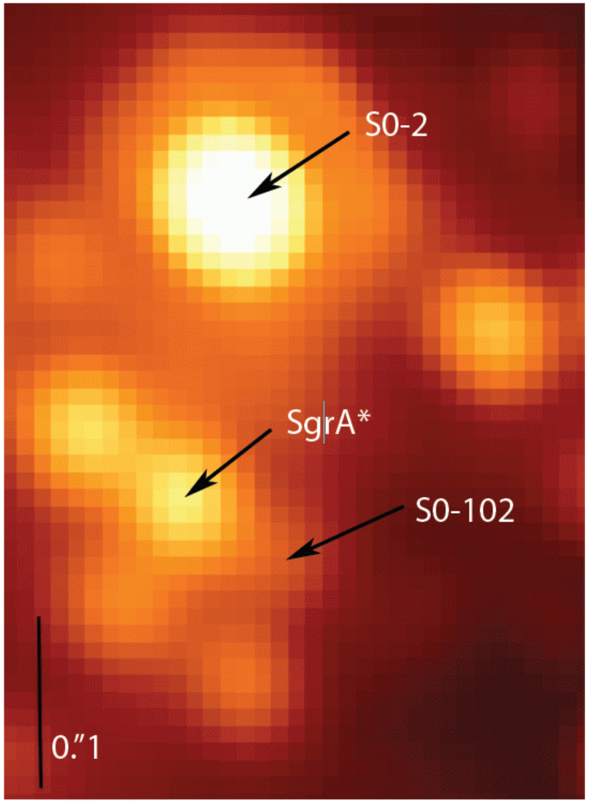

Shortest known period star with 11.5 years available to resolve degeneracies in the parameters describing the central gravitational potential (e=0.68) (Meyer et al. 2012 Sci 338, 84),

Bestimmung der Masse über S2

Für S2 ist der etwa 15 jährige Orbit geschlossen.
Die Kepler'schen Gesetze ergeben:

$$\boxed{M_{S2} = \frac{4\pi^2}{G} \frac{a^3}{T^2}}$$

mit der Umlaufzeit **T** und der großen Halbachse **a.**

Für S2 ergibt das::

$$\boxed{M_{SgrA*} \approx (4 \pm 0.3) \times 10^6 M_o}$$

Man kann gleichzeitig für die Entfernung lösen und erhält: 7.7+/-0.3 kpc

Eisenhauer et al. 2005

The Evironment of SgrA*

Orbital motion of high-velocity S-stars

On the possibility to detect relativistic and Newtonian peri-center shifts

- Granularity of scatterers
- Search for stellar probes

BH density in a dynamical core

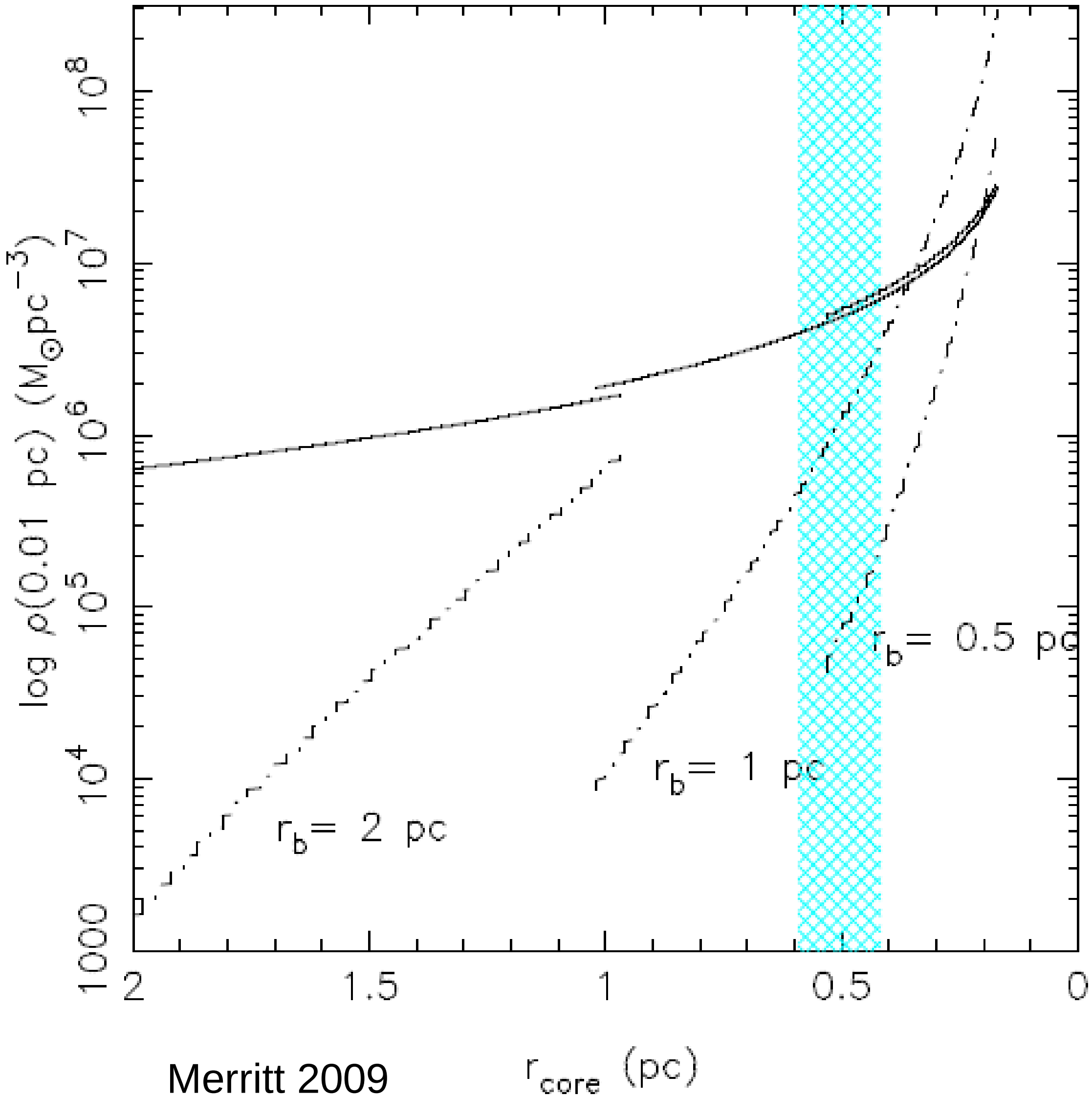

Merritt 2009

The stellar BH density is expected to be largest at a radius of a few 0.1 pc.

Most authors claim a ~10 Msol population of black holes residing at the 'bottom' of the central potential well

Chandra observations by Muno, Baganoff + 2008, 2009

and simulations by
Freitag et al. 2006
Merritt 2009

The Effect of Resonant Relaxation

$$\frac{|\Delta \mathbf{L}|}{L_c} \approx K\sqrt{N}\frac{m}{M_\bullet}\frac{\Delta t}{P}$$

change of torque due to filed stars

$$L_c = \sqrt{GM_\bullet a}$$

Equivalent angular momentum of test star on circular orbit

Changes in L over Δt imply
changes in e and orbital plane anges:

$$\cos(\Delta\theta) = \frac{\mathbf{L}_1 \cdot \mathbf{L}_2}{L_1 L_2}$$

Resonant relaxation:

Rauch & Tremaine 1996
Hopeman & Alexander 2006
Merritt et al. 2010

$$|\Delta e|_{\mathrm{RR}} \approx K_e\sqrt{N}\frac{m}{M_\bullet},$$

$$(\Delta\theta)_{\mathrm{RR}} \approx 2\pi K_t\sqrt{N}\frac{m}{M_\bullet}$$

Two stellar populations
Species 1 smooth
Species 2 perturbing

$$(\Delta\theta)_{RR} = K_t\left[\frac{m_1\sqrt{N_1} + m_2\sqrt{N_2}}{M_\bullet}\right]$$

Sabha, Eckart, Merritt et al. 2012

Average values of the changes in Δω, Δθ, Δe and for S2 over one orbital period (~16 yr) in the N-body integrations.

Filled circles are from integrations with m = 50 M⊙ and open circles are for m = 10 M⊙ ; number of field stars N = {25, 50, 100, 200} for both m. The abscissa is the distributed mass within S2's apo-apsis, at r =9.4 mpc. In each frame, the points are median values from the 100 N-body integrations.

(a) Changes in the argument of peri-bothron. The contribution from relativity has been subtracted.
(b) Changes in the eccentricity. Solid and dashed lines are with m = 50 M⊙ and m = 10 M⊙, respectively.
(c) The angle between initial and final values of L i.e. Δθ for S2. .

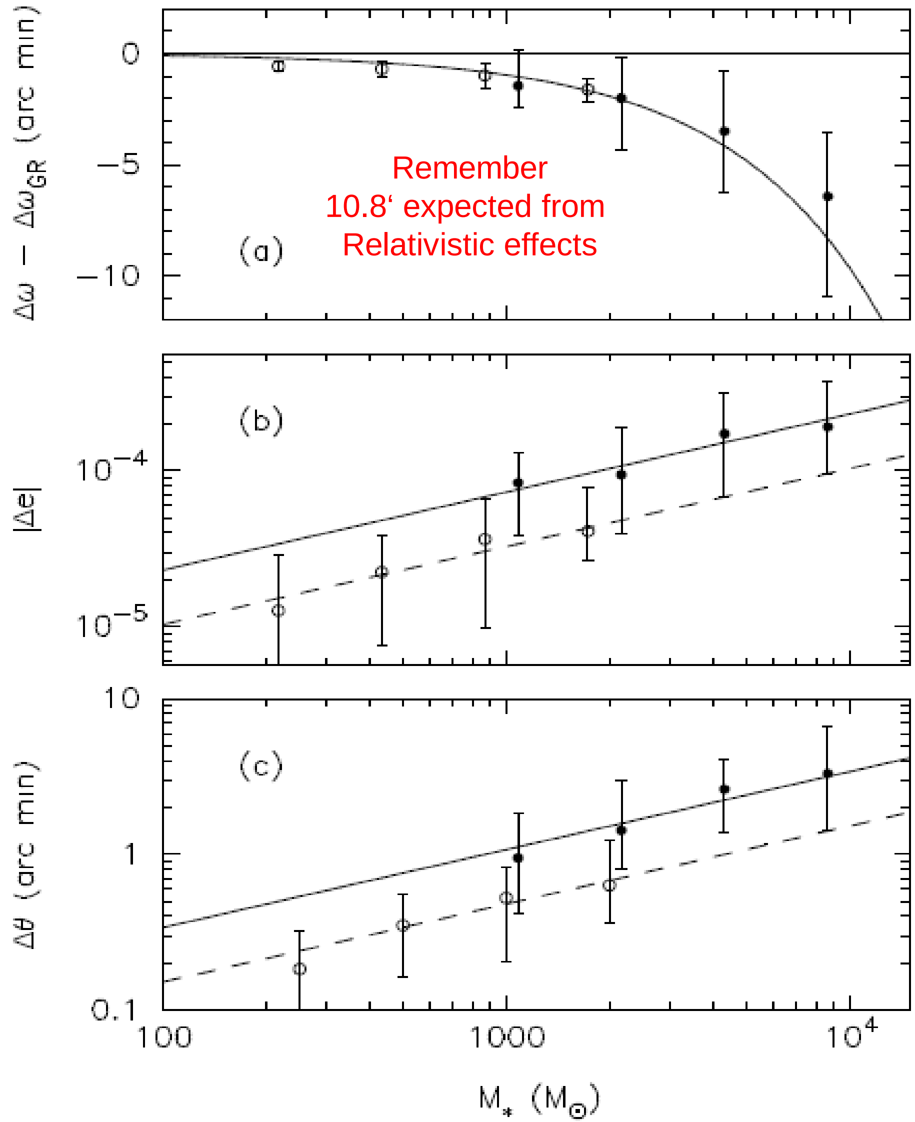

Sabha et al. 2012

Histograms of the predicted peri-bothron change of S2 over one orbital period (~16 yr).

The shift due to relativity (~11′), has been subtracted. What remains is due to Newtonian perturbations (peri-bothron shift and pertrubation/scattering) from the field stars.

$$\frac{|\Delta \mathbf{L}|}{L_c} \approx K\sqrt{N}\frac{m}{M_\bullet}\frac{\Delta t}{P}$$

$$|\Delta e|_{\rm RR} \approx K_e\sqrt{N}\frac{m}{M_\bullet},$$

$$(\Delta\theta)_{\rm RR} \approx 2\pi K_t\sqrt{N}\frac{m}{M_\bullet}$$

Resonant relaxation:

Rauch & Tremaine 1996
Hopeman & Alexander 2006
Merritt et al. 2010

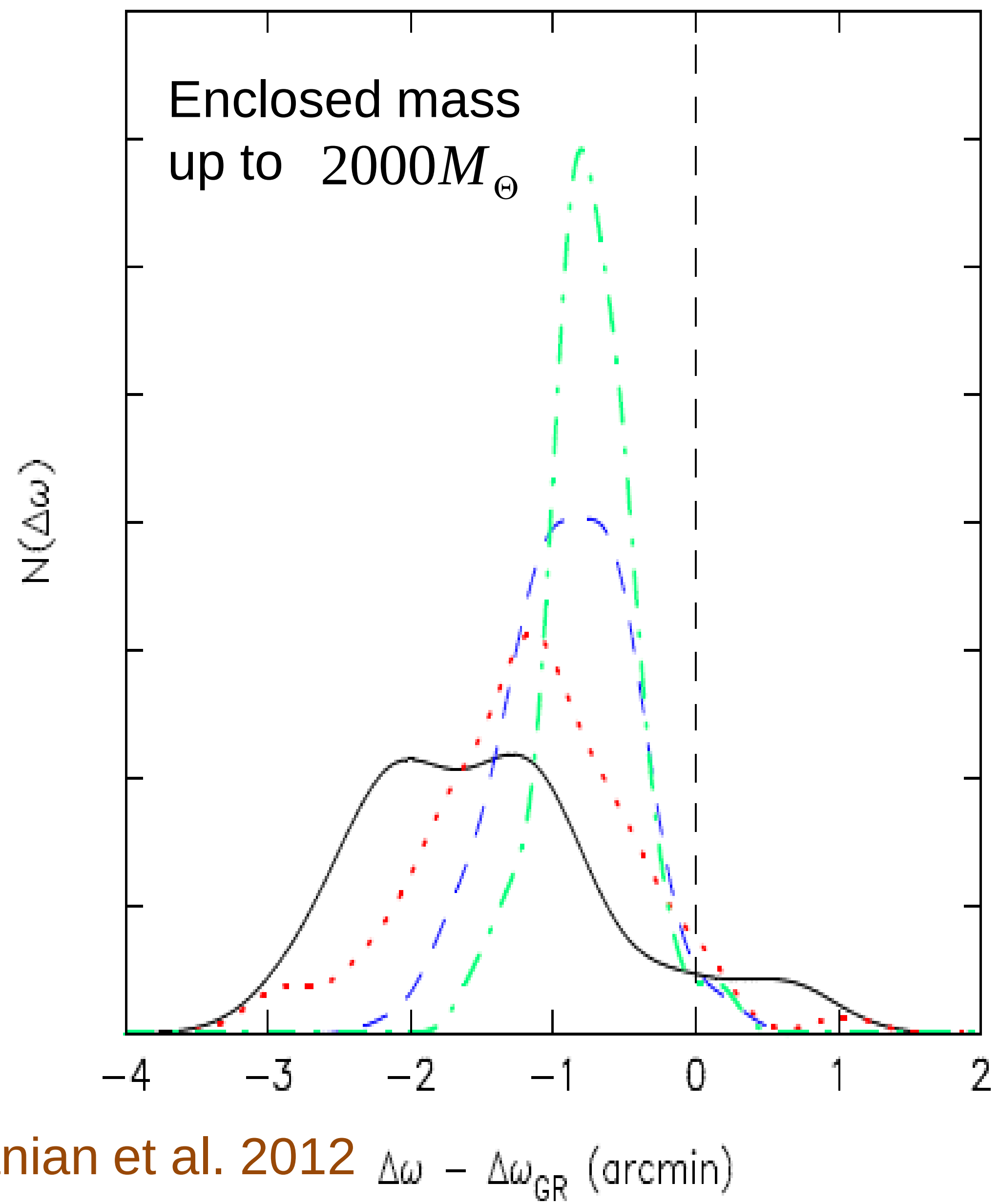

Sabha, Eckart, Merritt, Shahzamanian et al. 2012

Newtonian and relativistic periastron shift for S2

$$m_1 = 1\ \mathrm{M}_\odot, \quad m_2 = 10\ \mathrm{M}_\odot, \quad \boxed{N_1 = 10^4,} \quad N_2 = 1500$$

$$|\Delta e|_{\mathrm{RR}} \approx 1.7 \times 10^{-4}$$
$$(\Delta\theta)_{\mathrm{RR}} \approx 3'.0.$$

$$m_1 = 1\ \mathrm{M}_\odot, \quad m_2 = 10\ \mathrm{M}_\odot, \quad \boxed{N_1 = 10^5,} \quad N_2 = 15000$$

mass composition
following
Freitag et al. 2006

$$|\Delta e|_{\mathrm{RR}} \approx 5.4 \times 10^{-4}$$
$$(\Delta\theta)_{\mathrm{RR}} \approx 8'.0.$$

<u>Significant contributions </u>to perisatron shift $\Delta\omega$
from encounters
due to granulartiy of ‘scattering‘ population $\Delta\theta$: $\propto \sqrt{N_2}$
and
variation in enclosed mass due to scattering population: $\propto \sqrt{N_2}$

The variance in for S2 for one orbital period (~16 yr) in the N-body integrations.

Relative variance of peri-center shift as the absolute variance over the shift itself.

The absolute variance is large and of the order of the entire peri-center shift.

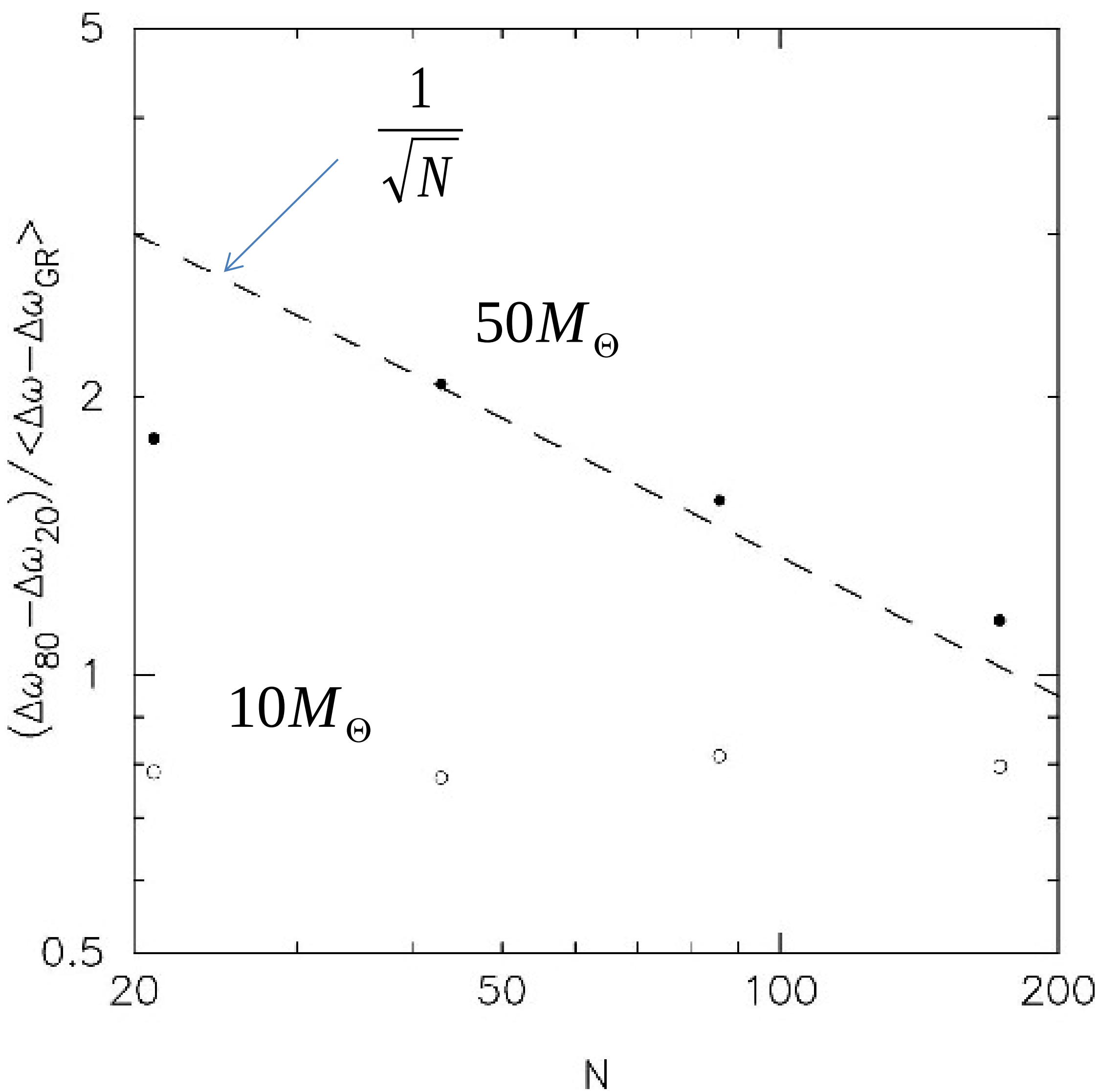

The Evironment of SgrA*

Orbital motion of high-velocity S-stars

On the possibility to detect relativistic and Newtonian peri-center shifts

- Granularity of scatterers
- Search for stellar probes

Subtraction of stars within R<0.7"

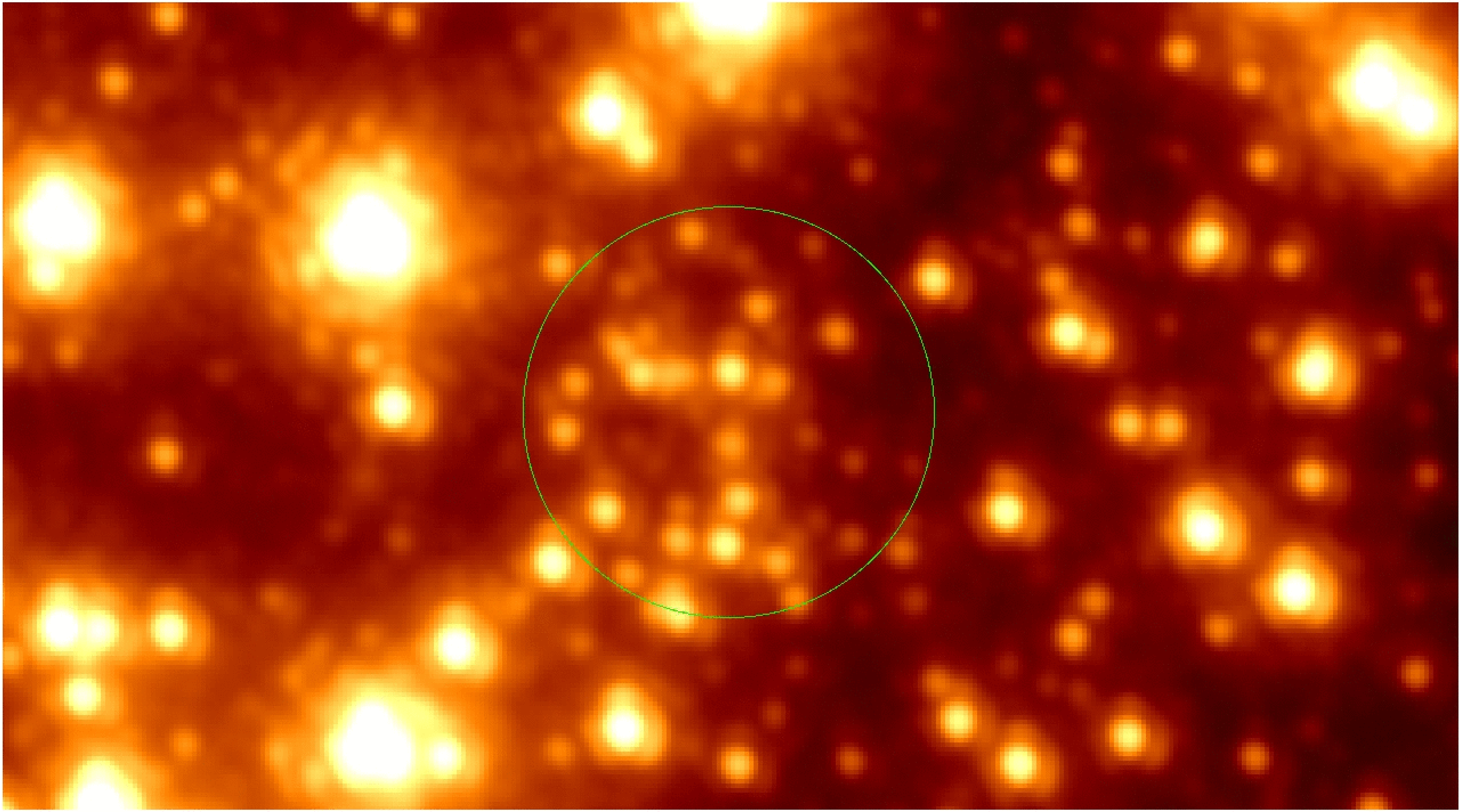

S<1mJy in the NIR K-band

Sabha et al. 2010

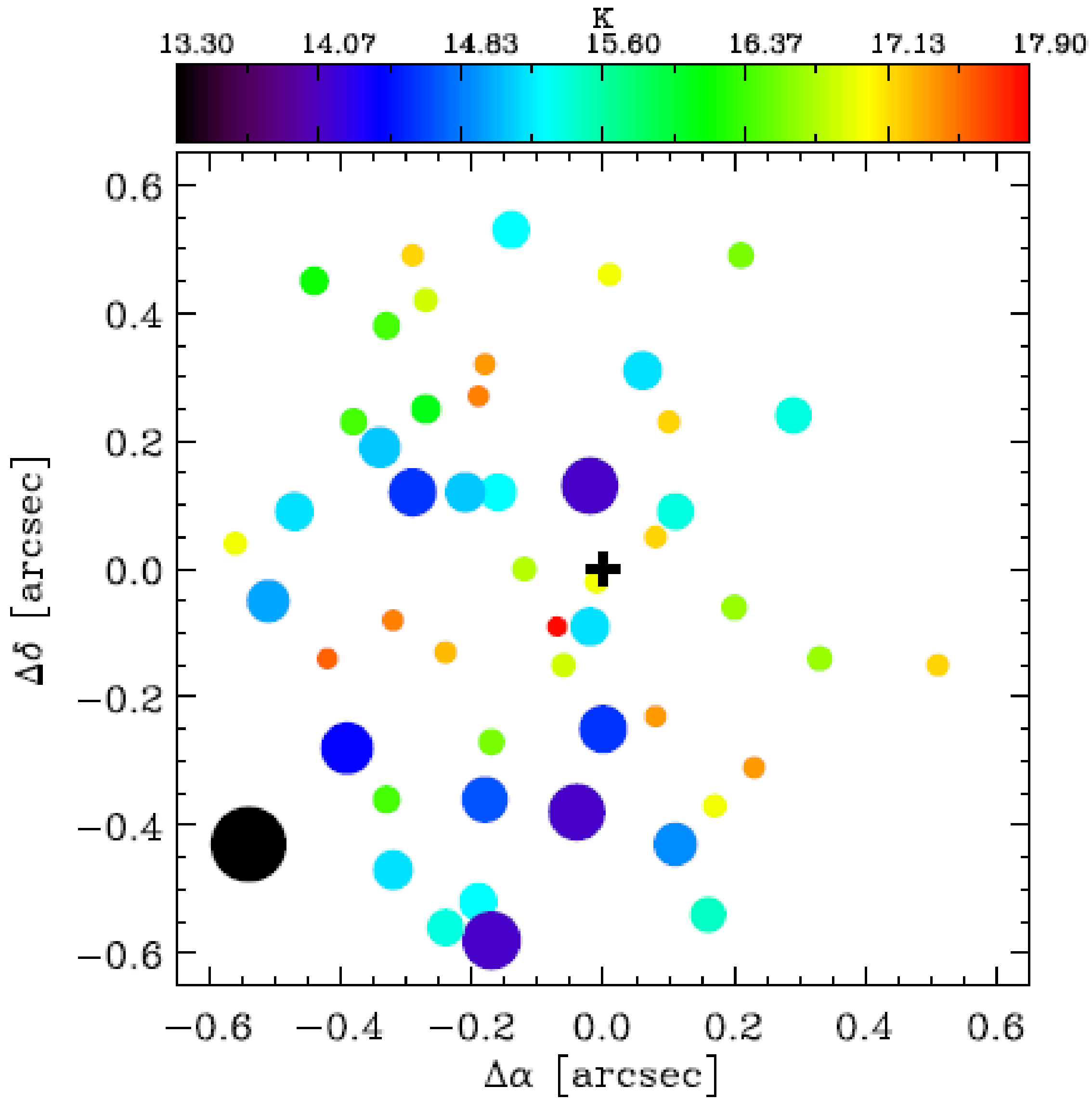

Map of the 51 brightest stars close to SgrA*. The color of each star indicates its K-magnitude. The size of each symbol is proportional to the flux of the corresponding star. The position of Sgr A* is indicated as a cross at the center

Sabha et al. 2012

The Central S-star Cluster

luminosity function exp(-Γ)

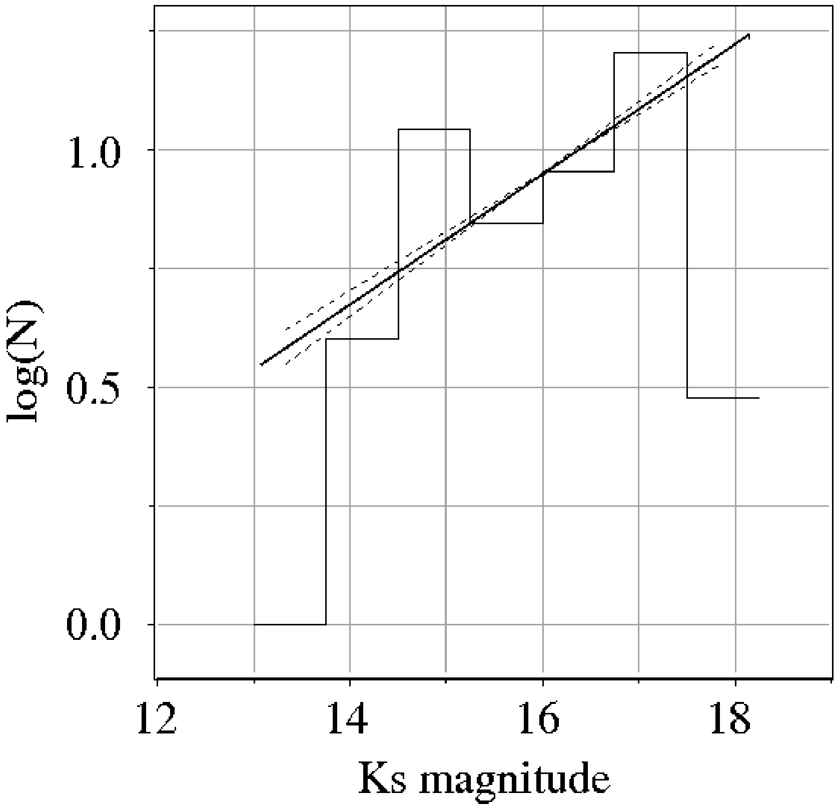

radial distribution exp(-α)

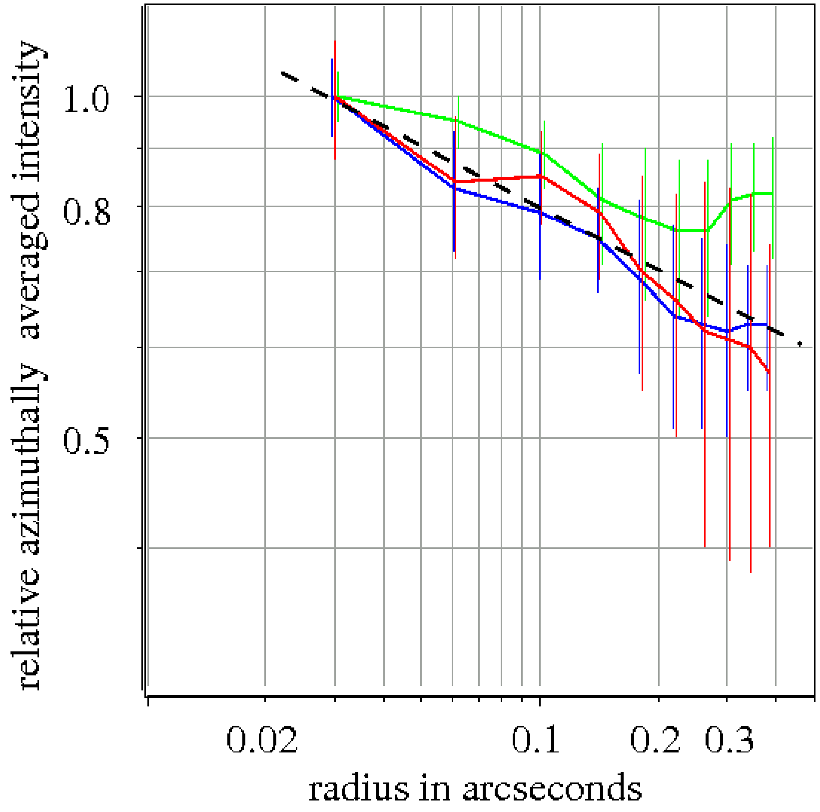

Sabha et al. 2011, 2012

S-stars: Extrapolation to fainter luminosities

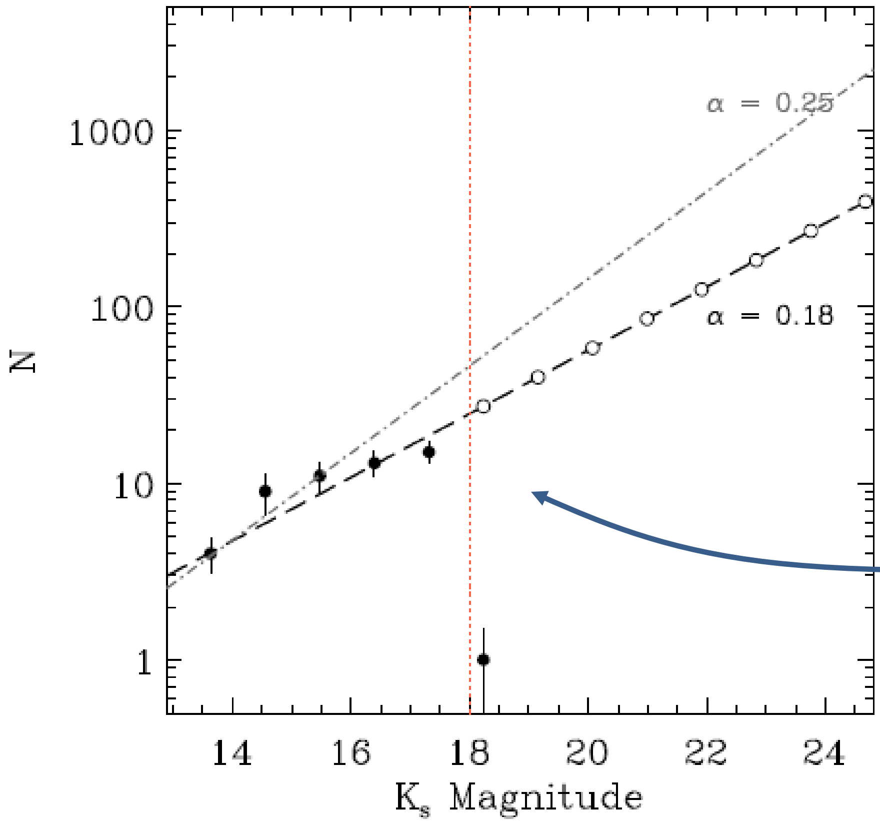

all stars fainter than the faintest stars detected in the central arcsecond.

Extrapolation of the KLF power-law fit. The KLF slope of α= 0.18 and the upper limit imposed by the uncertainty in the fit (α= 0.25) are plotted as dashed and dash-dotted lines, respectively. The black filled circles represent the data while the hollow circles represent new points based on the extrapolated KLF. The location of the detection limit is indicated by the red line.

Sabha et al. 2012

Apparent stars due to blends

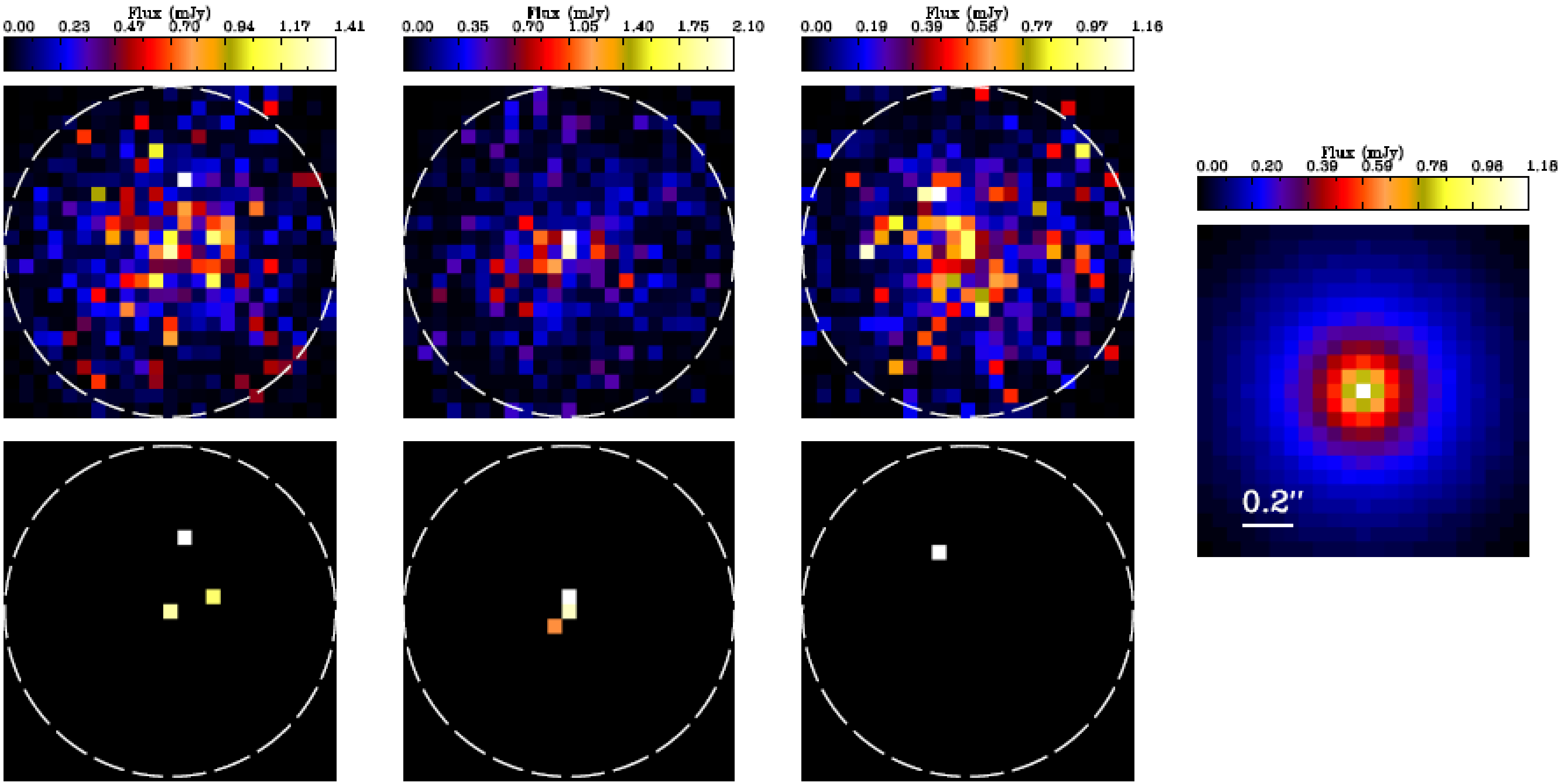

Upper panel: 3 different snapshots of the simulation for the α= 0.25 KLF slope, power-law index Γ = -0.3 and a ~25 K-magnitude cutoff.
Lower panel: The same as upper but with only the detectable blend stars visible.
Right: Average of all the 104 simulation snapshots for the same setup.

INTERFEROMETRY IS NEEDED to make progress! Sabha et al. 2012

SgrA* and its Environment

Orbits of High Velocity Stars
in the Central Arcsecond

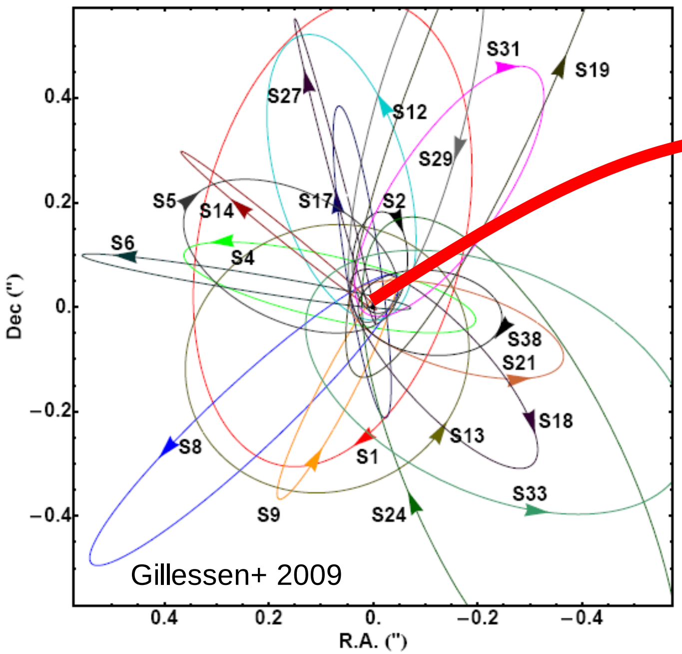

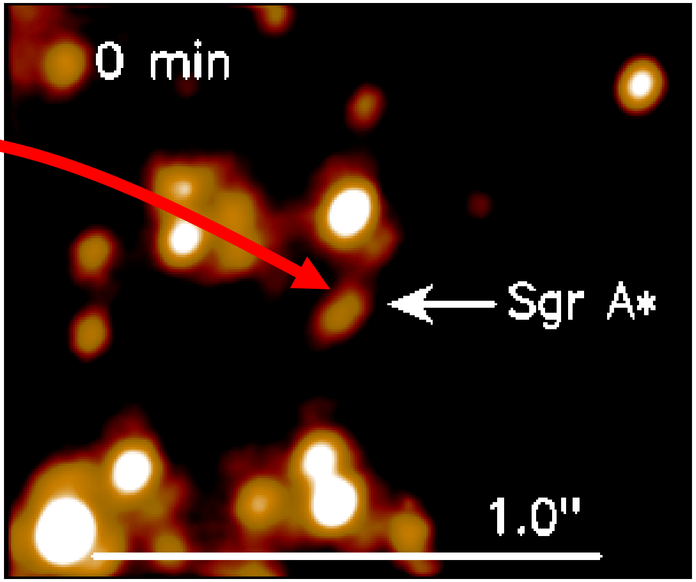

Eckart & Genzel 1996/1997 (first proper motions)
Eckart et al. 2002 (S2 is bound; first elements)
Schödel et al. 2002, 2003 (first detailed elements)
Ghez et al 2003 (detailed elements)
Eisenhauer 2005, Gillessen et al. 2009
(improved elements on more stars and distance)

~4 million solar masses
at a distance of
~8.3+-0.3 kpc

Progress expected in determining relativistic effects

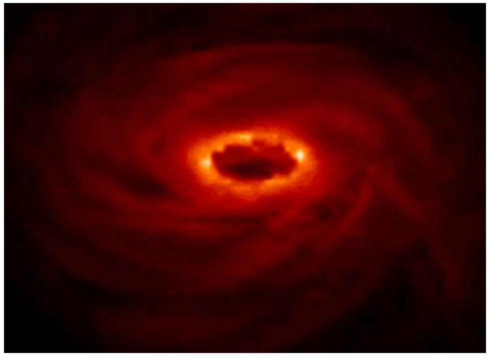

Possible hot spots orbiting SgrA* the detection of strong relativistic effects is complicated by processes in the accretion stream/outflow and relativistic disk effects

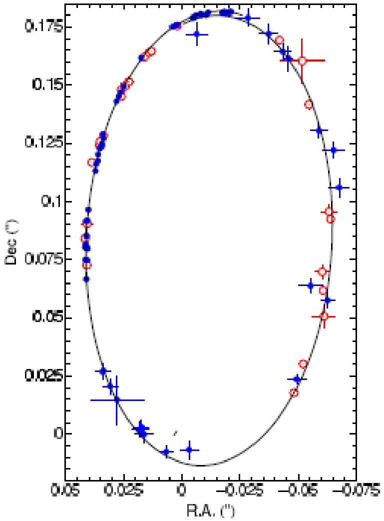

Stars are and remain the preferred (?) probs making use of NIR adaptive optics and interferometric measurments.

It is, however, unclear if there are any *preturbing effects* that may even further complicate the usage of stars for these high precision measurements.

Newtonian and relativistic periastron shift for S2

Newtonian:

retrograde shift $\Delta\phi$

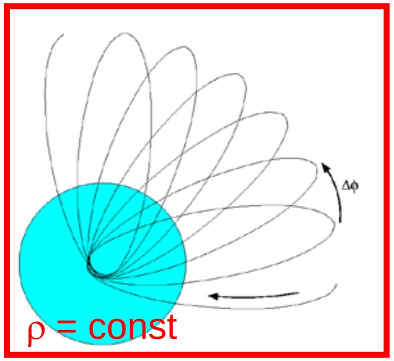

Relativistic:

prograde shift $\Delta\phi$

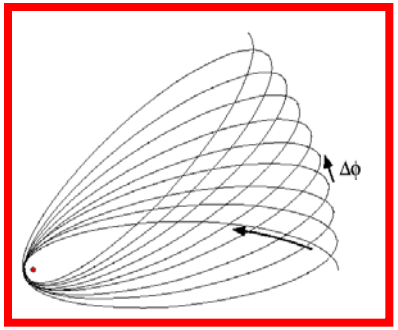

$$\boxed{(\Delta\omega)_{\rm M} = -2\pi G_{\rm M}(e,\gamma)\sqrt{1-e^2}\left[\frac{M_\star(r<a)}{M_\bullet}\right]}$$

$$G_{\rm M} = \left(1+\sqrt{1-e^2}\right)^{-1} \approx 0.68 \text{ for S2}$$

$$(\Delta\omega)_{\rm M} \approx -1.0' \left[\frac{M_\star(r<a)}{10^3\ {\rm M}_\odot}\right]$$

$$\boxed{(\Delta\omega)_{\rm GR} = \frac{6\pi G M_\bullet}{c^2 a(1-e^2)}}$$

$$a = 5.0 \text{ mpc}, \ e = 0.88 \text{ for S2}$$

$$\boxed{(\Delta\omega)_{\rm GR} \approx 10.8'}$$

Several stars are needed to disantangle the two effects.

Rubilar & Eckart 2002
Zucker + 2006;
Gillessen+ 2009;
Sabha + 2012

The high-velocity Galactic Center Stars are important probes for relativistic effects

average orbital distance: $$\langle d \rangle = a(1 + e^2 / 2)$$

ratio to gravitational radius: $$\rho = \frac{\langle d \rangle}{r_g} \qquad r_g = \frac{GM}{c^2}$$

$$\boxed{\frac{\rho_{Mercury}}{\rho_{S2}} \approx 1200}$$

Observed redshift as a function of the 3 dimensional velocity β

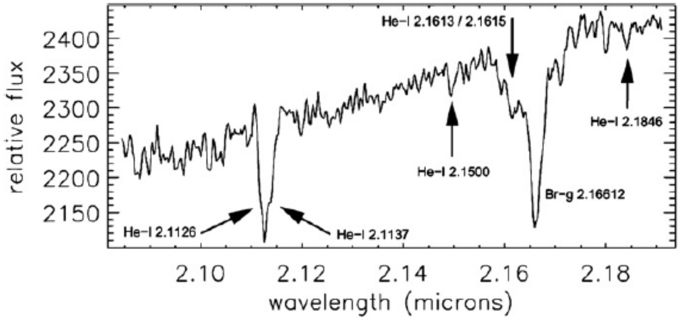

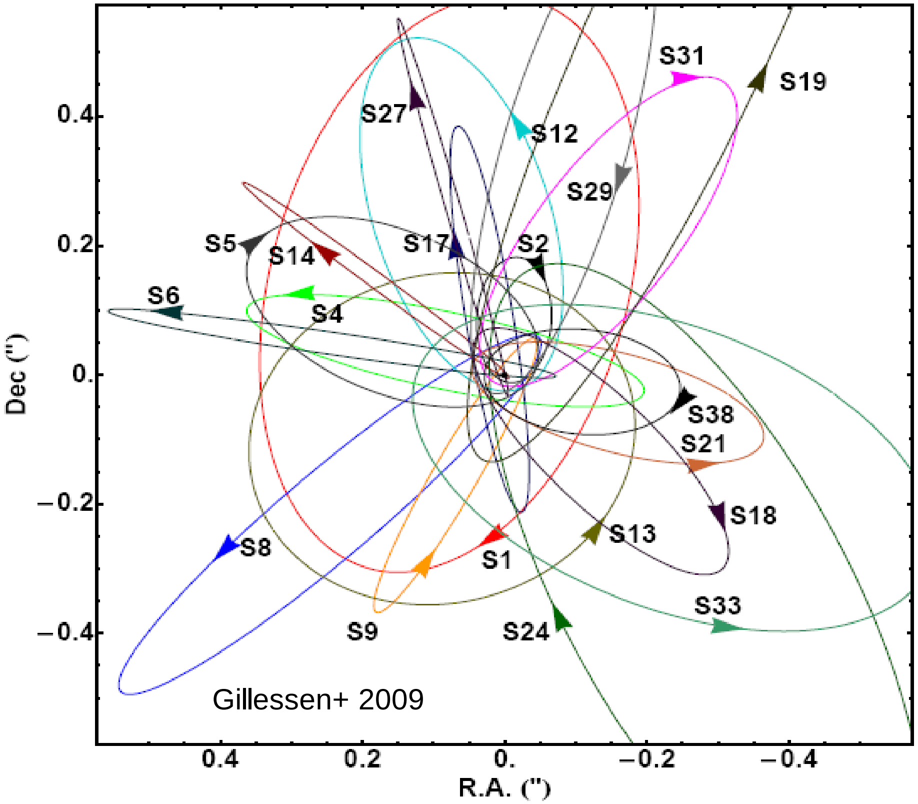

z: redshift

β: 3 dim. velocity

$$z = \Delta\lambda / \lambda = B_0 + B_1\beta + B_2\beta^2 + O(\beta^3)$$

offset ; Doppler; rel. effects

Zucker+ 2006, Gillesen+ 2009

Observed redshift as a function of the 3 dimensional velocity β

$$z = \Delta\lambda / \lambda = B_0 + B_1\beta + \boxed{B_2\beta^2} + O(\beta^3)$$

$$B_2 = B_{2,D} + B_{2,G} = \frac{1}{2} + \frac{1}{2}$$

$B_{2,G}$: gravitational redshift effect

$$z_G \equiv r_s / 4a + \frac{1}{2}\beta^2 = B_{0,G} + B_{2,G}\beta^2$$

$B_{2,D}$: special relativistic transverse Doppler effect

$$z_D \equiv (1 + \beta\cos\vartheta)(1-\beta^2)^{-1/2} - 1$$

$$z_D \equiv z_{Newton} + z_{transverse} = \beta\cos\vartheta + \beta^2 / 2 = B_1\beta + B_{2,D}\beta^2$$

Zucker et al. 2006

$O(\beta^2)-$ effects should be observable with today's instrumentation:

$$(B_{2,D}+B_{2,G})\beta_P^2 \sim 10^{-3} > \frac{\delta\lambda}{\lambda} \sim 10^{-4}$$

$$\beta_P \sim \frac{v_{Peri}}{c}$$

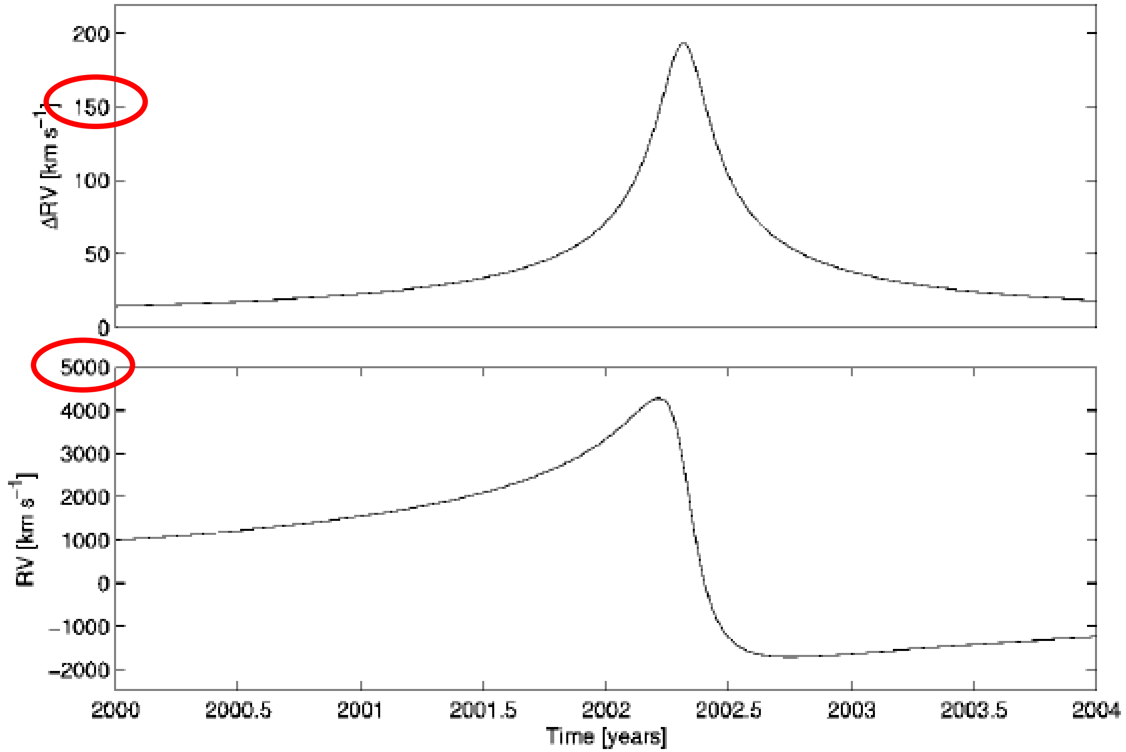

Contribution of the $O(\beta^2)-$ effects

full relativistic radial velocity of S2 near periaps

S2 e=0.88, r = 1500 rs

S14 e=0.94 r = 1400 rs

Zucker et al. 2006

Progress expected in determining relativistic effects

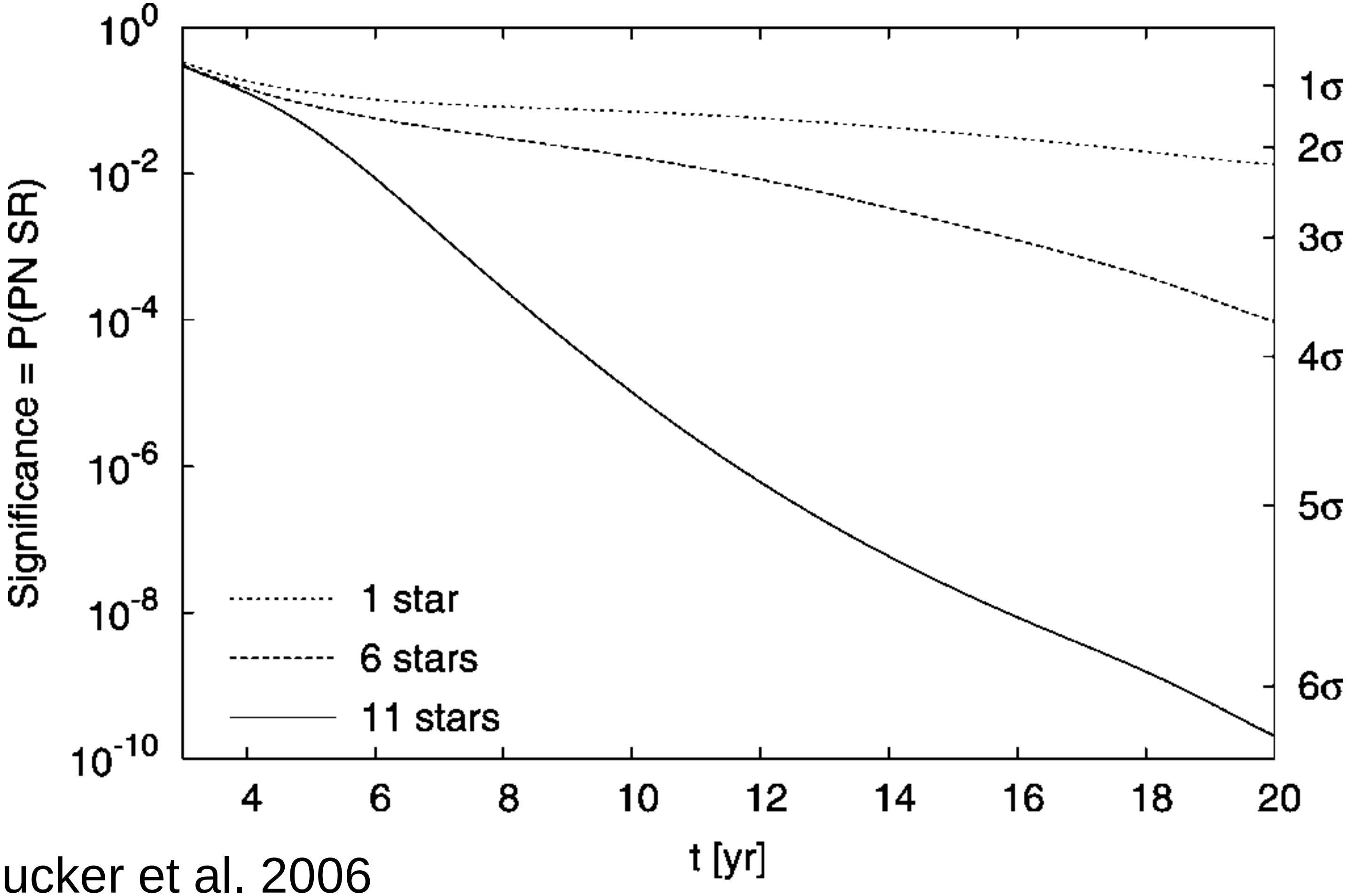

Zucker et al. 2006

For Schwarzschild, Kerr, quadrupol and non-luminous matter contributions see also Iorio 2011, MNRAS

Progress in measuring the orbits

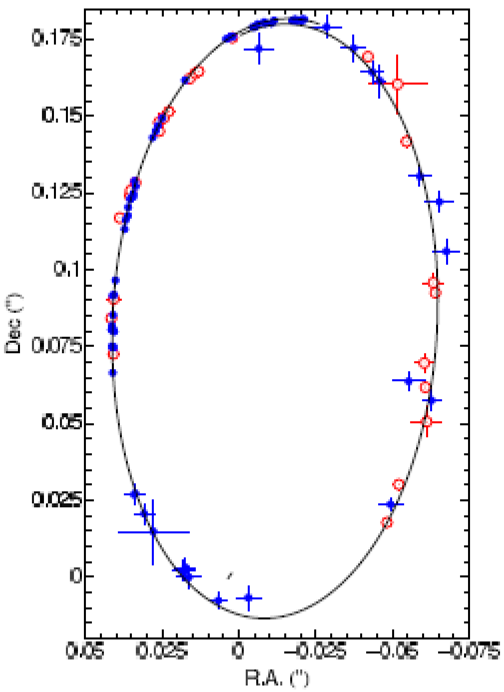

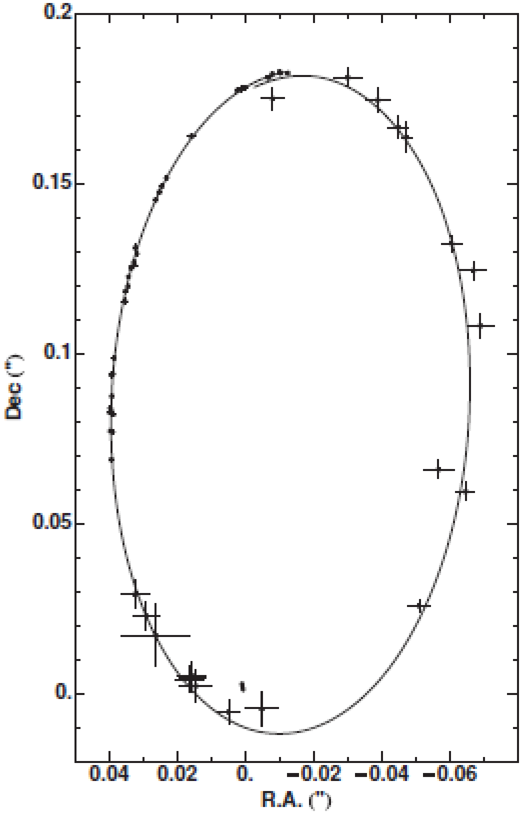

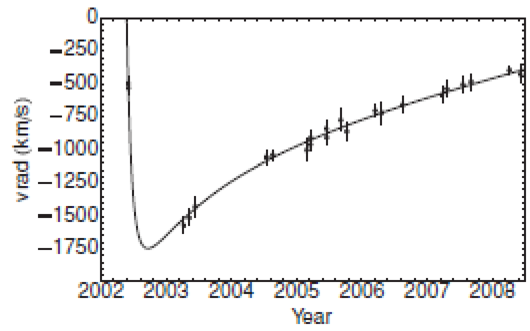

$$T_{orbit} = 15.6 \pm 0.4 yrs$$

$$e = 0.883 \pm 0.003$$

$$a = 0.125 \pm 0.002$$

$$R_0 = 8.28 \pm 0.15|_{\rm stat} \pm 0.29|_{\rm sys}\ {\rm kpc}$$

$$M_{\rm MBH} = 4.30 \pm 0.20|_{\rm stat} \pm 0.30|_{\rm sys} \times 10^6\ M_\odot$$

Gillessen+ 2009

Shortest known period star

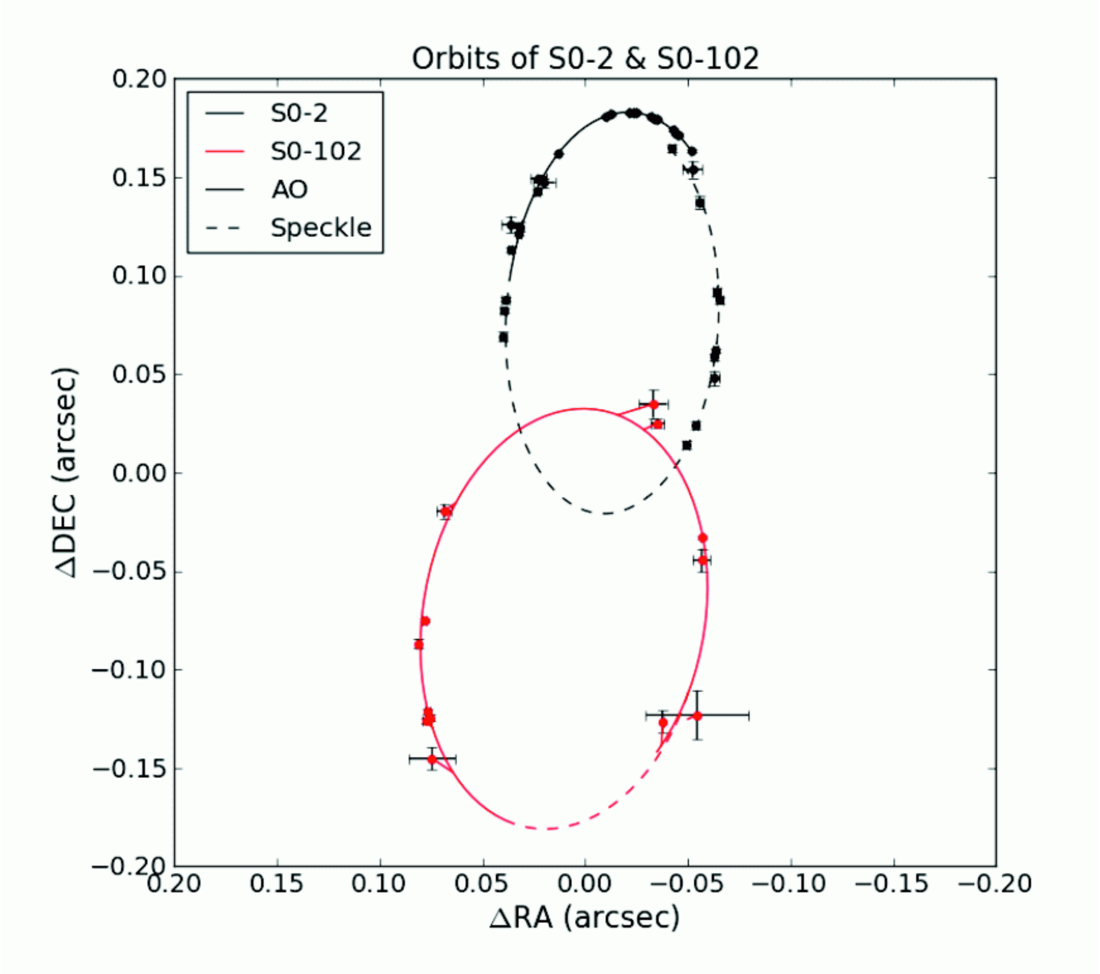

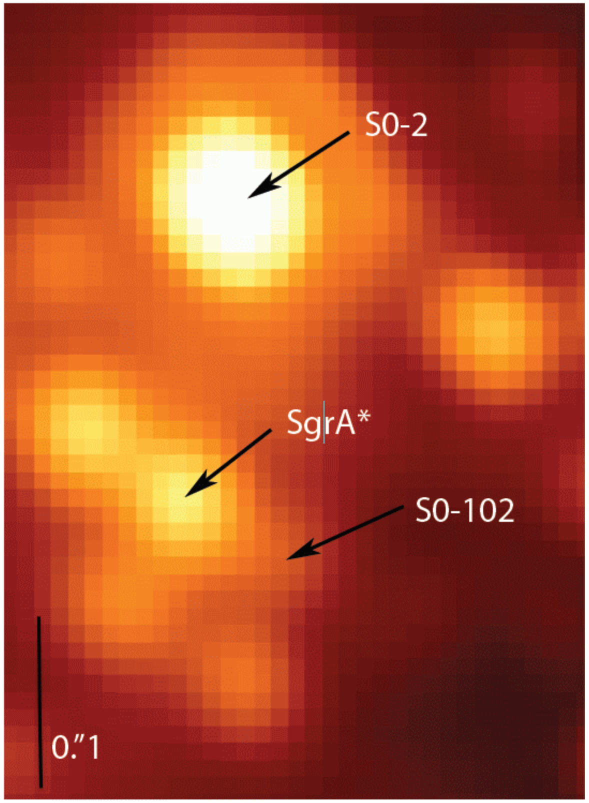

Shortest known period star with 11.5 years available to resolve degeneracies in the parameters describing the central gravitational potential (e=0.68) (Meyer et al. 2012 Sci 338, 84),

Relativity and evolution of S-star orbits

S0-102

$$T_{orbit} = 11.5 \pm 0.3 yrs$$
$$e = 0.68 \pm 0.02$$
$$a = 0.10 \pm 0.01$$

S2

$$T_{orbit} = 15.6 \pm 0.4 yrs$$
$$e = 0.883 \pm 0.003$$
$$a = 0.125 \pm 0.002$$

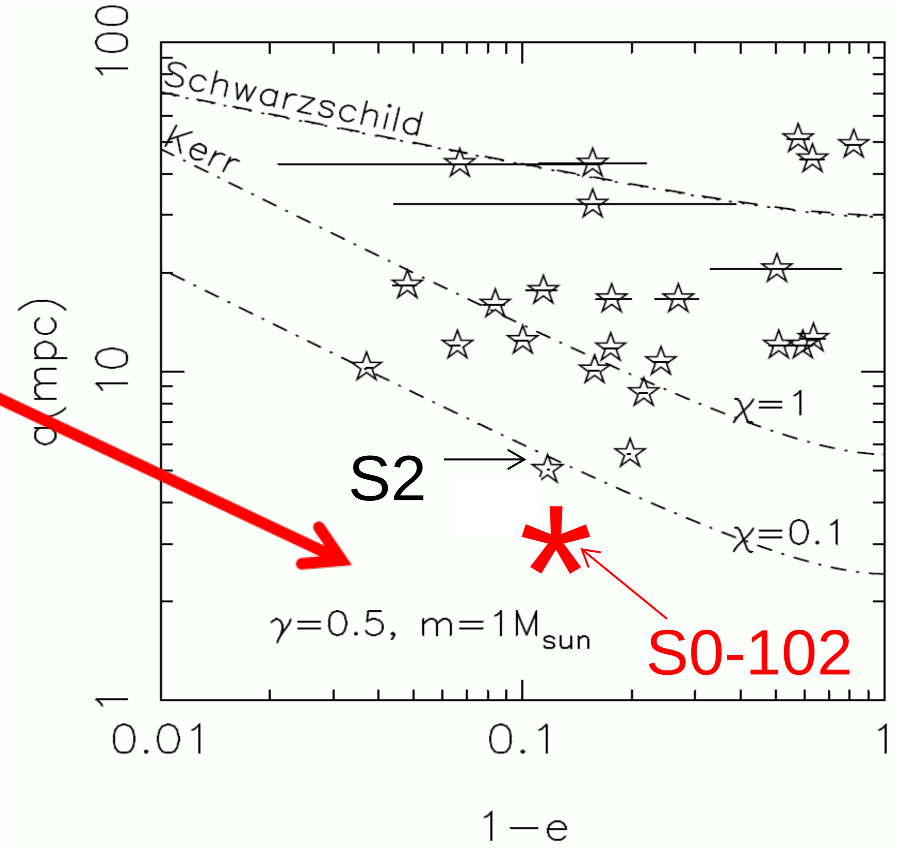

Orbits above (smaller *e*) the Schwarzschild line are subject to resonant relaxation and undergo a random walk in *e* . For stars below that curve the orbital torques of stars with smaller semi-major axis *a* compete with the SMBH torque (along dash-dotted curves with different spin   c).
Antonini & Merritt 2013, ApJ 763 ,L10

Staubquellen innerhalb von 2” of SgrA*

Staubquellen im galaktischen Zentrum

- Der Fall IRS13N
  fortlaufende Sternentstehung im GC?

- Das staubige S-cluster Objekt (DSO)

- Ausfluß und Akkretion

Proper Motions of Dusty Sources within 2” of SgrA*

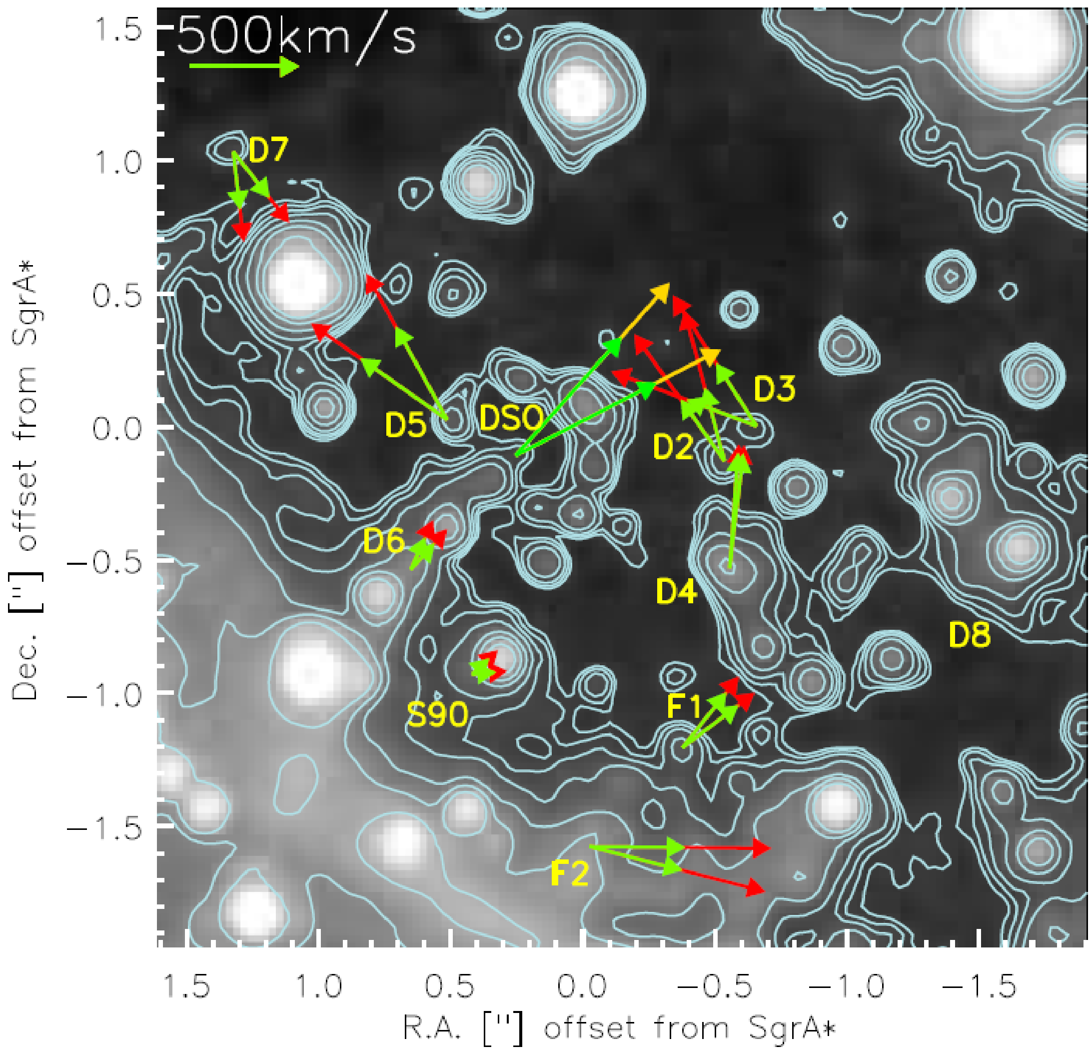

Eckart et al. 2012

Zooming in – towards IRS 13N

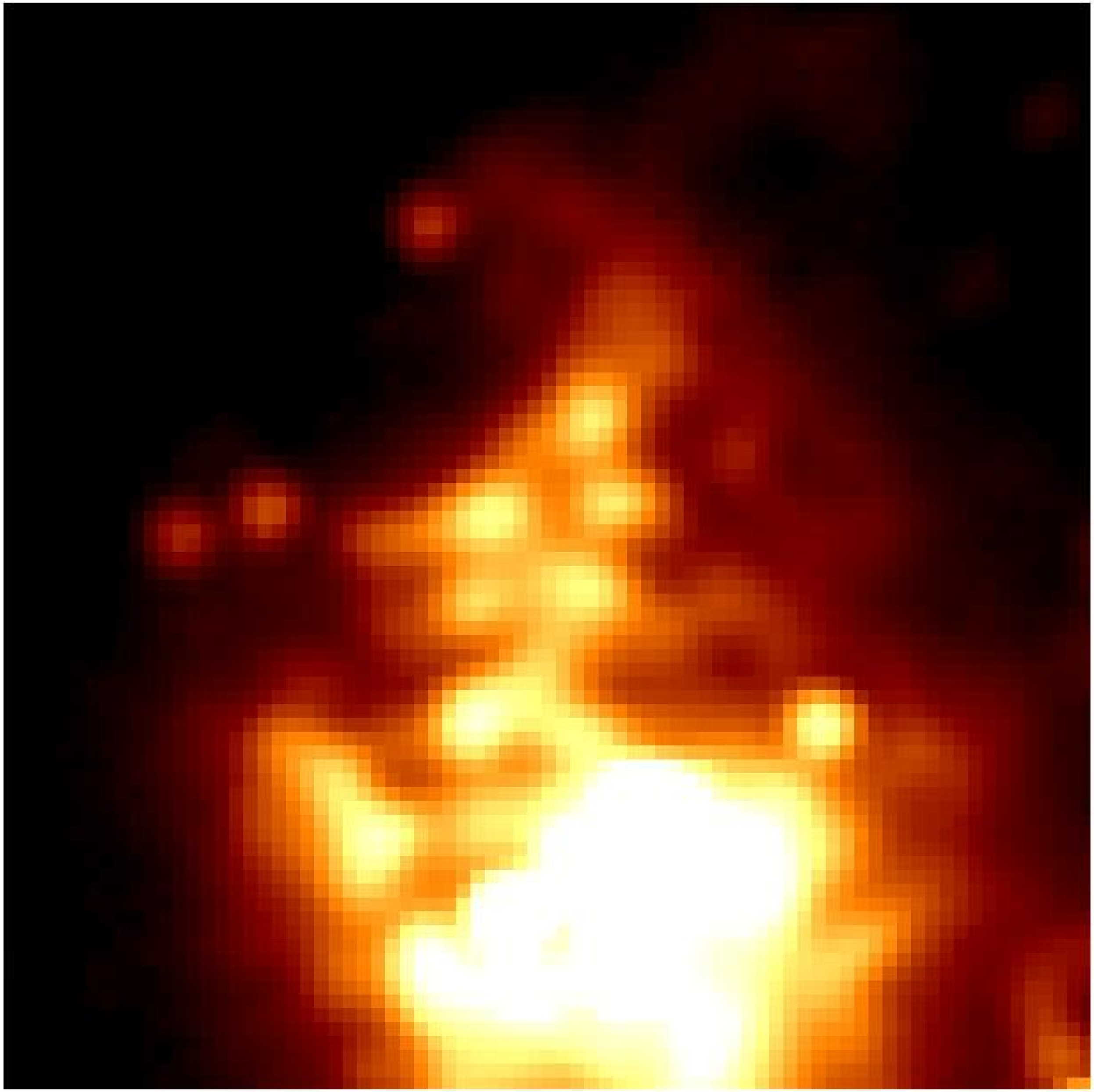

500mas
23 light days

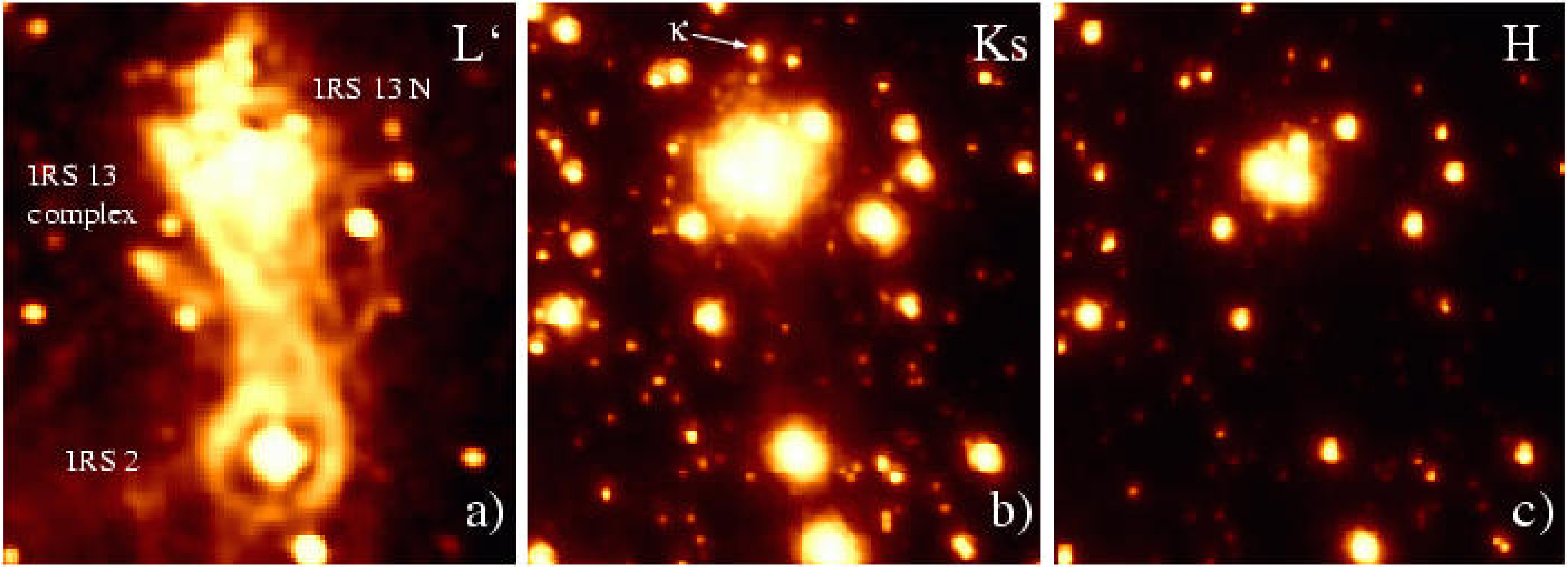

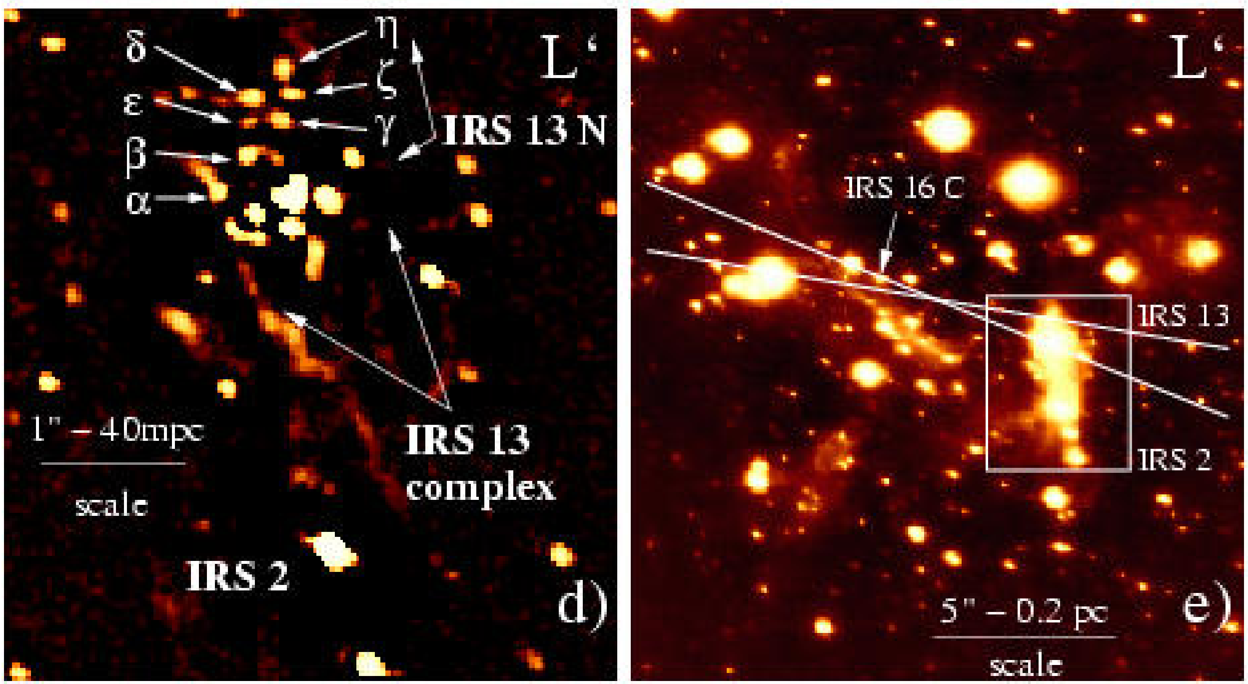

HKL-imaging
of the
IRS13N
complex
with NACO

Eckart et al. 2003

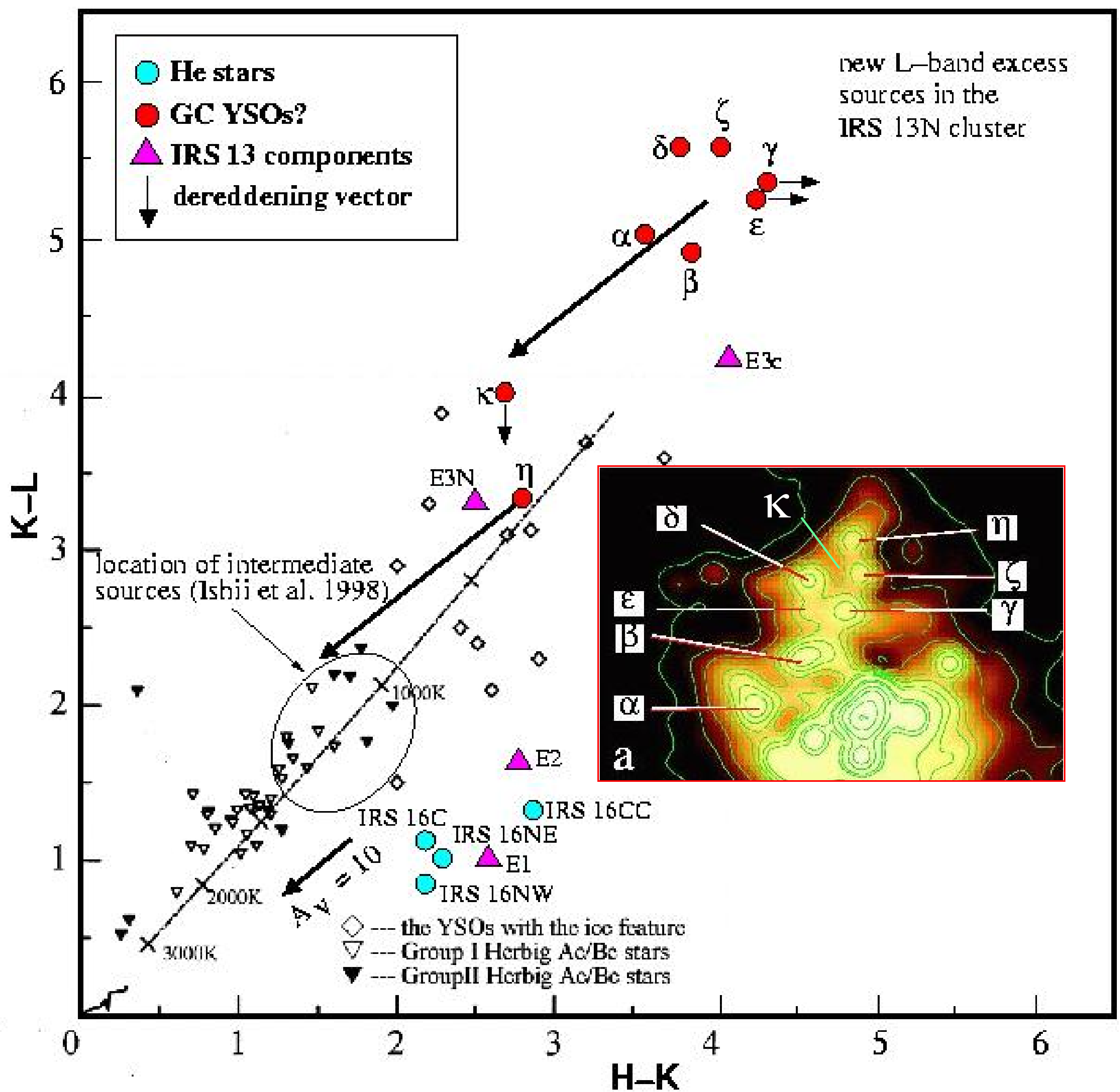

HKL-colors of sources in the IRS13N complex

$L=10^{2}-10^{4}$ Lsol
M=2-8 Msol

Low luminosity bow shock sources.

Are the IRS 13N sources at the GC Herbig Ae/Be stars?

Proper Motions in IRS13N

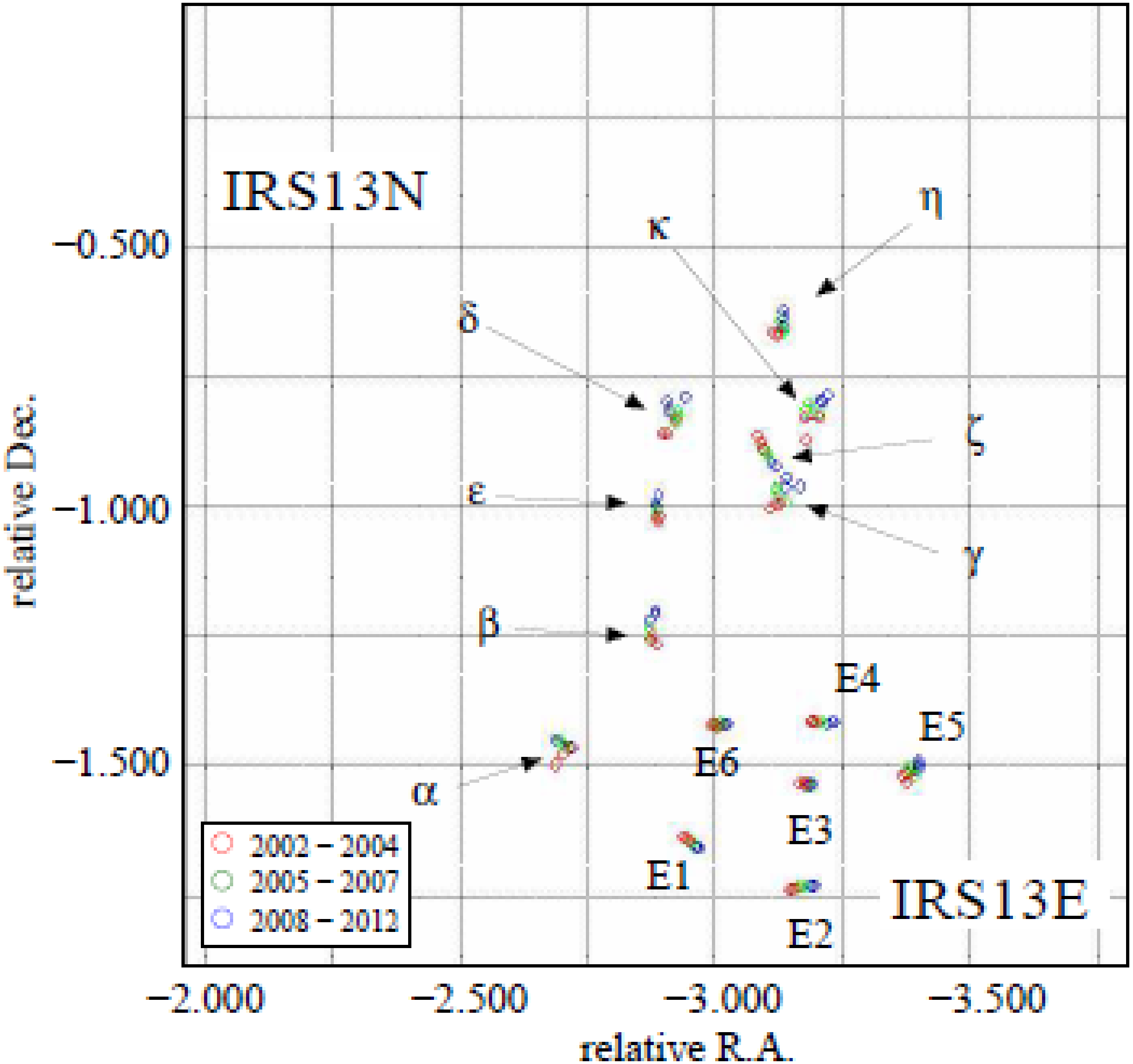

K-band proper motion from red to blue

Eckart et al. 2003, 2012
Muzic et al. 2009

Proper Motions in IRS13N

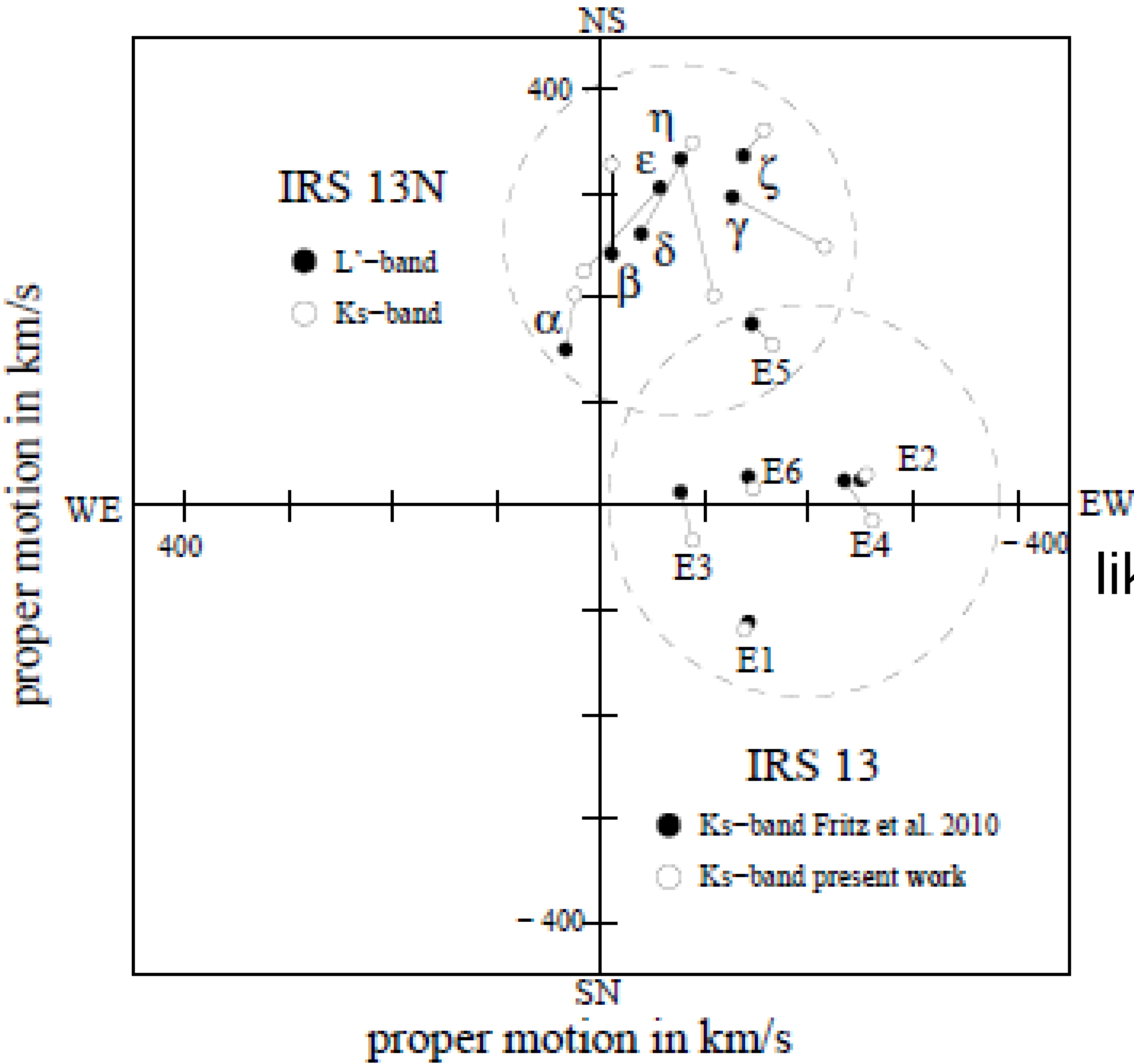

K- and L-band positions and proper motions agree

K-band emission likely to be photospheric e.i. from stars rather than from dust

Eckart et al. 2003, 2012

Muzic et al. 2009

1. Modeling Approach

100 Msun molecular clump,
0.2 pc radius,

Test with 10 & 50 Kelvin,
isothermal gas

Timescales:
clump free fall time ~ 10^5 yr
CND orbital period ~ 10^5 yr

Semi-major axis=1.8 pc →
orbital period ~10^5 yr,

two Orbits:
peri-center~0.1 pc → ecc.= 0.95
peri-center~0.9 pc → ecc.= 0.5

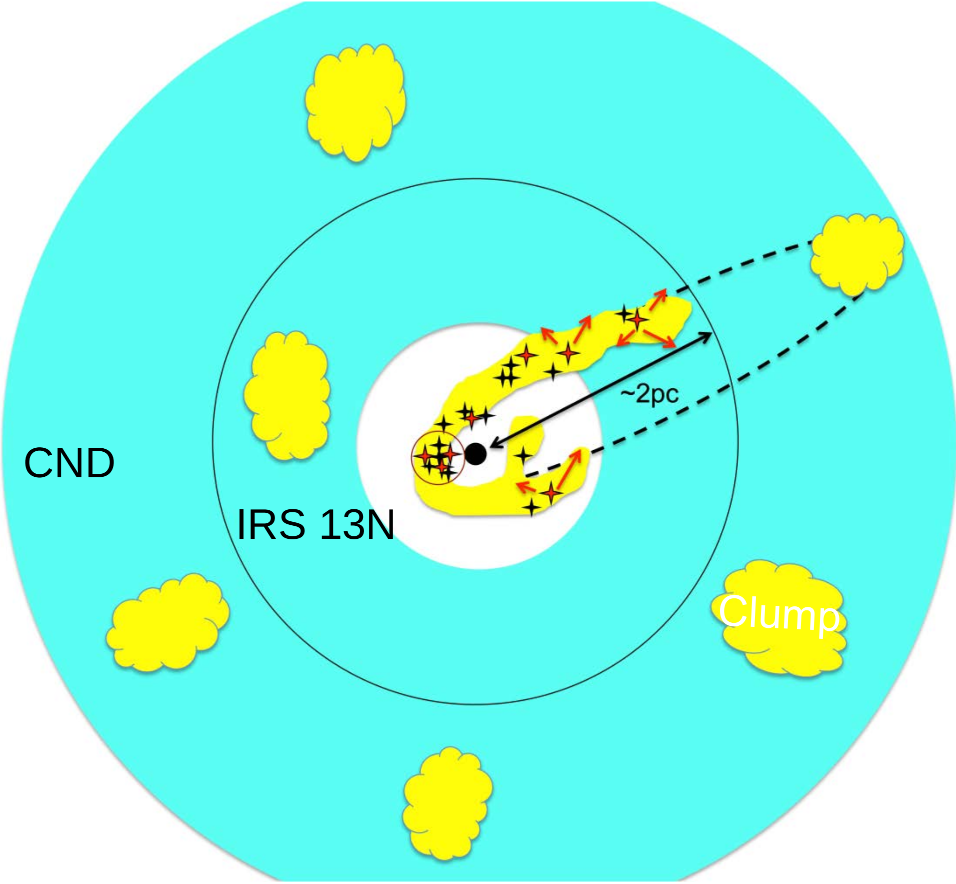

Jalali+2013 in prep.

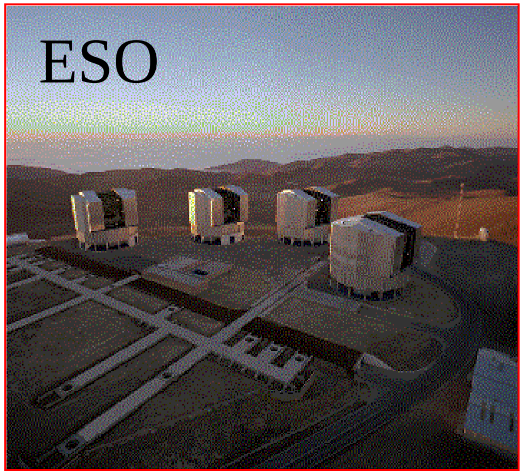

NL leads Euro-Team
Universitity of Cologne
studies for
METIS @ E-ELT

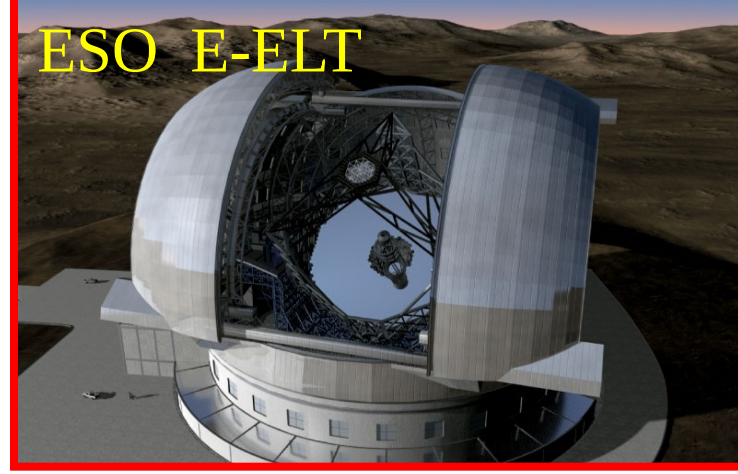

MPE, MPIA, Paris, SIM
Universitity of Cologne
participation
GRAVITY @ VLTI

The Galactic Center is a unique laboratory in which one can study signatures of strong gravity with GRAVITY

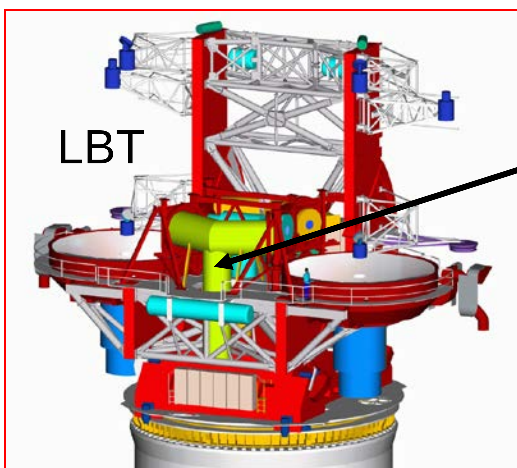

NIR Beam Combiner:
Universitity of Cologne
MPIA, Heidelberg
Osservatorio Astrofisico di Arcetri
MPIfR Bonn

Cologne
contribution to
MIRI on JWST

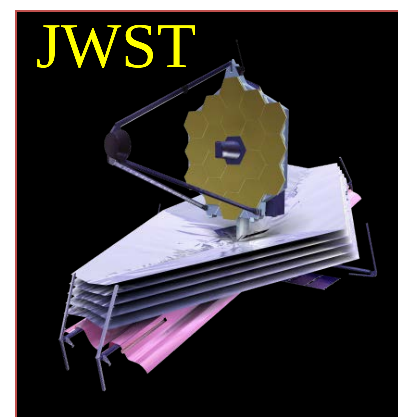

Sgr A*- the galactic center black hole - part 1 C

The COST action "Black Holes in a Violent Universe" (MP-0905) organizes a Summer School on "Black Holes at all scales Ioannina, Greece, September 16 and 18

Andreas Eckart

I.Physikalisches Institut der Universität zu Köln

Max-Planck-Institut für Radioastronomie, Bonn

STRONGGRAVITY EU FP7-SPACE research project 312789 2013 - 2017

SEVENTH FRAMEWORK PROGRAMME

Max-Planck-Institut für Radioastronomie

14:30-16:00 Part I: Observational methods to study the Galactic Center – SgrA and its environment CND/mini-spiral/central stellar cluster - dust sources in the central few arcseconds*

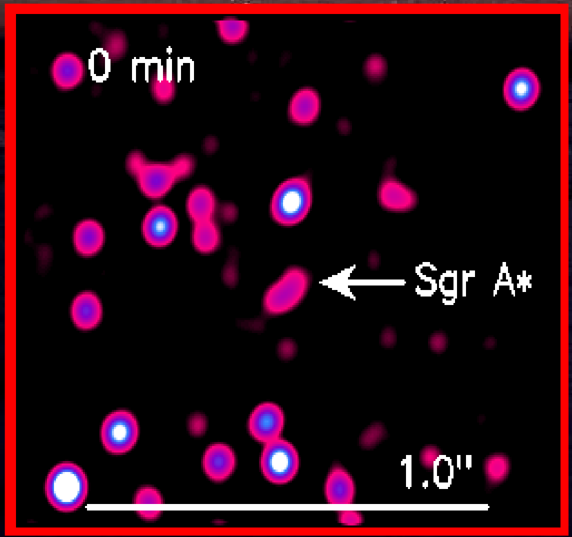

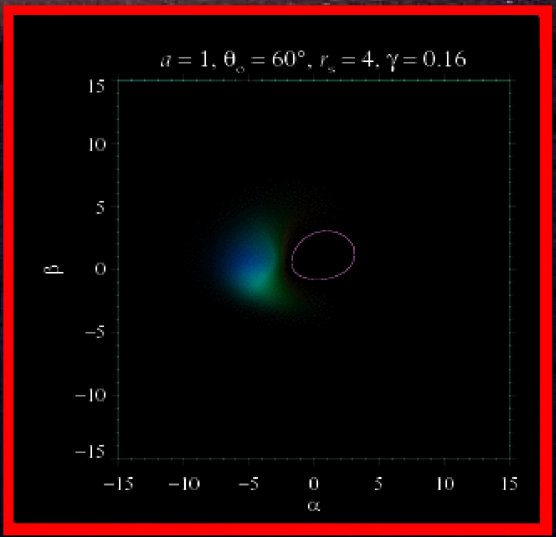

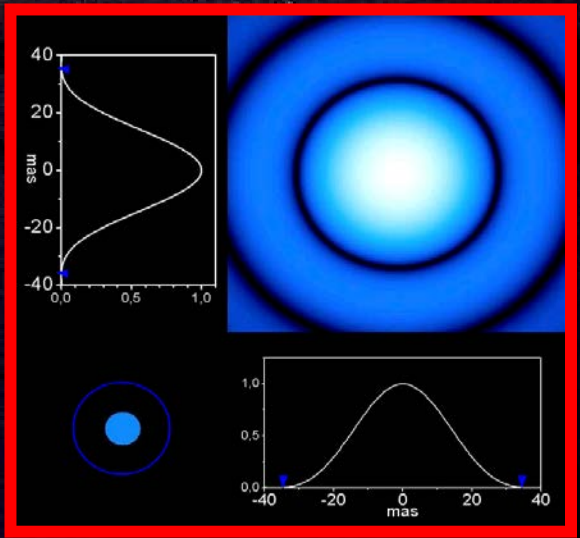

The Evironment of SgrA*

Orbital motion of high-velocity S-stars

On the possibility to detect relativistic and Newtonian peri-center shifts

- Granularity of scatterers
- Search for stellar probes

The Center of the Milky Way

Closest galactic genter at 8 kpc
High extinktion of Av=30 Ak=3
Stars can only be seen in the NIR

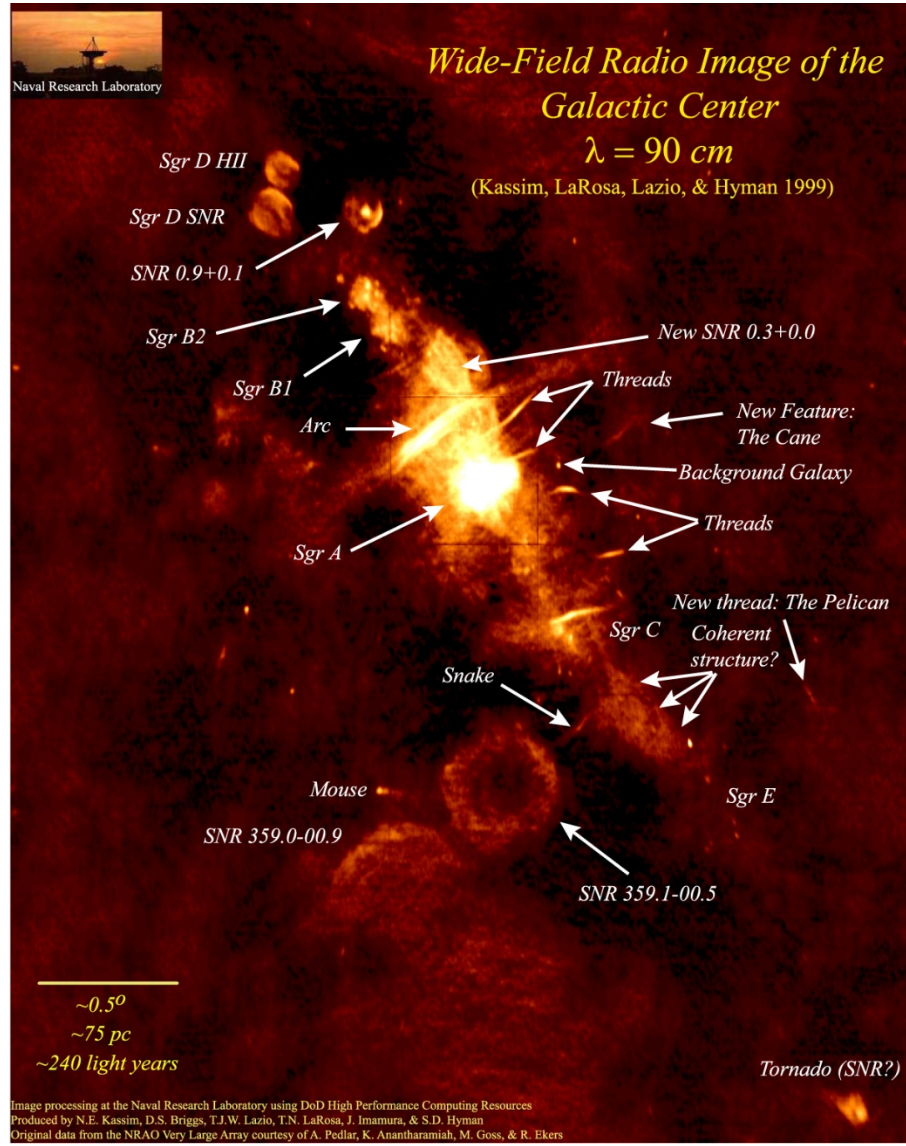

VLA 90cm

Kassim, Briggs, Lasio, LaRosa, Imamura, Hyman

SgrA* and its Environment

Orbits of High Velocity Stars
in the Central Arcsecond

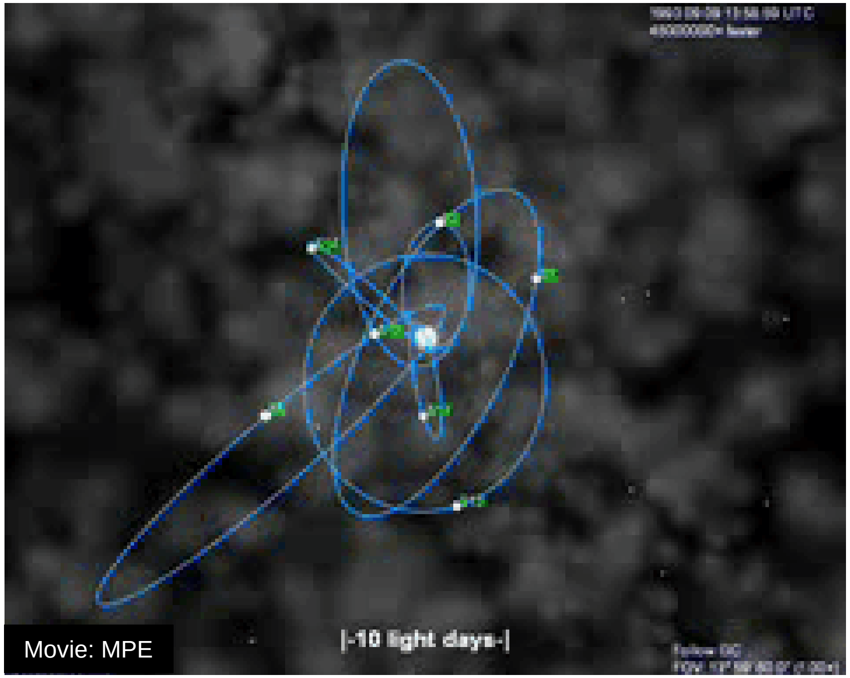

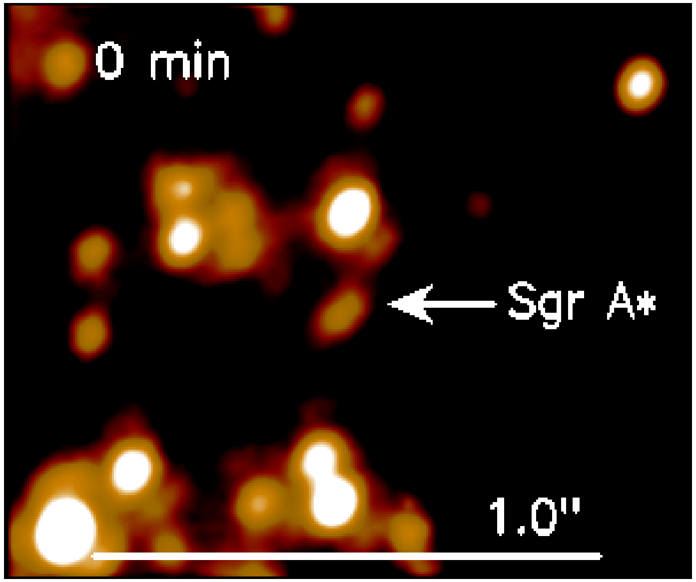

Eckart & Genzel 1996/1997 (first proper motions)
Eckart et al. 2002 (S2 is bound; first elements)
Schödel et al. 2002, 2003 (first detailed elements)
Ghez et al 2003 (detailed elements)
Eisenhauer 2005, Gillessen et al. 2009
(improved elements on more stars and distance)

~4 million solar masses
at a distance of
~8.3+-0.3 kpc

Progress in measuring the orbits

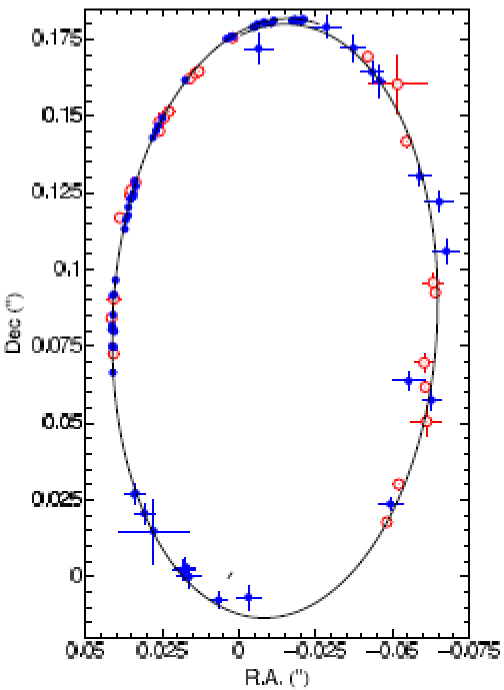

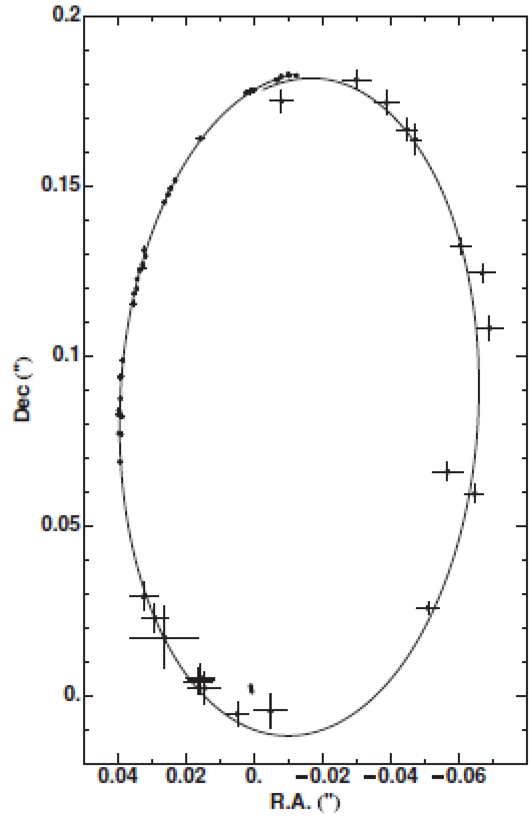

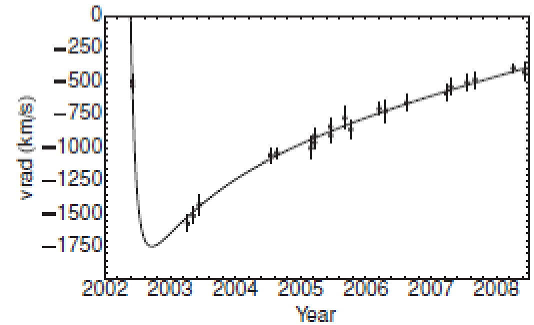

$$T_{orbit} = 15.6 \pm 0.4 yrs$$

$$e = 0.883 \pm 0.003$$

$$a = 0.125 \pm 0.002$$

$$R_0 = 8.28 \pm 0.15|_{\mathrm{stat}} \pm 0.29|_{\mathrm{sys}}\ \mathrm{kpc}$$

$$M_{\mathrm{MBH}} = 4.30 \pm 0.20|_{\mathrm{stat}} \pm 0.30|_{\mathrm{sys}} \times 10^6\ M_{\odot}$$

Gillessen+ 2009

Shortest known period star

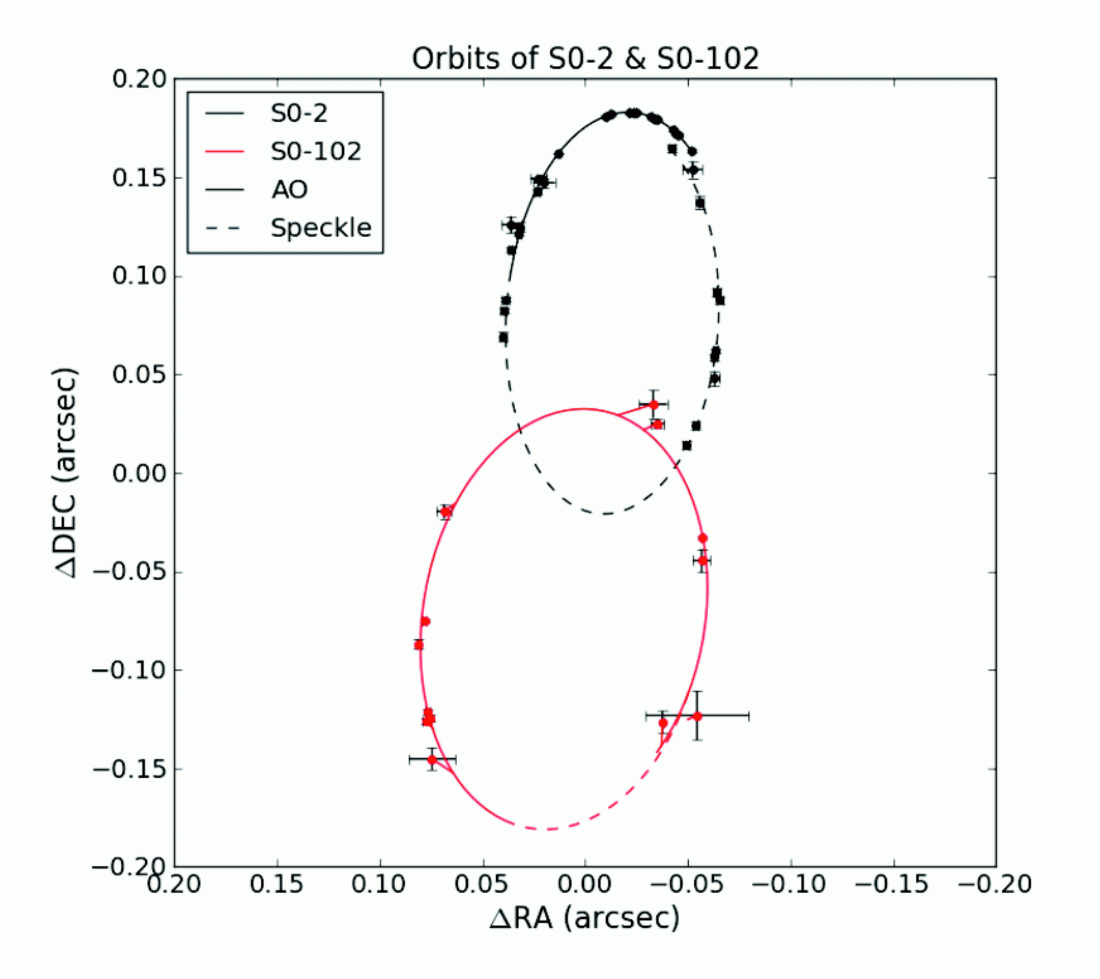

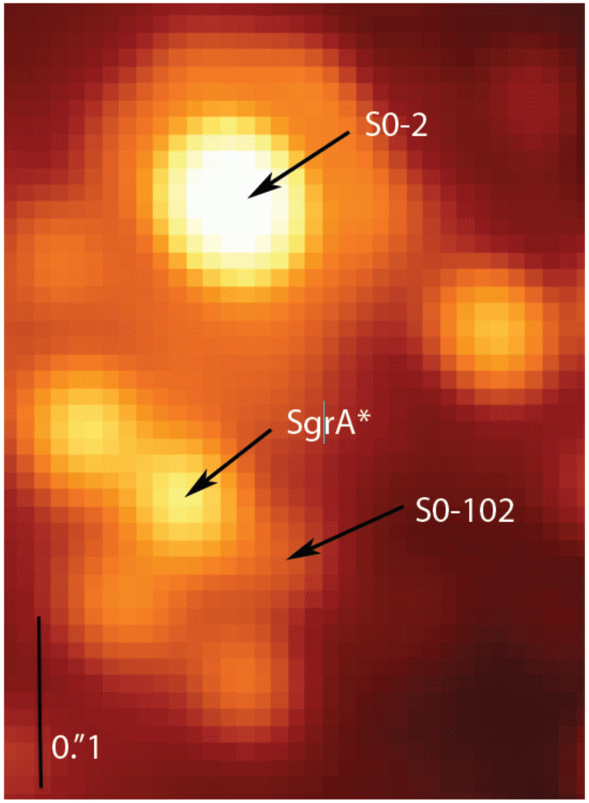

Shortest known period star with 11.5 years available to resolve degeneracies in the parameters describing the central gravitational potential (e=0.68) (Meyer et al. 2012 Sci 338, 84),

Bestimmung der Masse über S2

Für S2 ist der etwa 15 jährige Orbit geschlossen.
Die Kepler'schen Gesetze ergeben:

$$\boxed{M_{S2} = \frac{4\pi^2}{G}\frac{a^3}{T^2}}$$

mit der Umlaufzeit **T** und der großen Halbachse **a.**

Für S2 ergibt das::

$$\boxed{M_{SgrA*} \approx (4 \pm 0.3) \times 10^6 M_o}$$

Man kann gleichzeitig für die Entfernung lösen und erhält: 7.7+/-0.3 kpc

Eisenhauer et al. 2005

The Evironment of SgrA*

Orbital motion of high-velocity S-stars

On the possibility to detect relativistic and Newtonian peri-center shifts

- Granularity of scatterers
- Search for stellar probes

BH density in a dynamical core

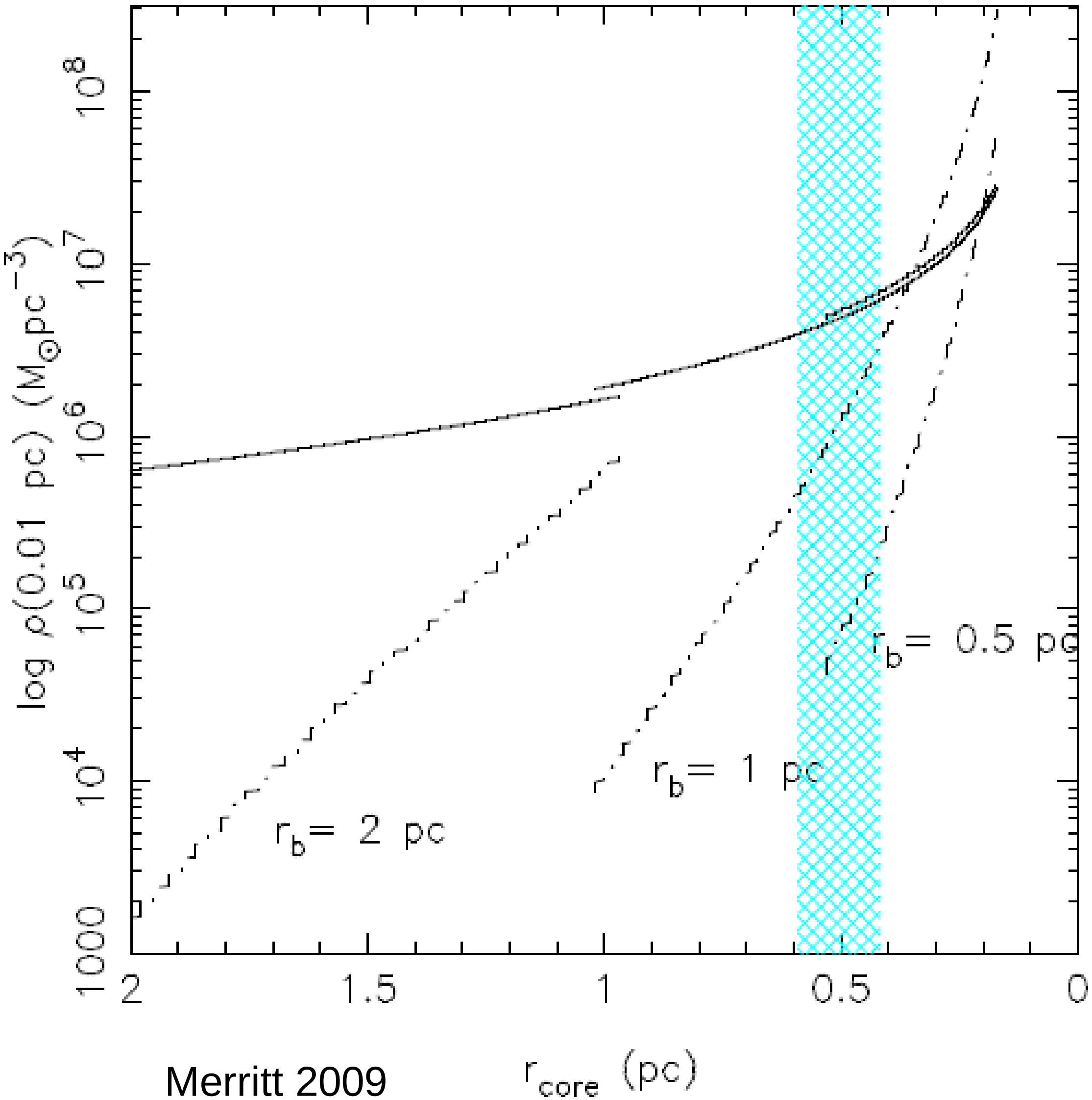

Merritt 2009

The stellar BH density is expected to be largest at a radius of a few 0.1 pc.

Most authors claim a ~10 Msol population of black holes residing at the 'bottom' of the central potential well

Chandra observations by Muno, Baganoff + 2008, 2009

and simulations by Freitag et al. 2006 Merritt 2009

The Effect of Resonant Relaxation

$$\frac{|\Delta \mathbf{L}|}{L_c} \approx K\sqrt{N}\frac{m}{M_\bullet}\frac{\Delta t}{P}$$

change of torque due to filed stars

$$L_c = \sqrt{GM_\bullet a}$$

Equivalent angular momentum of test star on circular orbit

Changes in L over Δt imply changes in e and orbital plane anges:

$$\cos(\Delta\theta) = \frac{\mathbf{L}_1 \cdot \mathbf{L}_2}{L_1 L_2}$$

Resonant relaxation:

$$|\Delta e|_{\mathrm{RR}} \approx K_e\sqrt{N}\frac{m}{M_\bullet},$$

$$(\Delta\theta)_{\mathrm{RR}} \approx 2\pi K_t\sqrt{N}\frac{m}{M_\bullet}$$

Rauch & Tremaine 1996
Hopeman & Alexander 2006
Merritt et al. 2010

Two stellar populations
Species 1 smooth
Species 2 perturbing

$$(\Delta\theta)_{RR} = K_t\left[\frac{m_1\sqrt{N_1} + m_2\sqrt{N_2}}{M_\bullet}\right]$$

Sabha, Eckart, Merritt et al. 2012

Average values of the changes in Δω, Δθ, Δe and for S2 over one orbital period (~16 yr) in the N-body integrations.

Filled circles are from integrations with m = 50 M⨀ and open circles are for m = 10 M⨀ ; number of field stars N = {25, 50, 100, 200} for both m. The abscissa is the distributed mass within S2's apo-apsis, at r =9.4 mpc. In each frame, the points are median values from the 100 N-body integrations.

(a) Changes in the argument of peri-bothron. The contribution from relativity has been subtracted.
(b) Changes in the eccentricity. Solid and dashed lines are with m = 50 M⨀ and m = 10 M⨀, respectively.
(c) The angle between initial and final values of L i.e. Δθ for S2. .

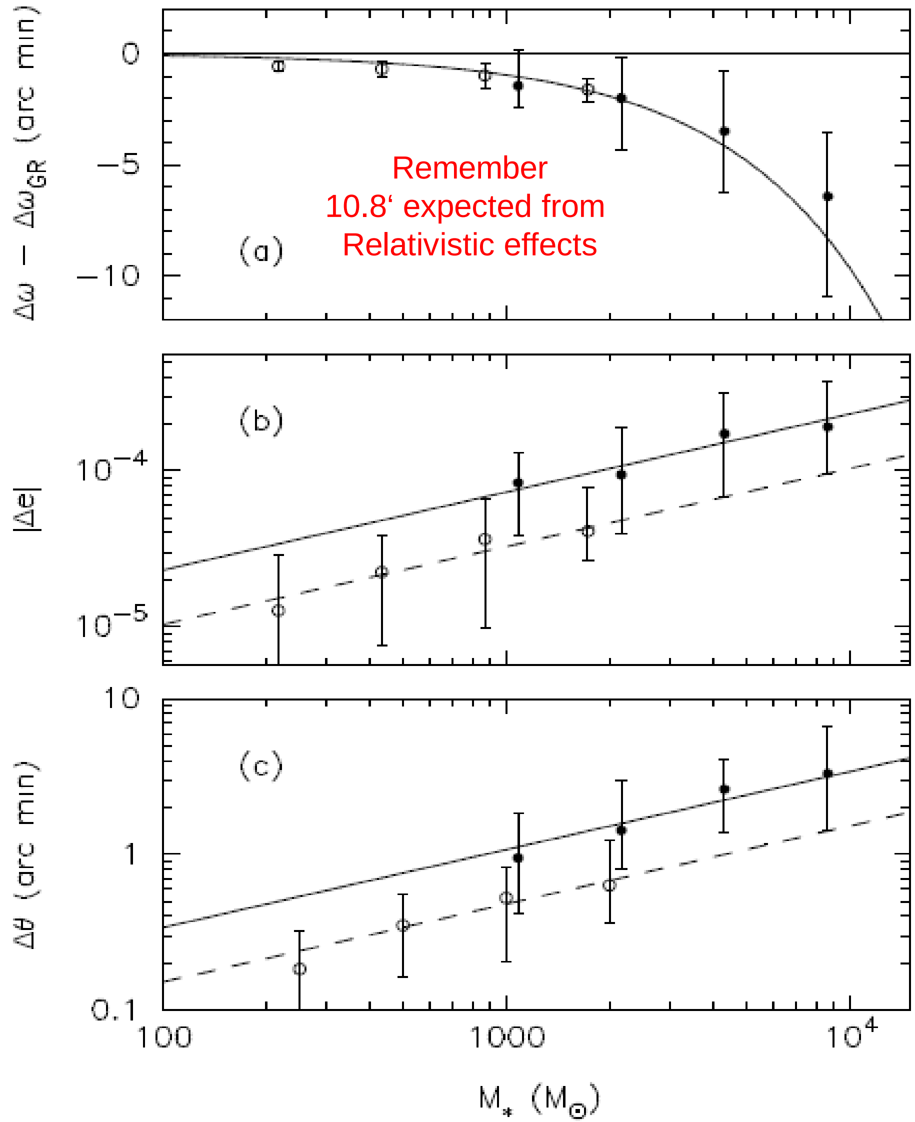

Sabha et al. 2012

Histograms of the predicted peri-bothron change of S2 over one orbital period (~16 yr).

The shift due to relativity (~11′), has been subtracted. What remains is due to Newtonian perturbations (peri-bothron shift and pertrubation/scattering) from the field stars.

$$\frac{|\Delta \mathbf{L}|}{L_c} \approx K\sqrt{N}\frac{m}{M_\bullet}\frac{\Delta t}{P}$$

$$|\Delta e|_{\mathrm{RR}} \approx K_e\sqrt{N}\frac{m}{M_\bullet},$$

$$(\Delta\theta)_{\mathrm{RR}} \approx 2\pi K_t\sqrt{N}\frac{m}{M_\bullet}$$

Resonant relaxation:

Rauch & Tremaine 1996
Hopeman & Alexander 2006
Merritt et al. 2010

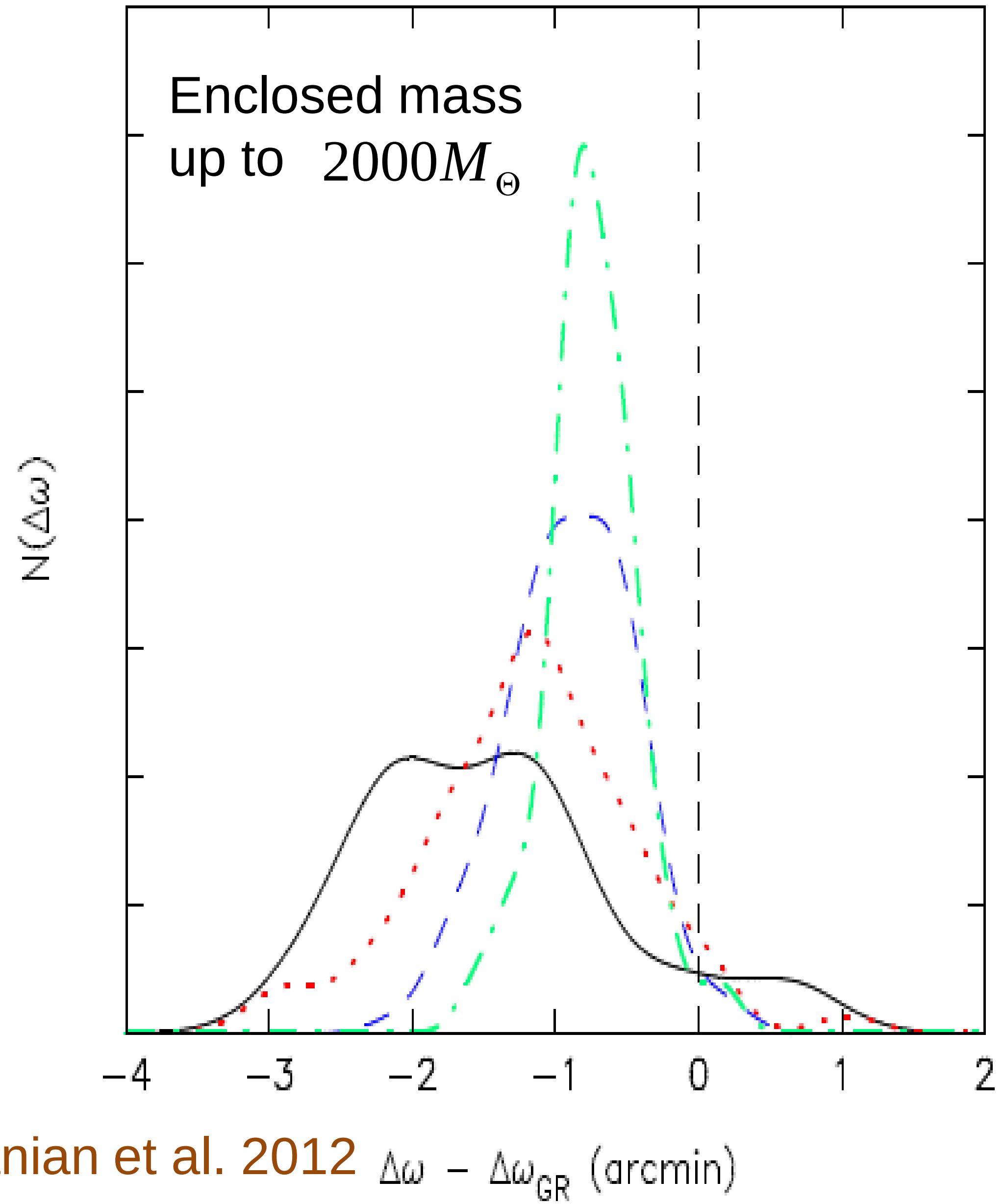

Sabha, Eckart, Merritt, Shahzamanian et al. 2012

Newtonian and relativistic periastron shift for S2

$$m_1 = 1\ \mathrm{M}_\odot, \quad m_2 = 10\ \mathrm{M}_\odot, \quad \boxed{N_1 = 10^4,} \quad N_2 = 1500$$

$$|\Delta e|_{\mathrm{RR}} \approx 1.7 \times 10^{-4}$$
$$(\Delta\theta)_{\mathrm{RR}} \approx 3'.0.$$

$$m_1 = 1\ \mathrm{M}_\odot, \quad m_2 = 10\ \mathrm{M}_\odot, \quad \boxed{N_1 = 10^5,} \quad N_2 = 15000$$

mass composition
following
Freitag et al. 2006

$$|\Delta e|_{\mathrm{RR}} \approx 5.4 \times 10^{-4}$$
$$(\Delta\theta)_{\mathrm{RR}} \approx 8'.0.$$

Significant contributions to perisatron shift $\Delta\omega$
from encounters
due to granulartiy of ‘scattering‘ population $\Delta\theta$: $\propto \sqrt{N_2}$
and
variation in enclosed mass due to scattering population: $\propto \sqrt{N_2}$

The variance in for S2 for one orbital period (~16 yr) in the N-body integrations.

Relative variance of peri-center shift as the absolute variance over the shift itself.

The absolute variance is large and of the order of the entire peri-center shift.

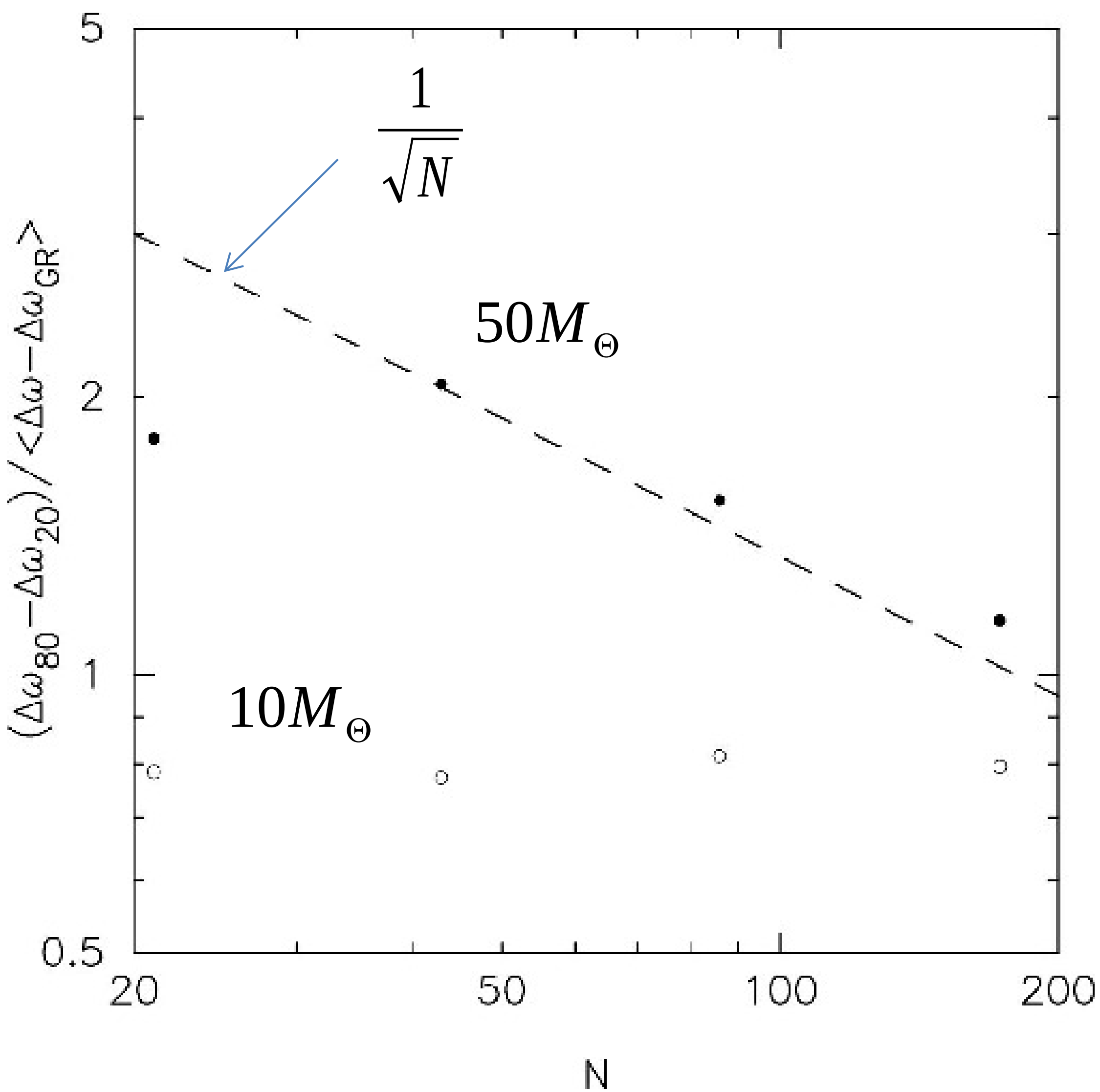

The Evironment of SgrA*

Orbital motion of high-velocity S-stars

On the possibility to detect relativistic and Newtonian peri-center shifts

- Granularity of scatterers
- Search for stellar probes

Subtraction of stars within R<0.7”

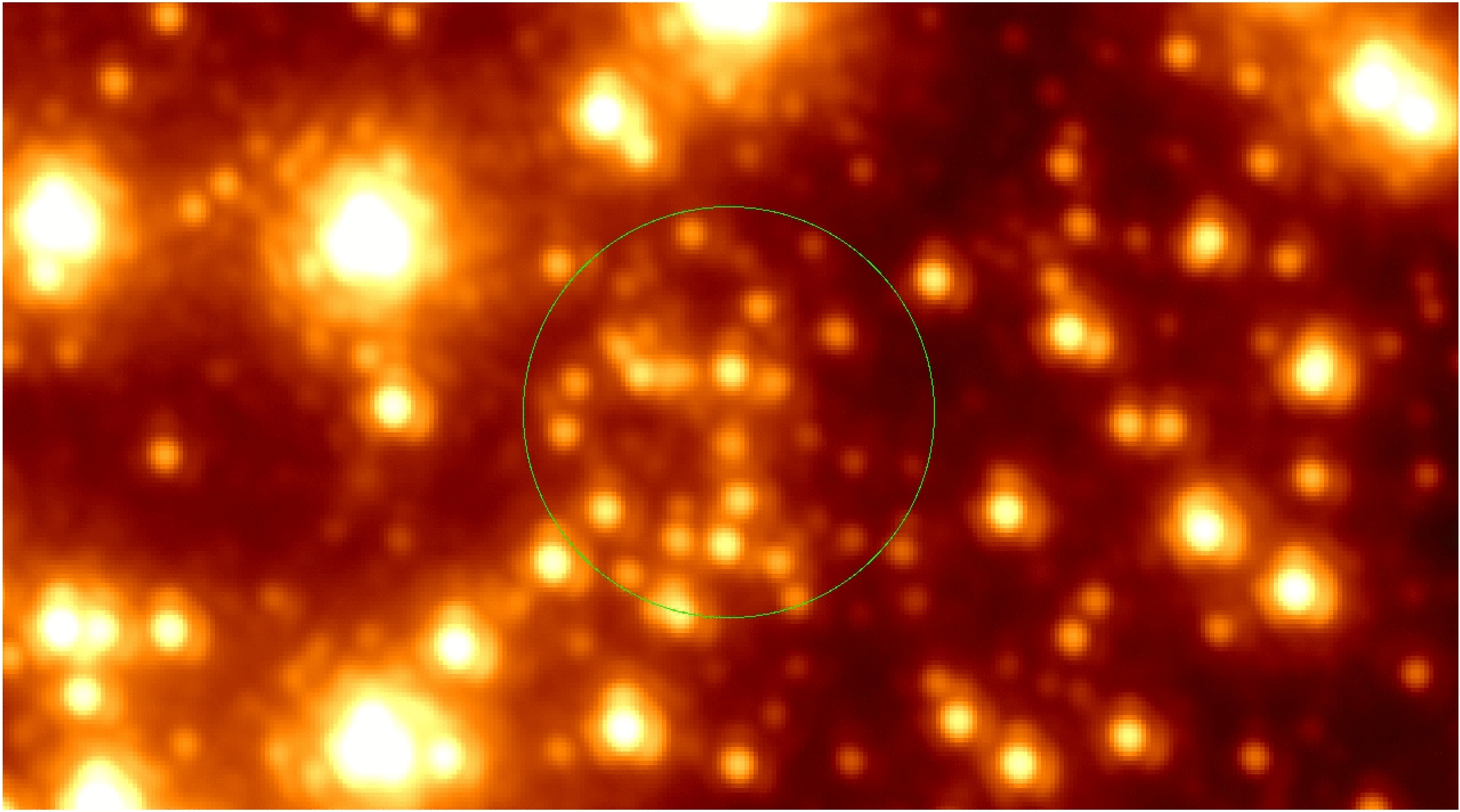

S<1mJy in the NIR K-band

Sabha et al. 2010

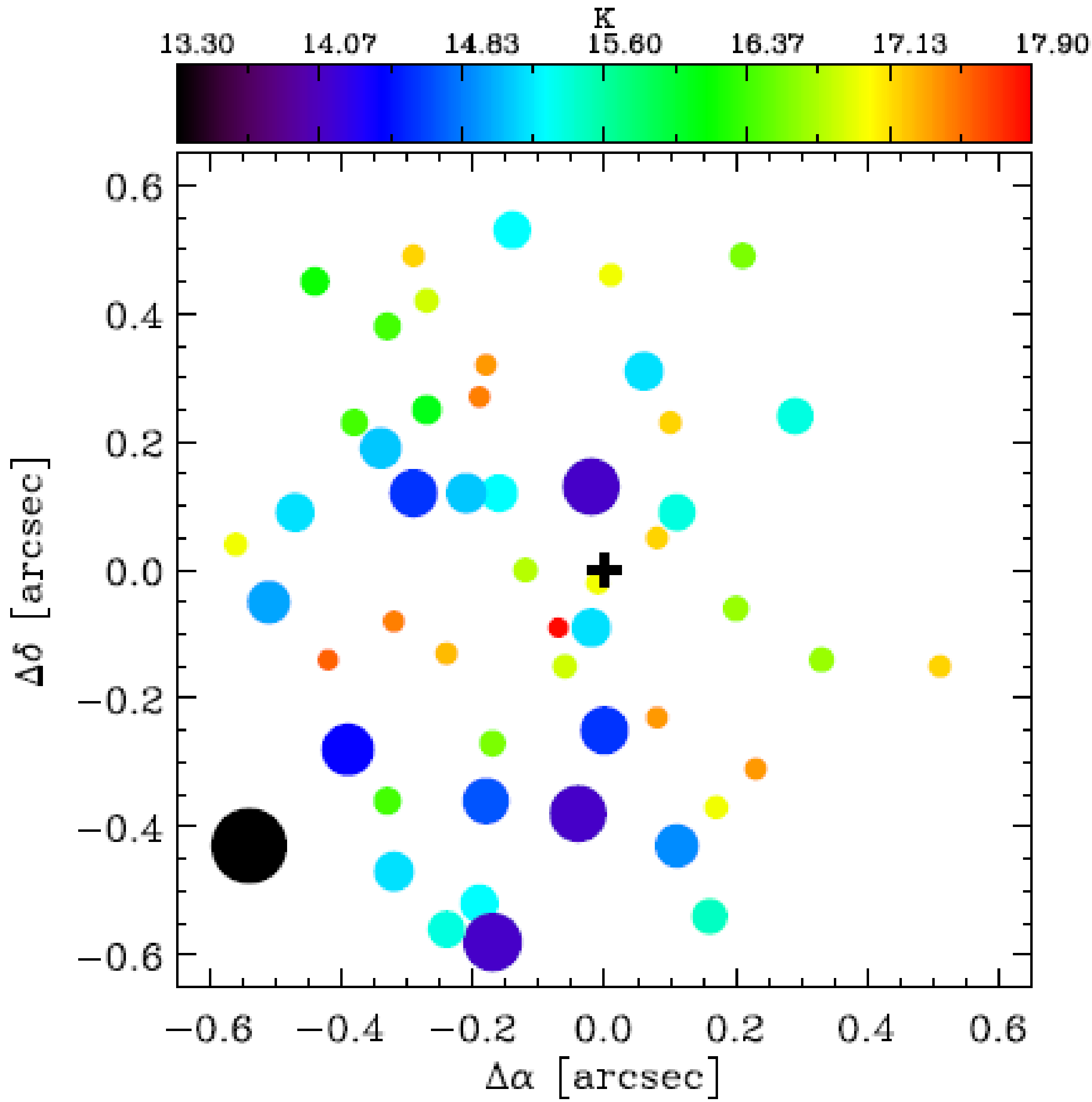

Map of the 51 brightest stars close to SgrA*. The color of each star indicates its K-magnitude. The size of each symbol is proportional to the flux of the corresponding star. The position of Sgr A* is indicated as a cross at the center

Sabha et al. 2012

The Central S-star Cluster

luminosity function exp(-Γ)

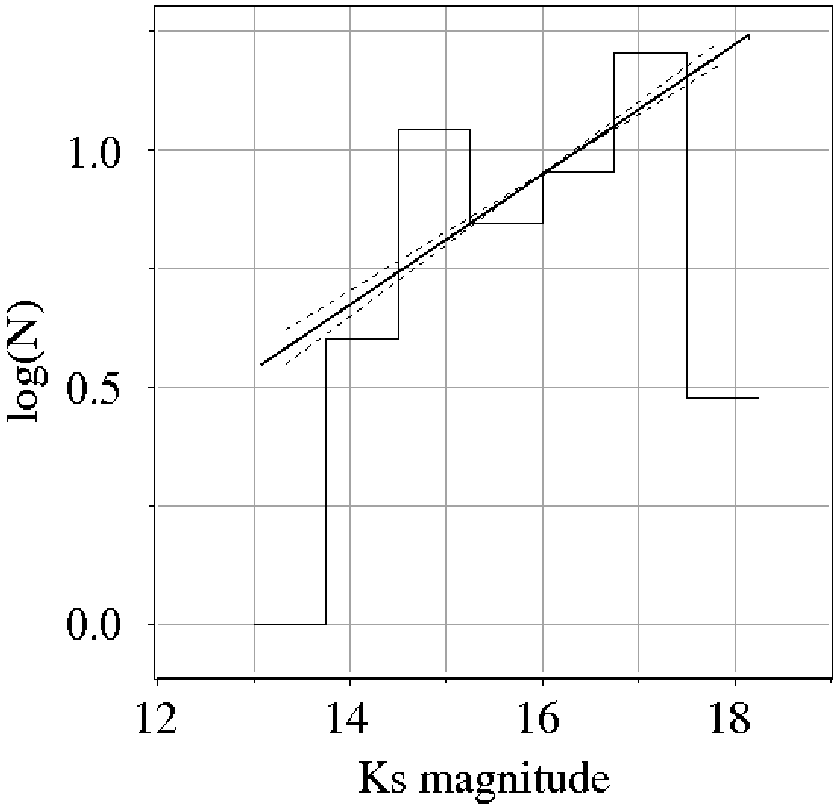

radial distribution exp(-α)

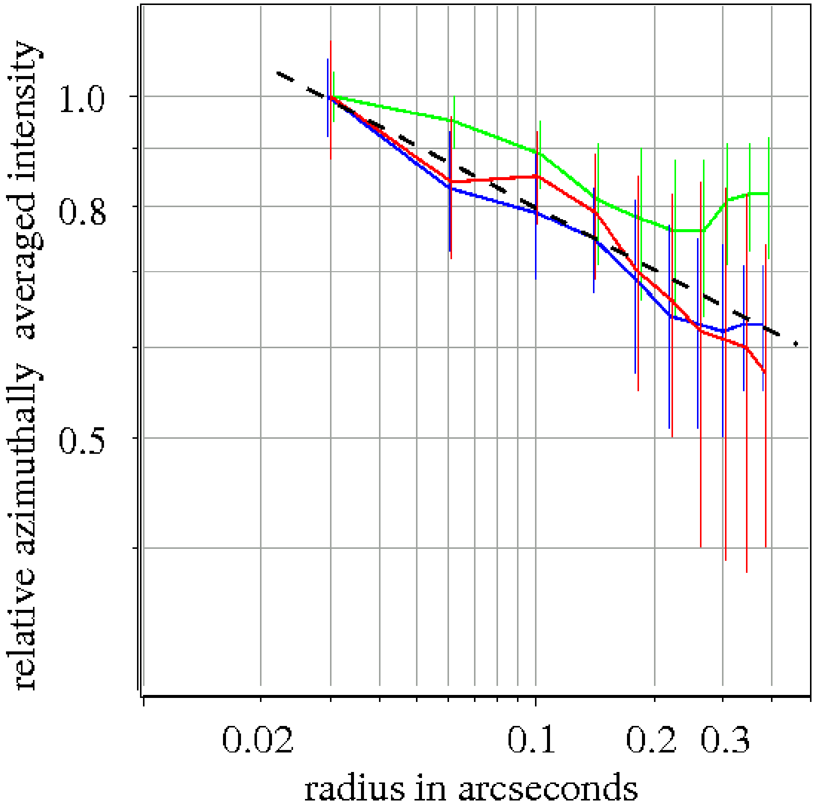

Sabha et al. 2011, 2012

S-stars: Extrapolation to fainter luminosities

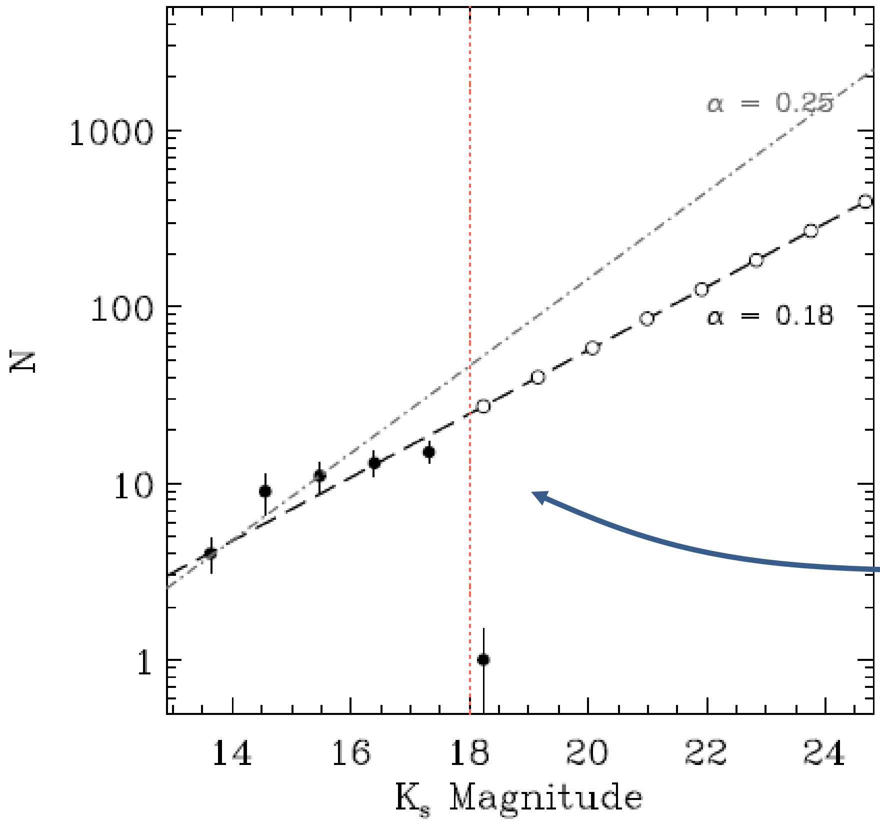

all stars fainter than the faintest stars detected in the central arcsecond.

Extrapolation of the KLF power-law fit. The KLF slope of α= 0.18 and the upper limit imposed by the uncertainty in the fit (α= 0.25) are plotted as dashed and dash-dotted lines, respectively. The black filled circles represent the data while the hollow circles represent new points based on the extrapolated KLF. The location of the detection limit is indicated by the red line.

Sabha et al. 2012

Apparent stars due to blends

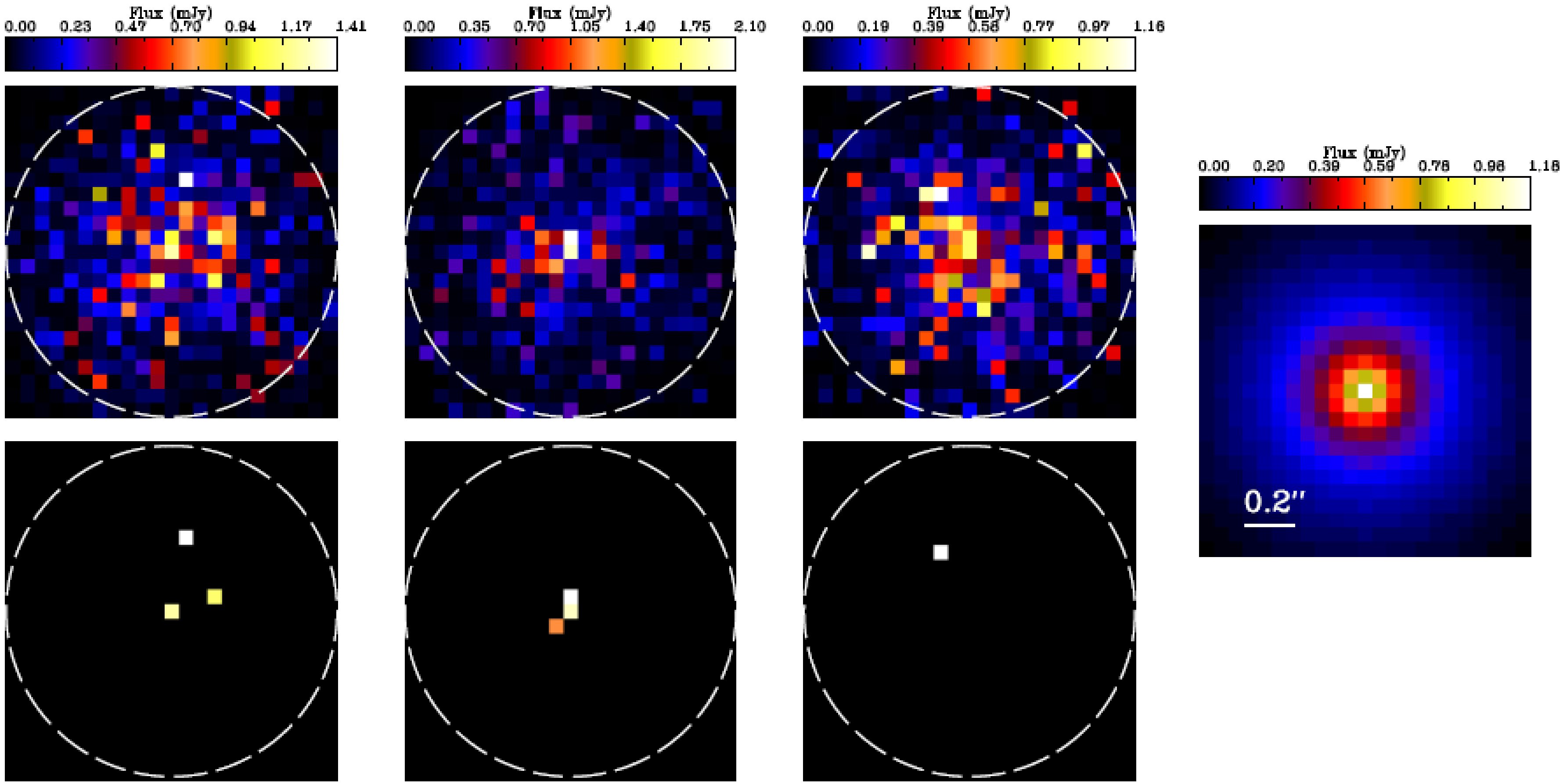

Upper panel: 3 different snapshots of the simulation for the α= 0.25 KLF slope, power-law index Γ = -0.3 and a ~25 K-magnitude cutoff.
Lower panel: The same as upper but with only the detectable blend stars visible.
Right: Average of all the 104 simulation snapshots for the same setup.

INTERFEROMETRY IS NEEDED to make progress! Sabha et al. 2012

SgrA* and its Environment

Orbits of High Velocity Stars
in the Central Arcsecond

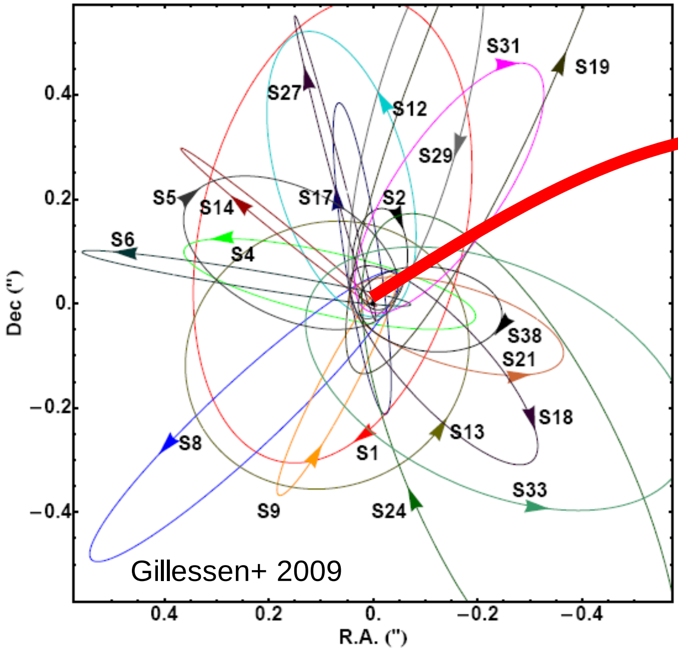

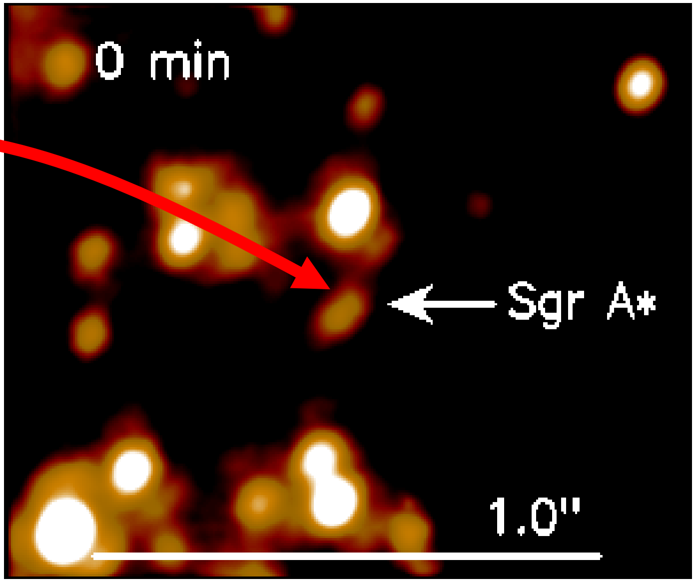

Eckart & Genzel 1996/1997 (first proper motions)
Eckart et al. 2002 (S2 is bound; first elements)
Schödel et al. 2002, 2003 (first detailed elements)
Ghez et al 2003 (detailed elements)
Eisenhauer 2005, Gillessen et al. 2009
(improved elements on more stars and distance)

~4 million solar masses
at a distance of
~8.3+-0.3 kpc

Progress expected in determining relativistic effects

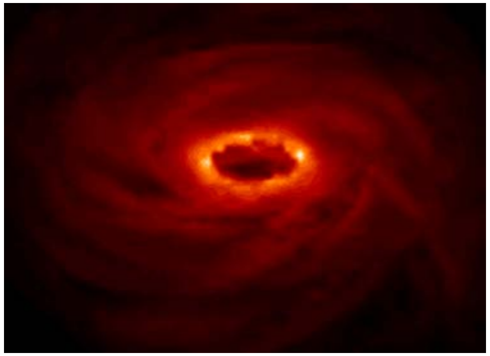

Possible hot spots orbiting SgrA* the detection of strong relativistic effects is complicated by processes in the accretion stream/outflow and relativistic disk effects

Stars are and remain the preferred (?) probs making use of NIR adaptive optics and interferometric measurments.

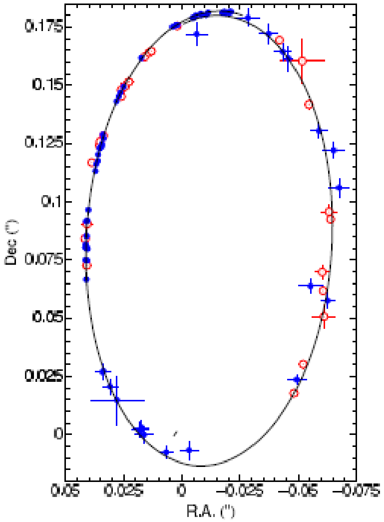

It is, however, unclear if there are any *preturbing effects* that may even further complicate the usage of stars for these high precision measurements.

Newtonian and relativistic periastron shift for S2

Newtonian:

retrograde shift Δϕ

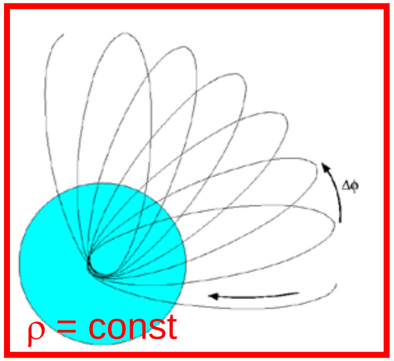

Relativistic:

prograde shift Δϕ

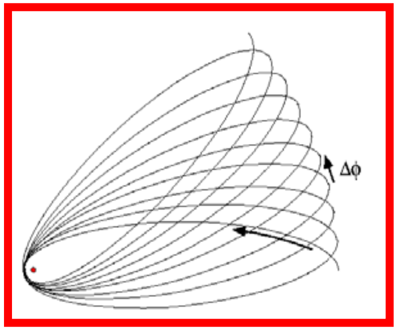

$$\boxed{(\Delta\omega)_{\mathrm{M}} = -2\pi G_{\mathrm{M}}(e,\gamma)\sqrt{1-e^2}\left[\frac{M_\star(r<a)}{M_\bullet}\right]}$$

$$G_{\mathrm{M}} = \left(1+\sqrt{1-e^2}\right)^{-1} \approx 0.68 \text{ for S2}$$

$$(\Delta\omega)_{\mathrm{M}} \approx -1.0' \left[\frac{M_\star(r<a)}{10^3\ \mathrm{M}_\odot}\right]$$

$$\boxed{(\Delta\omega)_{\mathrm{GR}} = \frac{6\pi G M_\bullet}{c^2 a(1-e^2)}}$$

$$a = 5.0 \text{ mpc}, \; e = 0.88 \text{ for S2}$$

$$\boxed{(\Delta\omega)_{\mathrm{GR}} \approx 10.8'}$$

Several stars are needed to disantangle the two effects.

Rubilar & Eckart 2002
Zucker + 2006;
Gillessen+ 2009;
Sabha + 2012

The high-velocity Galactic Center Stars are important probes for relativistic effects

average orbital distance: $\langle d \rangle = a(1 + e^2 / 2)$

ratio to gravitational radius: $\rho = \dfrac{\langle d \rangle}{r_g}$ $\quad r_g = \dfrac{GM}{c^2}$

$$\boxed{\frac{\rho_{Mercury}}{\rho_{S2}} \approx 1200}$$

Observed redshift as a function of the 3 dimensional velocity β

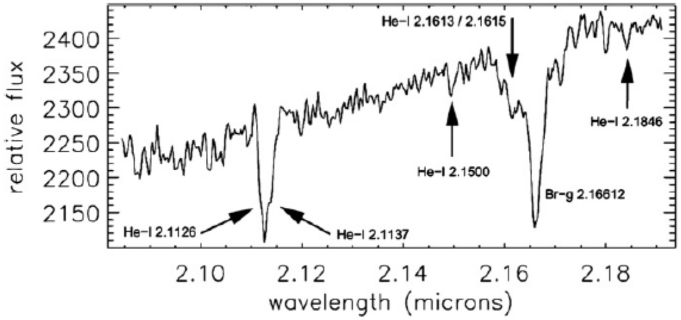

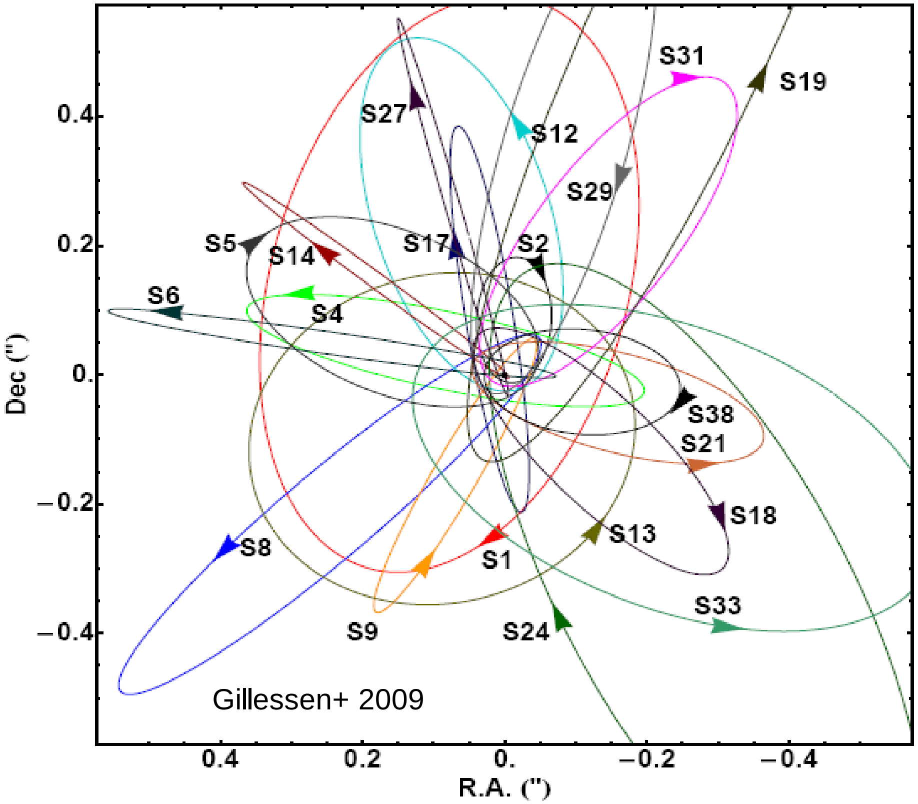

z: redshift

β: 3 dim. velocity

$$z = \Delta\lambda / \lambda = B_0 + B_1\beta + B_2\beta^2 + O(\beta^3)$$

offset ; Doppler; rel. effects

Zucker+ 2006, Gillesen+ 2009

Observed redshift as a function of the 3 dimensional velocity β

$$z = \Delta\lambda / \lambda = B_0 + B_1\beta + \boxed{B_2\beta^2} + O(\beta^3)$$

$$B_2 = B_{2,D} + B_{2,G} = \frac{1}{2} + \frac{1}{2}$$

$B_{2,G}$: gravitational redshift effect

$$z_G \equiv r_s / 4a + \frac{1}{2}\beta^2 = B_{0,G} + B_{2,G}\beta^2$$

$B_{2,D}$: special relativistic transverse Doppler effect

$$z_D \equiv (1+\beta\cos\vartheta)(1-\beta^2)^{-1/2} - 1$$

$$z_D \equiv z_{Newton} + z_{transverse} = \beta\cos\vartheta + \beta^2/2 = B_1\beta + B_{2,D}\beta^2$$

Zucker et al. 2006

$O(\beta^2)-$ effects should be observable with today's instrumentation:

$$\boxed{(B_{2,D}+B_{2,G})\beta_P^2 \sim 10^{-3} > \frac{\delta\lambda}{\lambda} \sim 10^{-4}}$$

$$\beta_P \sim \frac{v_{Peri}}{c}$$

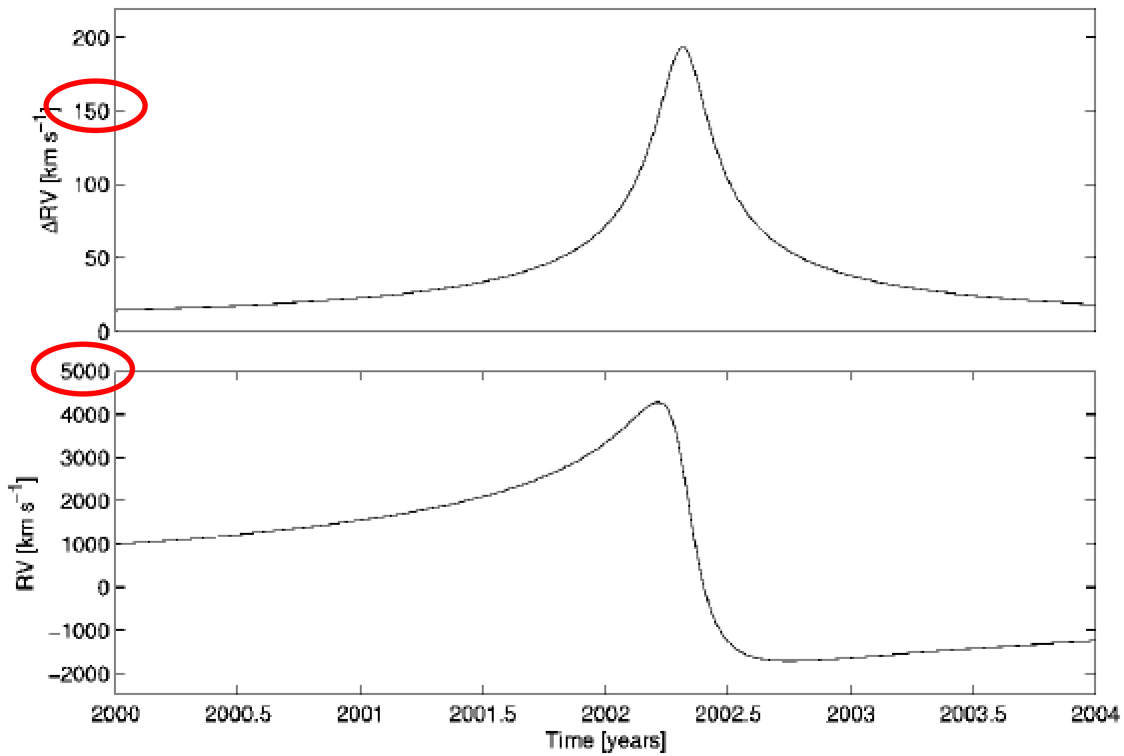

Contribution of the $O(\beta^2)-$ effects

full relativistic radial velocity of S2 near periaps

S2 e=0.88, r = 1500 rs

S14 e=0.94 r = 1400 rs

Zucker et al. 2006

Progress expected in determining relativistic effects

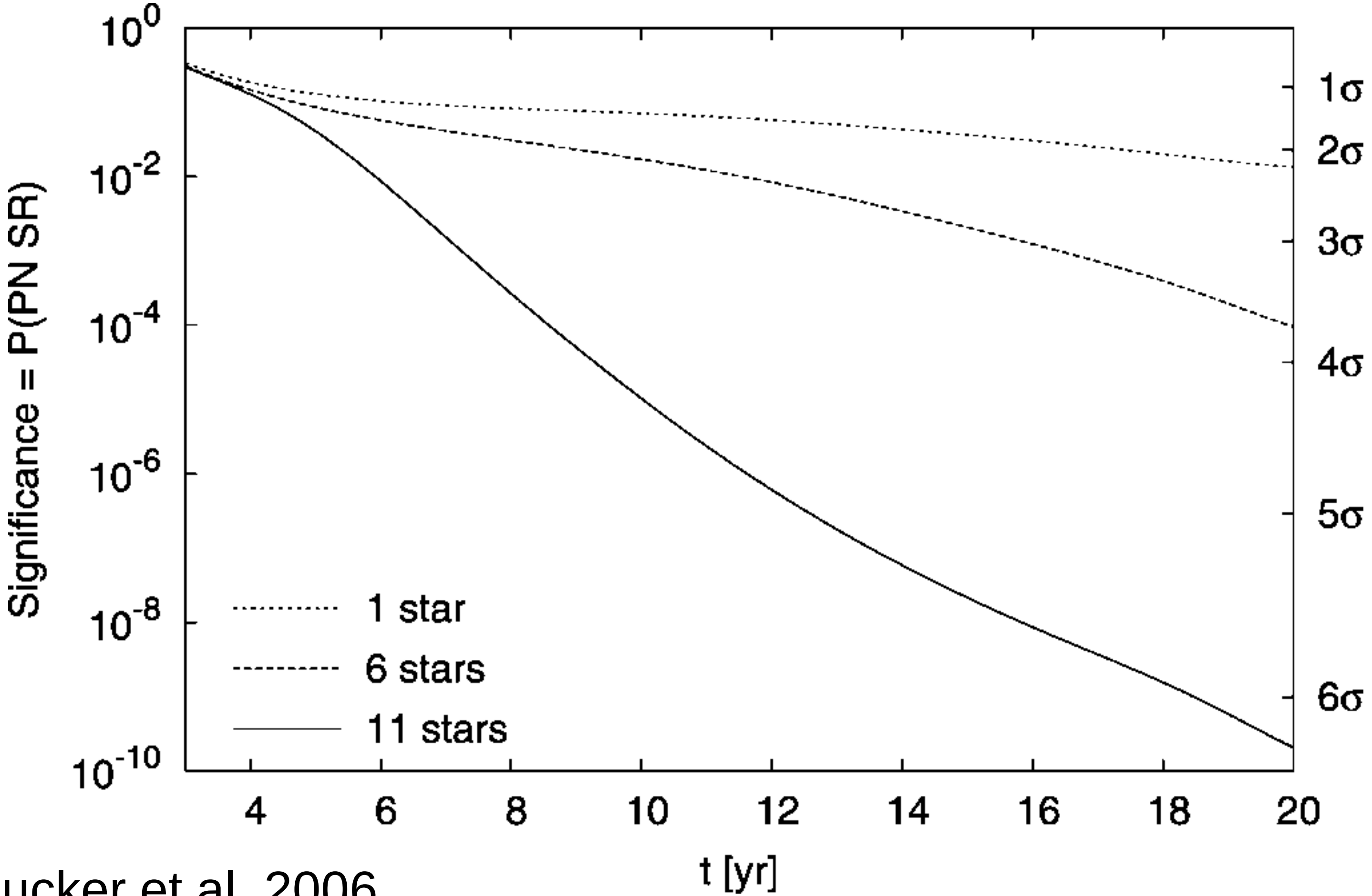

Zucker et al. 2006

For Schwarzschild, Kerr, quadrupol and non-luminous matter contributions see also Iorio 2011, MNRAS

Progress in measuring the orbits

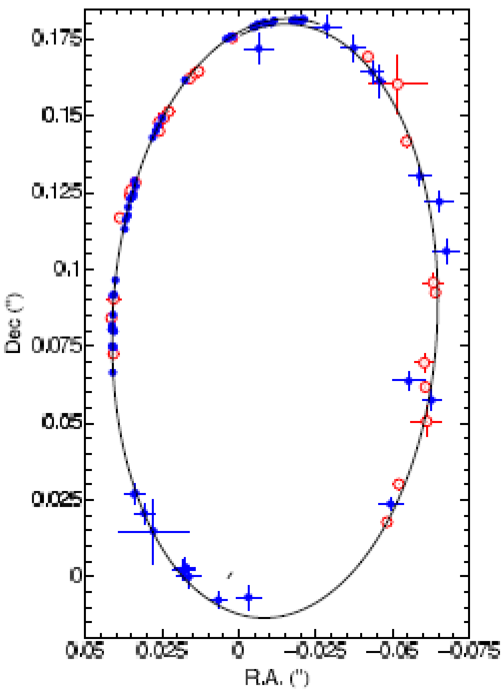

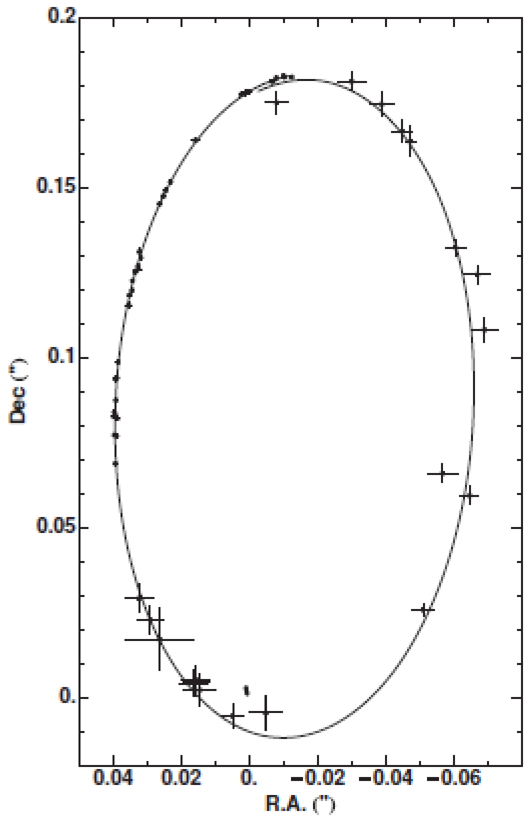

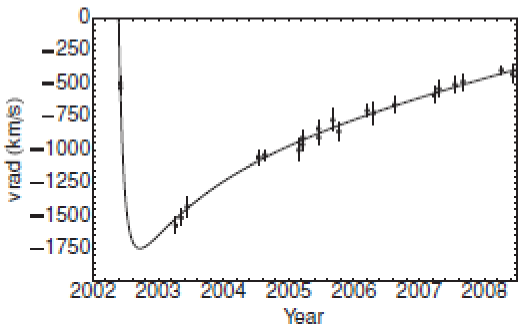

$$T_{orbit} = 15.6 \pm 0.4 yrs$$

$$e = 0.883 \pm 0.003$$

$$a = 0.125 \pm 0.002$$

$$R_0 = 8.28 \pm 0.15|_{\mathrm{stat}} \pm 0.29|_{\mathrm{sys}}\ \mathrm{kpc}$$

$$M_{\mathrm{MBH}} = 4.30 \pm 0.20|_{\mathrm{stat}} \pm 0.30|_{\mathrm{sys}} \times 10^6\ M_\odot$$

Gillessen+ 2009

Shortest known period star

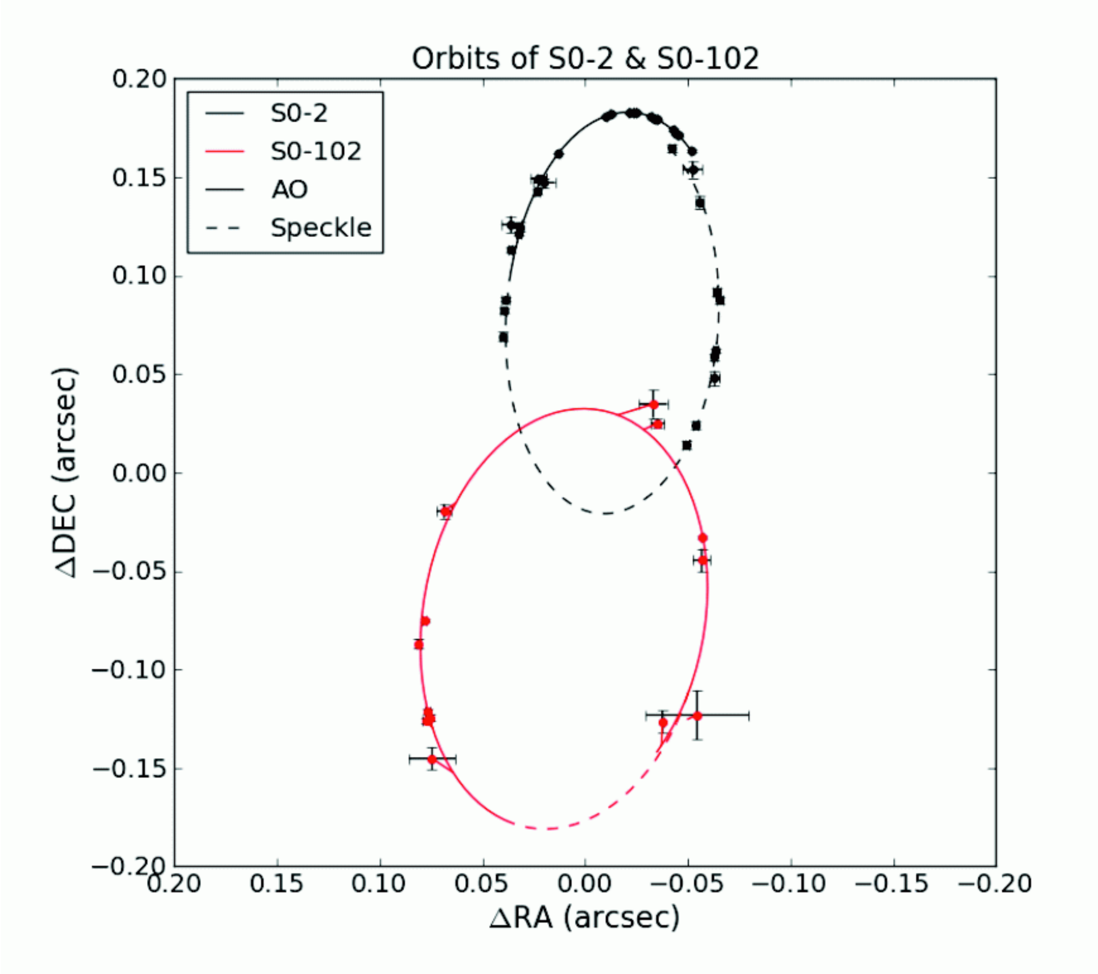

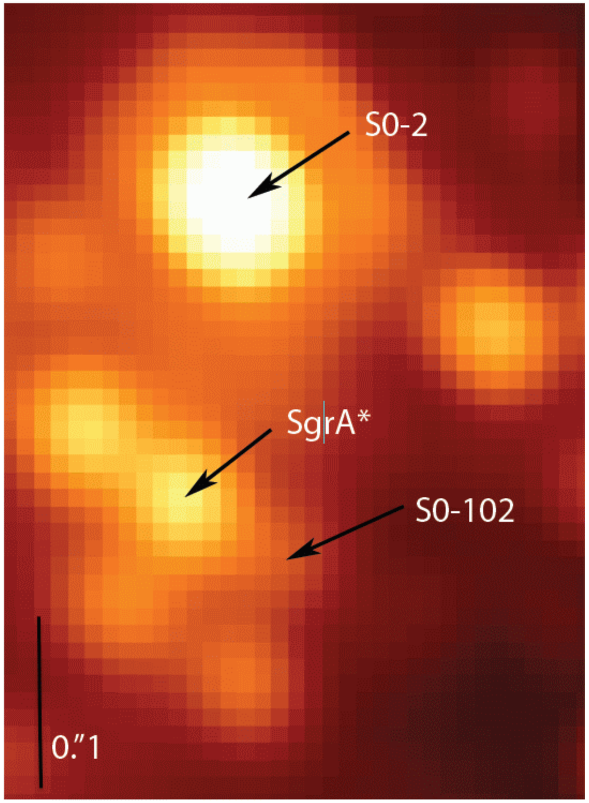

Shortest known period star with 11.5 years available to resolve degeneracies in the parameters describing the central gravitational potential (e=0.68) (Meyer et al. 2012 Sci 338, 84),

Relativity and evolution of S-star orbits

S0-102

$$T_{orbit} = 11.5 \pm 0.3 yrs$$
$$e = 0.68 \pm 0.02$$
$$a = 0.10 \pm 0.01$$

S2

$$T_{orbit} = 15.6 \pm 0.4 yrs$$
$$e = 0.883 \pm 0.003$$
$$a = 0.125 \pm 0.002$$

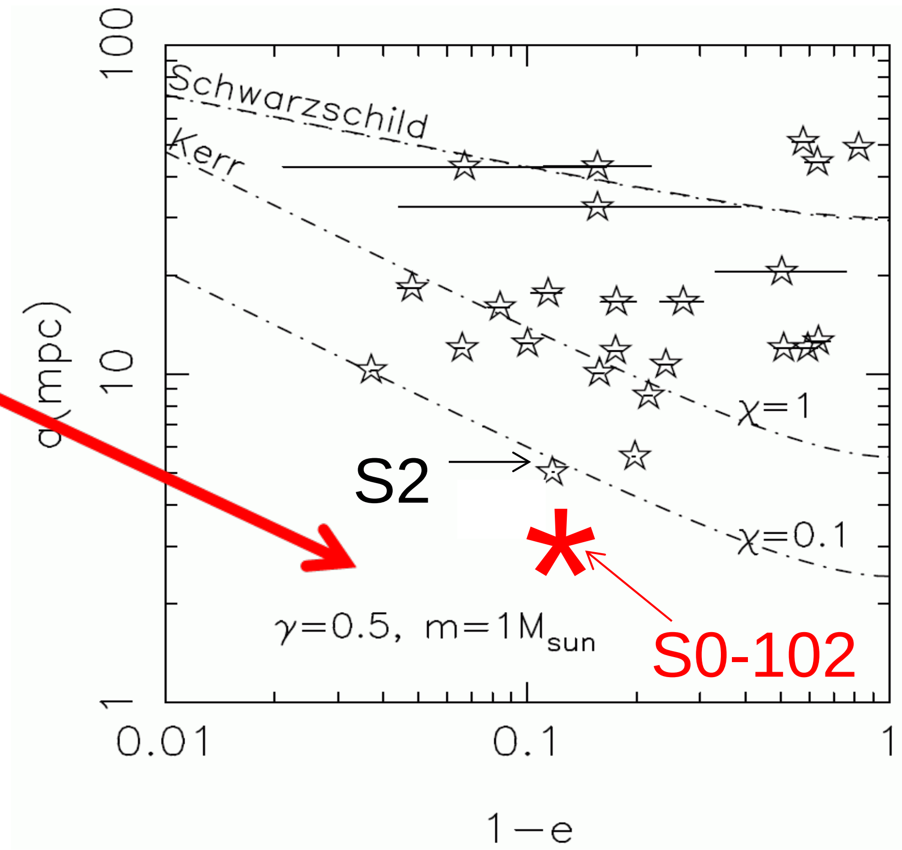

Orbits above (smaller e) the Schwarzschild line are subject to resonant relaxation and undergo a random walk in e . For stars below that curve the orbital torques of stars with smaller semi-major axis a compete with the SMBH torque (along dash-dotted curves with different spin c).

Antonini & Merritt 2013, ApJ 763 ,L10

Staubquellen innerhalb von 2” of SgrA*

Staubquellen im galaktischen Zentrum

- Der Fall IRS13N
  fortlaufende Sternentstehung im GC?

- Das staubige S-cluster Objekt (DSO)

- Ausfluß und Akkretion

Proper Motions of Dusty Sources within 2” of SgrA*

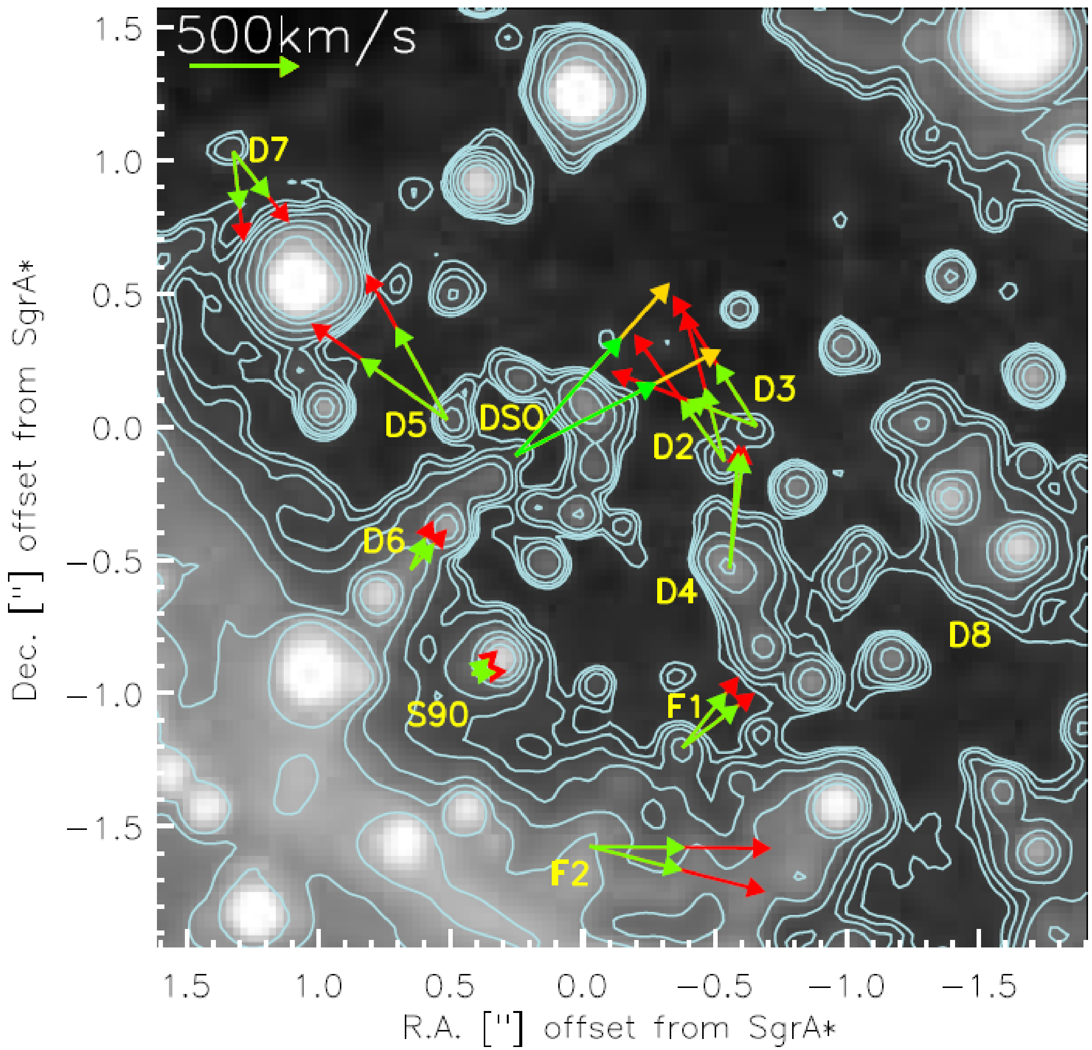

Eckart et al. 2012

Zooming in – towards IRS 13N

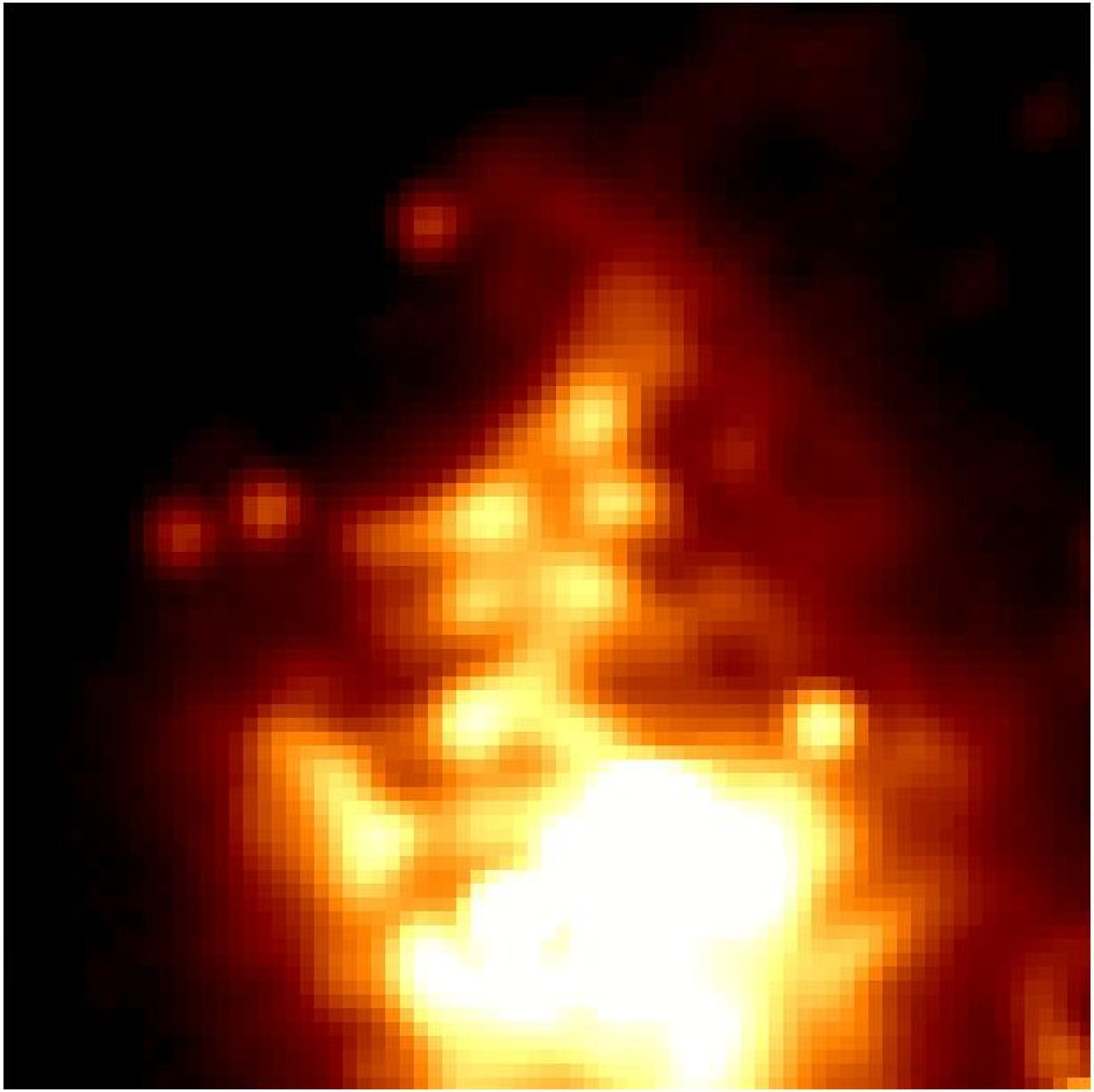

500mas
23 light days

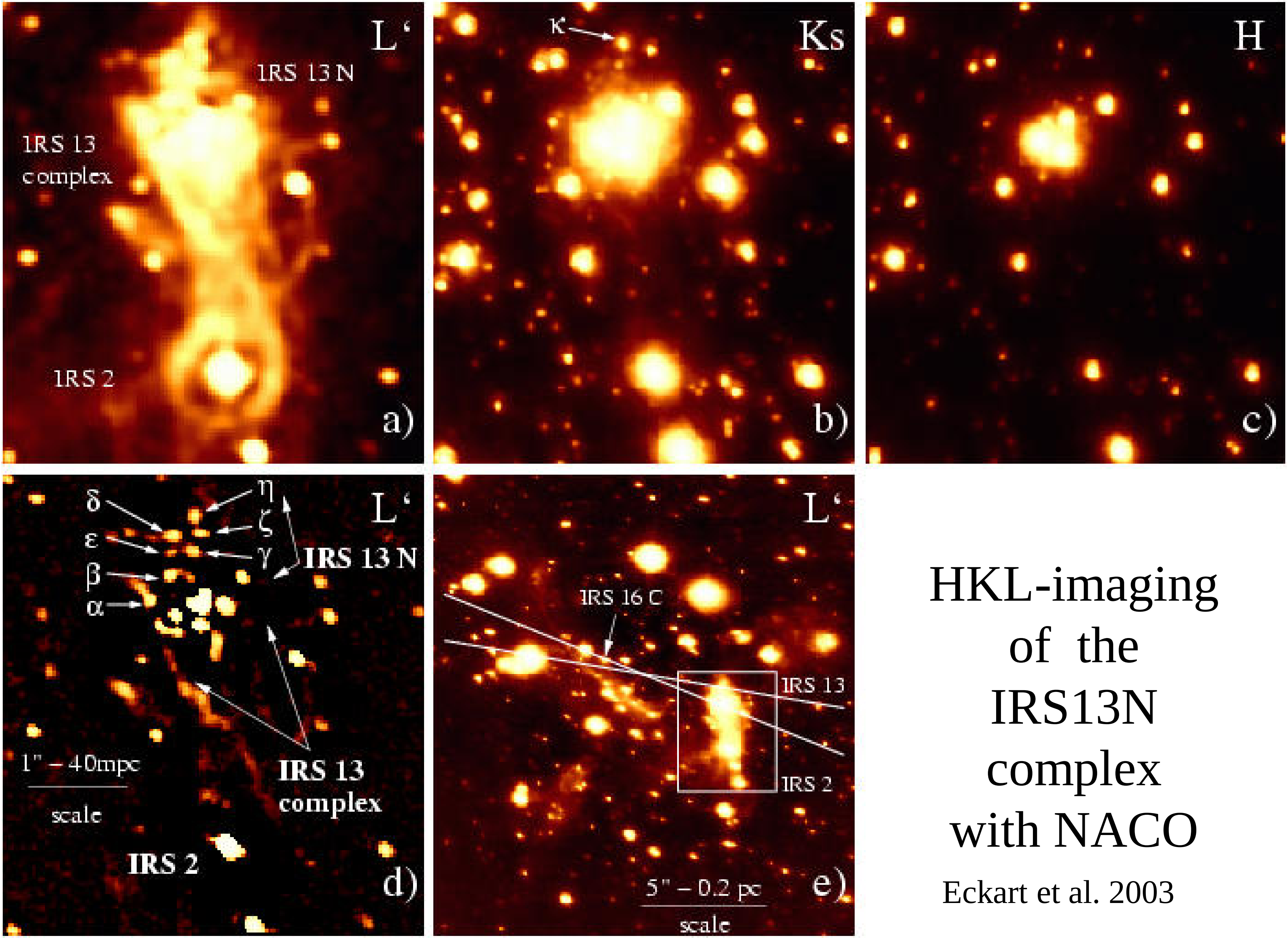

HKL-imaging of the IRS13N complex with NACO

Eckart et al. 2003

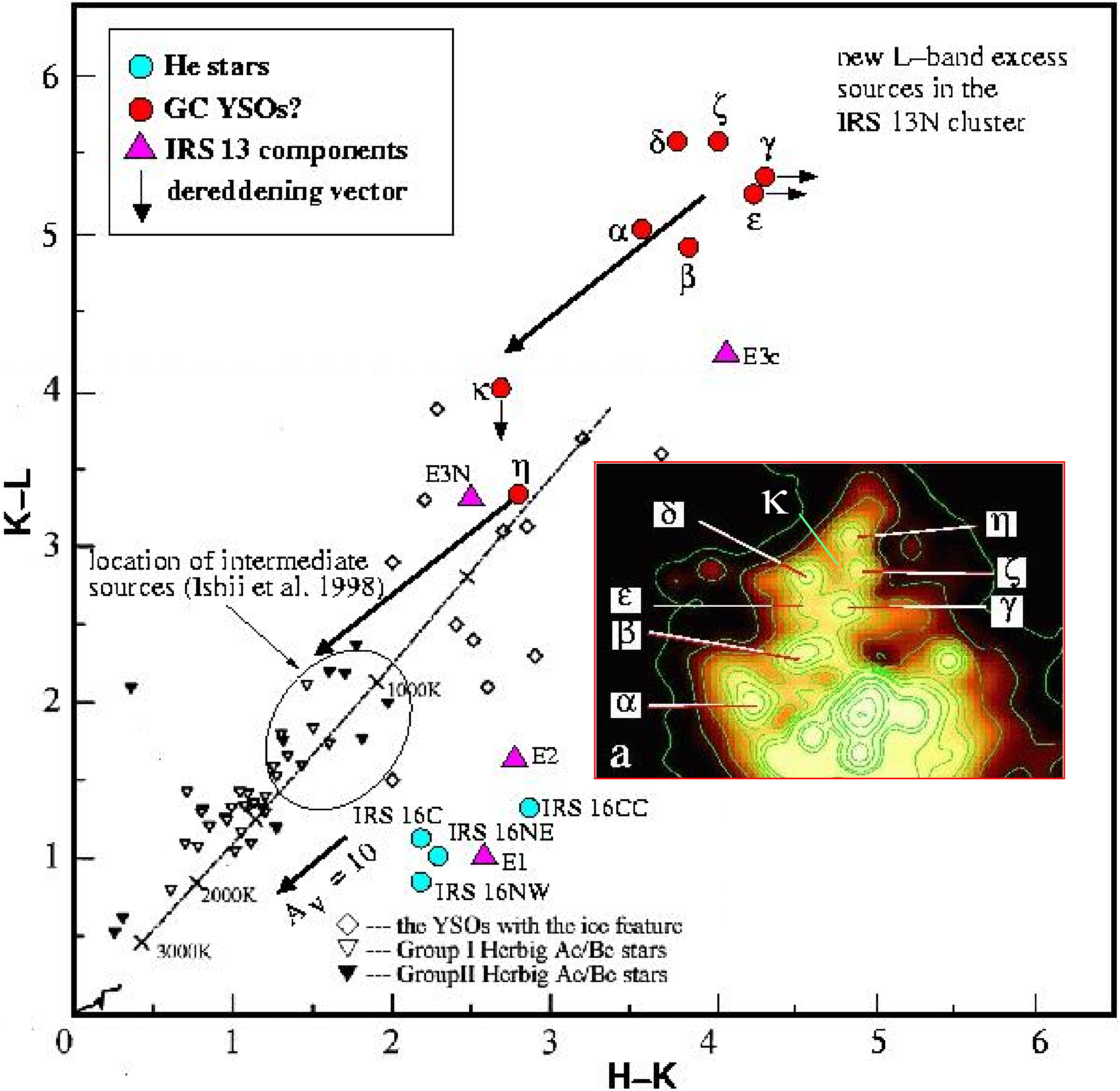

HKL-colors of sources in the IRS13N complex

$L=10^2 - 10^4$ Lsol
M=2-8 Msol

Low luminosity bow shock sources.

Are the IRS 13N sources at the GC Herbig Ae/Be stars?

Proper Motions in IRS13N

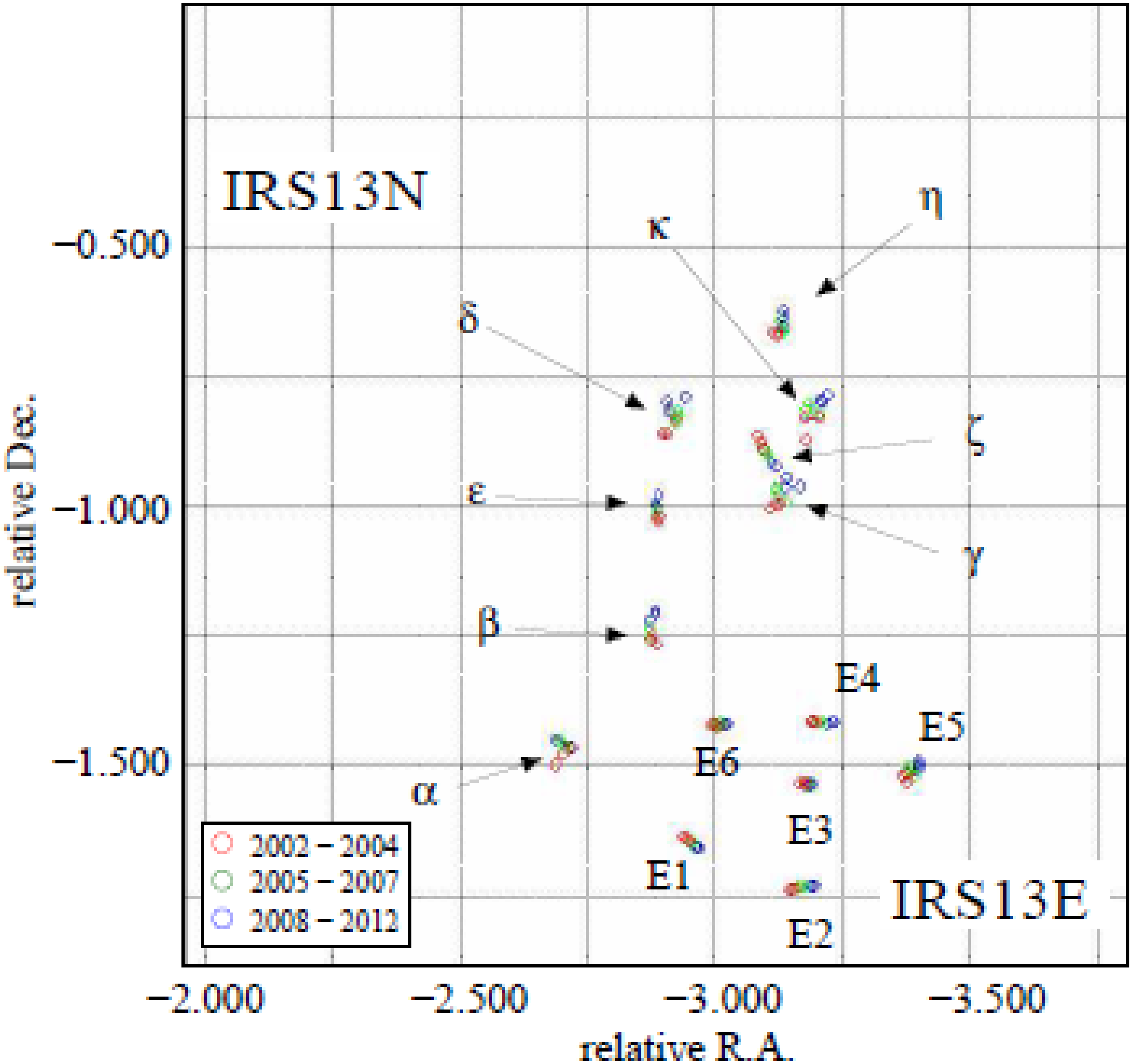

K-band proper motion from red to blue

Eckart et al. 2003, 2012
Muzic et al. 2009

Proper Motions in IRS13N

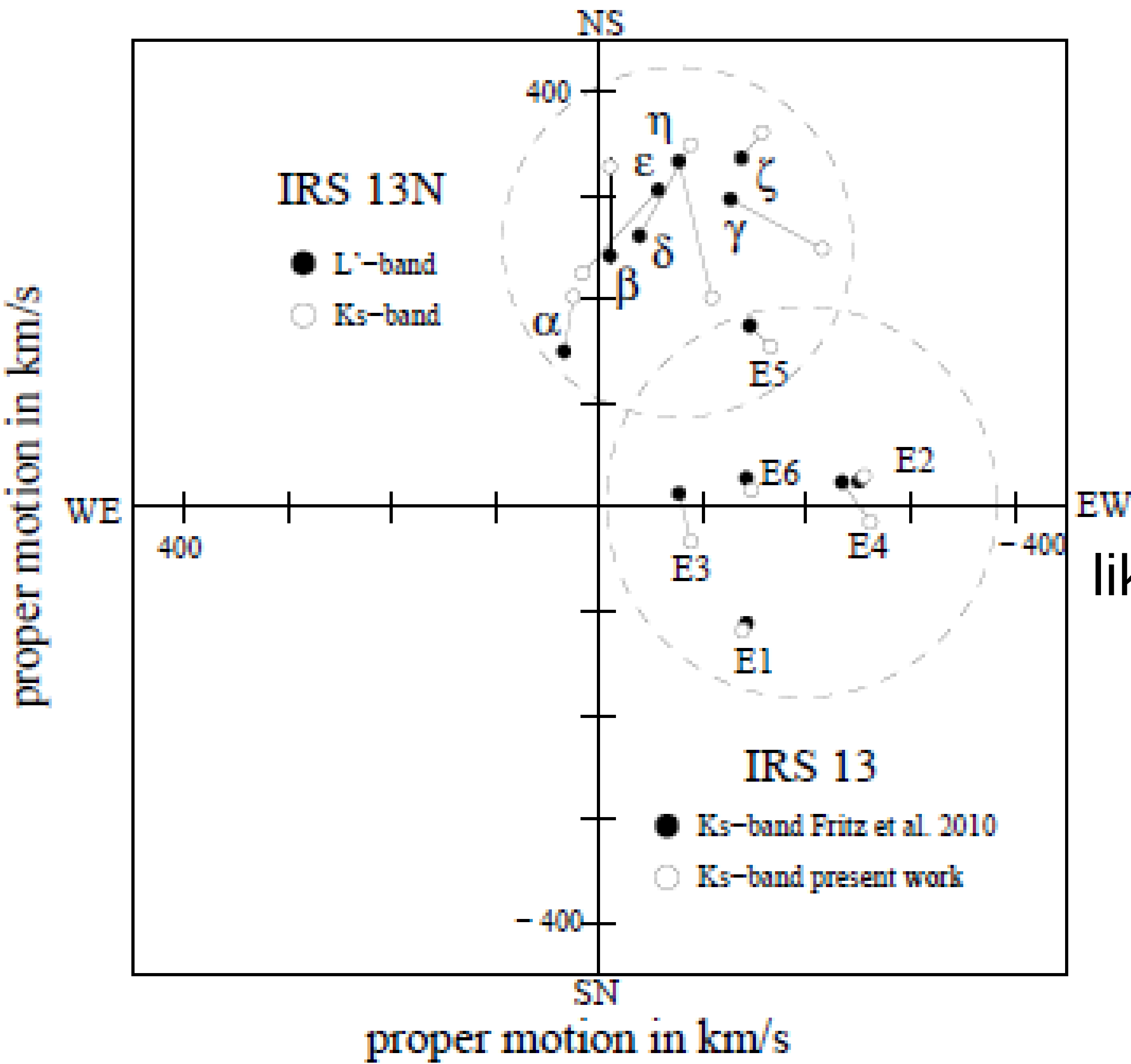

K- and L-band positions and proper motions agree
K-band emission likely to be photospheric e.i. from stars rather than from dust

Eckart et al. 2003, 2012
Muzic et al. 2009

1. Modeling Approach

100 Msun molecular clump, 0.2 pc radius,

Test with 10 & 50 Kelvin, isothermal gas

Timescales:
clump free fall time ~ 10^5 yr
CND orbital period ~ 10^5 yr

Semi-major axis=1.8 pc → orbital period ~10^5 yr,

two Orbits:
peri-center~0.1 pc → ecc.= 0.95
peri-center~0.9 pc → ecc.= 0.5

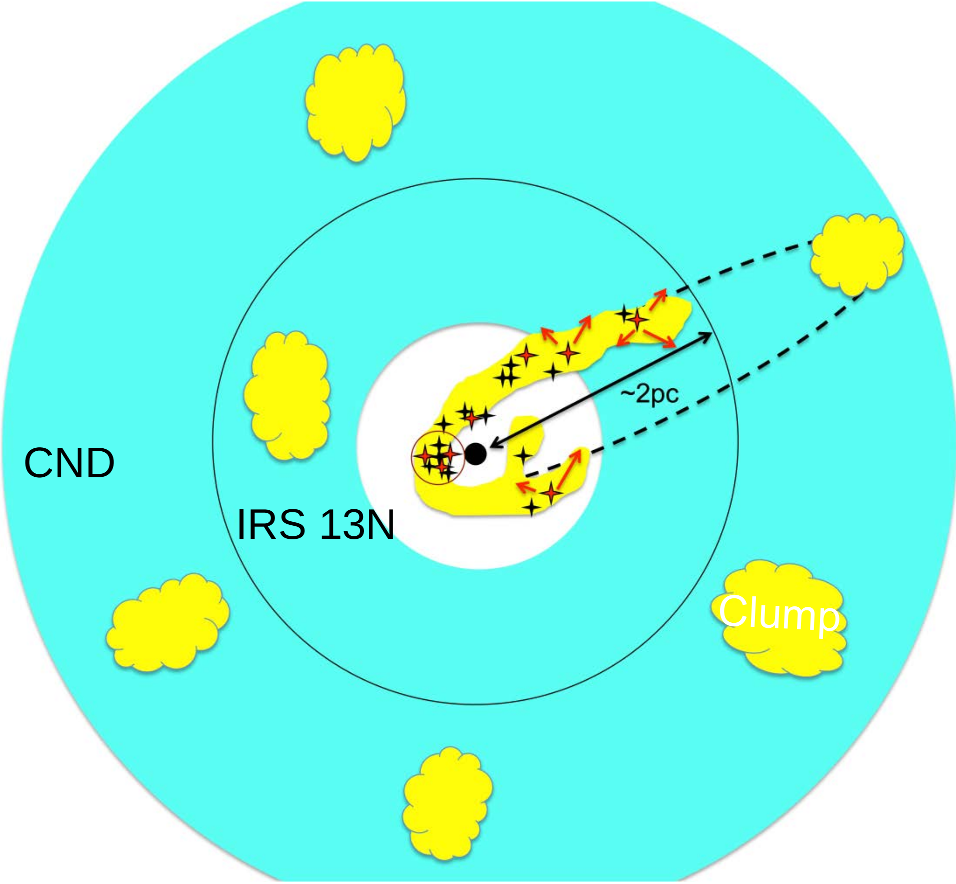

Jalali+2013 in prep.

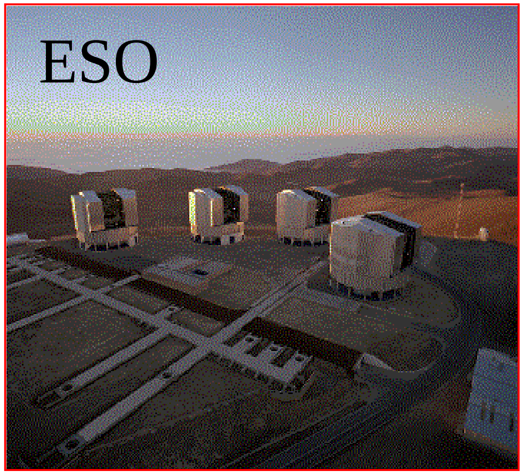

NL leads Euro-Team
Universitity of Cologne
studies for
METIS @ E-ELT

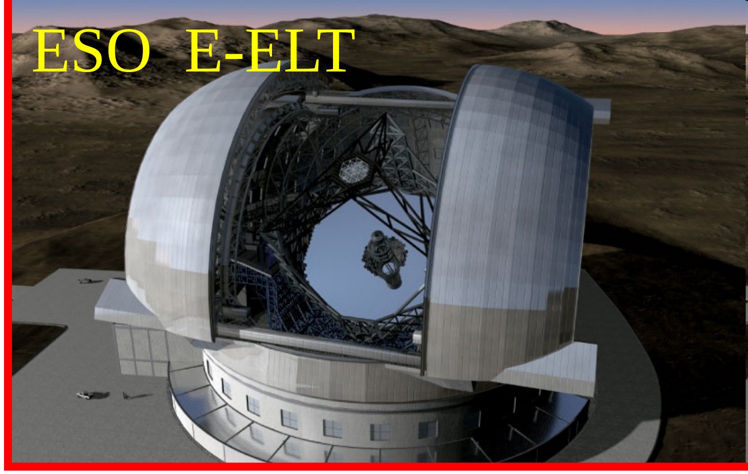

MPE, MPIA, Paris, SIM
Universitity of Cologne
participation
GRAVITY @ VLTI

The Galactic Center is a unique laboratory in which one can study signatures of strong gravity with GRAVITY

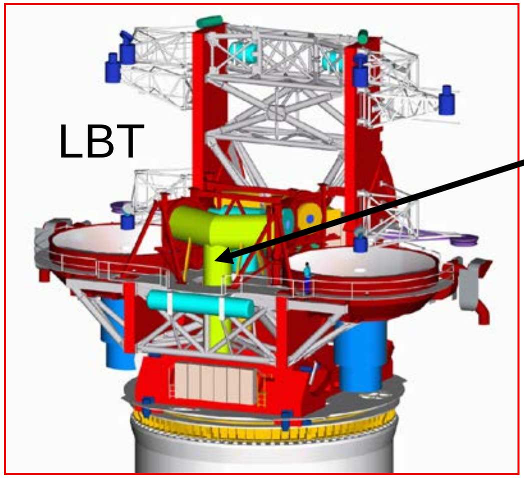

NIR Beam Combiner:
Universitity of Cologne
MPIA, Heidelberg
Osservatorio Astrofisico di Arcetri
MPIfR Bonn

Cologne
contribution to
MIRI on JWST